7-6-2015 12:00 AM

Modulation of synaptic plasticity by hippocampal theta rhythm

Clayton Law
The University of Western Ontario

Supervisor
Dr. Stan Leung
The University of Western Ontario

Graduate Program in Physiology and Pharmacology
A thesis submitted in partial fulfillment of the requirements for the degree in Master of Science

MODULATION OF SYNAPTIC PLASTICITY AND PYRAMIDAL CELL EXCITABILITY BY HIPPOCAMPAL THETA RHYTHM

(Thesis format: Monograph)

by

Clayton SH Law

Graduate Program in Physiology and Pharmacology

A thesis submitted in partial fulfillment of the

requirements for the degree of

Master of Science

The School of Graduate and Postdoctoral Studies

The University of Western Ontario

London, Ontario, Canada

July 2015

ABSTRACT

Hippocampal theta rhythm facilitates memory formation. This study investigated the temporal relation of long-term potentiation (LTP) with the hippocampal theta rhythm. I hypothesize that the population spike excitability evoked by excitation of the apical and basal dendrites peak at a similar phase of the theta rhythm. I also expect that LTP at the basal and apical dendritic synapses to be maximal at a similar theta phase. Extracellular potentials were recorded in hippocampal CA1 of urethane-anaesthetized rats. Maximal population spikes evoked by single-pulse stimulation of the apical and basal dendrites occurred at the falling phase of theta (120°-160°). LTP was maximal when the burst stimulation occurred during the rising phase of theta, which was 306°-30° (basal LTP) and 333°-24° (apical LTP). Thus, theta rhythm sets up a temporal (or phase) gradient of synaptic plasticity at the basal and apical dendrites of hippocampal pyramidal cells.

Keywords: synaptic plasticity; hippocampus; memory formation; theta rhythm; neural networks; basal dendrites; apical dendrites; CA1; rats; current source density; population spike

ACKNOWLEDGEMENTS

I would like to thank everyone who has supported me during my academic career. First and foremost, I would like to extend my deepest gratitude to my supervisor, Dr. Stan Leung, who has provided me with the opportunity to participate in such an exciting research project. I am honored to have worked with one of the world-leading experts in the field of electrophysiology. His dedication to research and commitment to producing quality work has inspired me and allowed me to grow as an individual. I would also like to thank all the members of my lab for making the lab a comfortable place to work. Without their support and assistance, my research would not have been conducted with the same efficiency. I would like to extend a special acknowledgement to Dr. Min-Ching Kuo for teaching me the technical skills necessary to start and complete this project. Thank you for being patient with me when I was still trying to orient myself to an unfamiliar and complex environment. I would also like to thank my advisory committee, Dr. Donglin Bai, and Dr. Susanne Schmid, for providing helpful advice and encouragement along the way.

TABLE OF CONTENTS

LIST OF FIGURES AND TABLES

Figure

Table

Supplementary Figure

LIST OF ABBREVIATIONS

-	negative
+	positive
AEP	average evoked potential
AMPA	α-amino-3-hydroxy-5-methyl-4-isoxazolepropionic acid
AMPAR	α-amino-3-hydroxy-5-methyl-4-isoxazolepropionic acid receptor
ANOVA	analysis of variance
AP	action potential
CA	cornu ammonis
Ca^{2+}	calcium
CAMKII	calcium/calmodulin (CaM)-dependent protein kinase II
CPI	combined phase index
CSD	current source density
AP5	2-amino-5-phosphoneopentanoic acid
DG	dentate gyrus
EC	entorhinal cortex
EEG	electroencephalogram
EPSP	excitatory post synaptic potential
fEPSP	field excitatory post synaptic potential
GABA	γ-Aminobutyric acid
HFS	high frequency stimulation
IPSP	inhibitory postsynaptic potential
K^+	potassium
LFS	low frequency stimulation
LTD	long-term depression
LTP	long-term potentiation
mGluR	metabotropic glutamate receptor
Na^+	sodium
NOS	nitric oxide synthase
NMDA	N-methyl-D-aspartate
NMDAR	N-methyl-D-aspartate receptor
pEPSP	population excitatory post synaptic potential
PPI	positive combined phase index
PnO	nucleus pontis oralis
PS	population spike
REM	rapid eye movement
SLM	stratum lacunosum moleculare
SUM	supramammillary nucleus
VDCC	voltage-dependent calcium channel

1. LITERATURE REVIEW

1.1 General Introduction

The greatest endeavor in neuroscience is possibly trying to understand the nature of the human mind. How can unique human experiences such as consciousness, thought, and emotion be attributed to a physical structure known as the brain? This question poses a problem in neuroscience: phenomena of the mind may not be observable in a physical realm; trying to explain how the physical connections between neurons can produce metaphysical phenomena may ultimately be a futile effort. A prominent philosopher, René Descartes, described this as the Mind-Body Dichotomy, a problem that still currently exists within the fields of neuroscience and philosophy. Although we may never be able to experience thoughts, feelings or emotions outside our own mind, I believe these unique states have corresponding physical manifestations in the brain which can be observed. Much like studying earth's history, although we may never really know the entire truth, which would require us to travel back in time, artifacts can allow us to paint a clear picture of what may have happened in the past. In trying to understand human thought, one has to determine the underlying template in which thought is created (the evidence). Space and time are innate concepts that help humans orient themselves to their environment. Episodic memories serve as a recollection of past events in space and time, which can then be consciously used to establish future behaviours. Understanding how memory is formed may ultimately allow for greater insight into the more elaborate faculties of human cognition.

1.2 Hippocampus and memory formation

Karl Lashley (1950), in search of where the memory trace (engram) was located, lesioned different cortical regions of the brain and observed how it affected the learning ability of different animals. Contrary to his hypothesis, where he believed that a specific region of the brain contained all memories, he found that lesioning any area of the brain will impair learning ability. This observation led Lashley to conclude that memory was equally distributed among all cortical areas. However, Lashley's experiments could not elucidate the different functions of each region that may contribute to creating a memory trace. Thus, the current view of memory is in partial agreement with Lashley's conclusion in that memory is distributed across the brain, but not equally distributed in all cortical areas.

The hippocampus is a medial cortical brain structure involved with learning and memory in many different animal species, including humans. Hippocampal involvement in human memory has been proposed following earlier clinical observations where lesion or damage to the hippocampus resulted in memory loss (Scoville and Milner, 1957).In fact, a lesion to the CA1 region of the hippocampus proper is sufficient to induce moderately severe memory impairment (Zola-Morgan et al., 1986). Most human subjects with hippocampal damage experience anterograde amnesia, the inability to form new memories, and some show minor retrograde amnesia, the inability to recall previously formed memories. Although these patients had anterograde amnesia, they were still able to show day-to-day improvement in a hand-eye coordination skill (Milner, 1962). This observation necessitated a paradigm shift in how memory was defined. Perhaps memory

could not be considered as a single entity, but a combination of multiple, distinct processes, with different contributions from different brain regions.

The hippocampus specifically contributes to declarative memory. Declarative (explicit) memory is the ability to consciously recall general factual knowledge that is independent of personal experience (semantic memory) or observational information attached to specific events that one has experienced (episodic memories). In contrast, nondeclarative (implicit) memory is learning of skills or habits that can be unconsciously executed. The hippocampus plays a time-sensitive role in memory formation. Information storage in the hippocampus is only temporary as memory is gradually reorganized into more permanent representations in the neocortex (Squire, 1992). Although the hippocampus is undoubtedly involved in learning and memory formation, its contribution to specific learning processes such as encoding, consolidation, and retrieval remains unclear (Nadel and Moscovitch, 1997).

Clinical human studies have provided a foundation for studying the hippocampal role in memory formation. However, to gain an even further understanding of learning, cellular mechanisms must be explored, which would require the use of *in vitro* or *in vivo* models. These techniques may be too invasive for human application and using human tissue poses various technical challenges. Therefore, a suitable model organism would enable further efforts in research. The rat hippocampus has a similar role in learning to that of the human hippocampus. In rats, the hippocampus is required for declarative memory, similar to findings in humans (Bunsey and Eichenbaum, 1996); thus making the rat an appropriate model for studying the hippocampal role in memory formation.

The discovery of place cells in rats has provided physiological evidence of the hippocampus' role in memory formation (O'Keefe and Dostrovsky, 1971). Place cells are believed to be pyramidal neurons found throughout the hippocampal structure that encode for spatial information. When a rat navigates through a maze, individual place cells will fire correspondingly to the rat's spatial location in the maze. Other types of specialized cells (e.g., time cells, grid cells) also exist to help the brain understand its position in space and time (MacDonald et al., 2011; Moser et al., 2008). Considering that episodic memories are a recollection of space and time, the hippocampus has a crucial role in memory and learning.

1.3 Hippocampal Anatomy

The hippocampus is a convoluted structure found in the medial temporal lobe of the brain. Its distinct curved shape resembles that of a sea horse, which it is named after in Greek (*hippos* meaning "horse" and *kampos* meaning "sea monster"). The hippocampal formation includes the hippocampus proper, the dentate gyrus and the subiculum.

The hippocampus is unique in its lamellar organization. Different distinct layers can be defined based on functionality and anatomy. The subiculum is divided into stratum pyramidale, where the pyramidal cell somas are located, and the dendritic stratum moleculare. The CA subregions of the hippocampus can be divided into several layers. The alveus is contiguous with the fimbria, and is found overlying CA1 and CA2. Stratum oriens layer is found between the alveus and stratum pyramidale, the pyramidal cell soma layer. Stratum radiatum is found below stratum pyramidale, and stratum lacunosummoleculare is found beneath stratum radiatum**(Fig. 1B)**. CA region is separated from the dentate gyrus by the hippocampal sulcus. The stratum moleculare of

the dentate gyrus is found between the hippocampal sulcus and the stratum granulosum, where the soma of granule cells are located (Knowles, 1992).

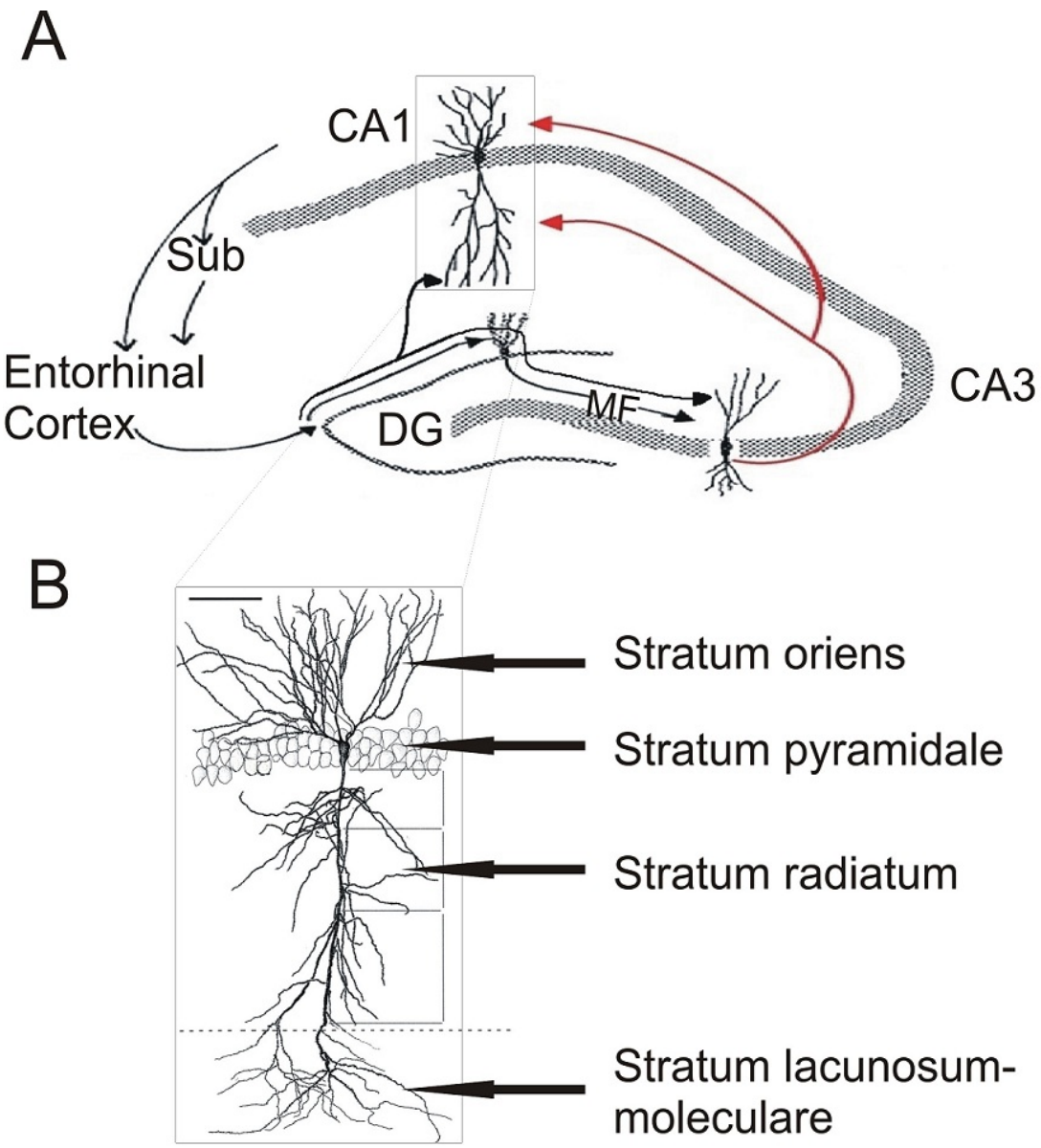

Figure 1. Schematic diagram of hippocampal connections. **(A)** Coronal section of rat hippocampus depicting major subregions and circuitry. Arrows indicate the direction of information propagation. Information enters the entorhinal cortex from neocortex and projects to DG, CA3 and distal dendrites of CA1 directly. DG projects to CA3 via mossy fiber pathway. CA3 projects to CA1 via Schaeffer collateral pathway. Information exits from CA1 to entorhinal cortex. Abbreviations: DG (dentate gyrus), MF (mossy fibers), Sub (subiculum) **(B)** Organization of different layers of CA1 subregion. Basal dendrites project to stratum oriens, proximal apical dendrites project to stratum radiatum and distal apical dendrites project to stratum lacunosummoleculare (originally illustrated by Megias et al., 2001).

Anatomically, the hippocampus is a candidate location for information processing: the neocortex provides multisensory signals to the hippocampus through the entorhinal cortex using the perforant pathway. These neurons project monosynaptically to the hippocampal dentate gyrus, CA3 and CA1. Perforant path projections to the dentate gyrus arise from layer II of the EC. Subsequent activation of the "trisynaptic loop" involves dentate gyrus projections to CA3 via mossy fiber pathway, and CA3 projections to CA1 via the Schaeffer collateral pathway, synapsing onto both basal and apical dendrites **(Fig. 1A)**. CA3 projects to CA1 both ipsilaterally and contralaterally. Commissural fibers connect CA3 to the contralateral CA1 region (Amaral and Witter, 1989; Andersen et al., 1971).The CA3 subregion can be further divided into CA3a, CA3b, and CA3c. CA3a is more distal to the dentate gyrus, bordering CA2, whereas CA3c penetrates the dentate hilus (Lorente de Nó, 1934). Subdividing CA3 serves both an anatomical and functional purpose as CA3a cells preferentially synapse on the basal dendrites of CA1, whereas CA3c cells preferentially synapse onto apical dendrites. CA3b cells project to both apical and basal dendrites of CA1 (Ishizuka et al., 1990; Laurberg, 1979; Li et al., 1993). CA3 and CA1 distal apical dendritic synapses at the level of stratum lacunosummoleculare are also monosynaptically activated via temporoammonic pathway (Blackstad, 1958; Lorente de Nó, 1934; Ramon y Cajal, 1911) input from entorhinal cortex layer III pyramidal cells (Steward &Scoville, 1976). CA1 pyramidal cells then extrinsically project to the subiculum and entorhinal cortex. Other limbic cortical areas and the lateral septum, nucleus accumbens and olfactory bulb are also targets for CA1. Therefore, CA1 (together with the subiculum) can be considered as the major output structure from the hippocampus back to the neocortex.

The hippocampus consists of principal cells and interneurons. Principal cells are responsible for excitatory neurotransmission, using glutamate as a neurotransmitter. Granule cells are principal cells of the dentate gyrus. Pyramidal cells represent the principal cells of CA3 and CA1. Hippocampal pyramidal cells have a distinct, triangular cell body with basal dendrites extending obliquely into stratum oriens and apical dendrites extending radially into stratum radiatum and stratum lacunosum-moleculare, giving rise to smaller side branches that may reach the hippocampal fissure or the border of the hilus proper. Basal dendrites are more numerous than apical dendrites. Pyramidal cells in CA1 are smaller than those in CA3, and form a narrow layer (stratum pyramidale) of 50-100 µm thickness. (Blackstad, 1958; Lorente de Nó, 1934; Ramon y Cajal, 1911).While principal cells may have axonal projections extending beyond where their cell bodies and dendrites are located, the axons and dendrites of interneurons are limited to a single brain area.

Interneurons play a significant role in modulating principal cell ensembles by providing an inhibitory component in excitatory networks, and temporally regulating pyramidal cell activity. Interneurons primarily use gamma-aminobutyric acid (GABA) to inhibit their targets (Freund and Buzsaki, 1996). A CA1 pyramidal cell receives around 30 000 inputs through the dendritic framework, while the cell body and axon-initial segment receive only GABAergic synapses. There are a wide variety of interneurons and they are classified based upon shape, location and neurophysiology. Different types of parvalbumin (PV)-expressing GABAergic interneurons innervate specific subcellular domains.Axo-axonic cells exclusively innervate the axon-initial segment of pyramidal cells. Interneurons that inhibit pyramidal cells at the axon initial segment include

oriens/alveus interneurons, moleculare-lacunosum interneurons and chandelier cells (Lorente de No, 1934). Basket cells can be found near stratum pyramidale and inhibit pyramidal cells via axosomatic synapses. Bistratified cells innervate basal and oblique dendrites coaligned with CA3 glutamatergic input. Oriens-lacunosummoleculare (O-LM) interneurons innervate the apical dendritic tuft and are aligned with entorhinal cortical input. These different interneurons defined by their axonal target domain on the pyramidal cell fire action potentials at distinct times during network oscillations, indicating the important time-dependent modulatory role of interneurons. Basket and bistratified cells strongly increase their firing rate during ripple oscillations and discharge in a manner phase-coupled to the oscillatory cycles. However, axo-axonic cells sometimes fire before the ripple oscillations, but are silenced during and after it. OL-M cell firing is suppressed during ripple oscillations. During theta oscillations, O-LM and bistratified cells increase in activity, modulating pyramidal cell dendrites one-quarter of a theta cycle after PV-expressing basket cells discharge. PV-expressing basket cells in turn fire later than axo-axonic cells. Thus, different domains on the CA1 pyramidal cell receive GABAergic input at different time points. However, the same domain on the CA1 pyramidal cell can also receive differentially timed GABAergic input from distinct sources. In addition to PV-expressing cells, cholecystokinin (CCK)-expressing GABAergic interneurons innervate pyramidal cells at the soma, proximal dendrites, apical dendrites, dendrites receiving glutamatergic CA3 input, and at the apical tuft. During theta oscillations, CCK-expressing cells fire at a phase when CA1 pyramidal cells fire due to the rat entering its place field (Klausberger and Somogyi, 2008).

There are some notable anatomical differences between human and rodent hippocampus. In rodents, CA1 pyramidal neurons are densely packed, whereas in humans it tends to be more dispersed (Duvernoy, 1988). In humans, CA2 is a distinct region between CA1 and CA3, whereas in rodents, CA2 is smaller and much less distinct.

1.4 Synaptic plasticity in the hippocampus

1.4.1 Physiological mechanism of learning and memory

Learning and memory can be observed behaviorally, but should also manifest as a measurable physiological phenomenon. The cellular basis of memory formation is widely believed to exist between neuronal connections known as synapses. Donald Hebb (1949) proposed a theory of how learning and memory is the result of changing associative strengths between neurons. The more one cell participates in the firing of another cell, the greater that connection will be. The theory of Hebbian Learning can be summarized as "cells that fire together, wire together".

Long-term potentiation (LTP) is a persistent increase in synaptic signaling due to repetitive activation of specific synapses (Bliss and Lomo, 1973). Although LTP appears to be the phenomenon that is described in Hebbian Learning, a unidirectional change in excitatory signaling is insufficient to describe how learning and memory occurs. There is no mechanism for how connections get weaker and no upper limit for maximum excitability. Therefore, the Bienenstock-Cooper-Munro (BCM) theory of learning proposed a sliding threshold of postsynaptic excitation and inhibition to account for changes that occur during memory formation (Bienenstock et al., 1982).

LTP accounted for increases in postsynaptic response; however a similar phenomenon needed to be discovered to account for persistent decreases in postsynaptic response. Long-term depression (LTD) is the persistent decrease in synaptic signaling due to repetitive low-frequency activation of excitatory synapses (Dudek and Bear, 1992). Selective disruption of NMDA receptors required for LTP and LTD results in impaired spatial memory (Tsien et al., 1996; Ge et al., 2010).Therefore, both LTP and LTD are believed to contribute to learning and memory.

1.4.2 Long-term potentiation (LTP)

LTP is widely-regarded as a cellular correlate of behaviour learning due to similar features between the two phenomena: 1) associativity, 2) input-specificity, and 3) temporal persistence. Associativity in LTP is demonstrated through spike-timing dependent plasticity (STDP) experiments where pairing a weak input with a strong input can cause potentiation of the weak input (Dan and Poo, 2004). This cellular phenomenon is similar to what is observed in classical conditioning where a previously neutral stimulus can be associated with an unconditioned stimulus to produce a desired response from the neutral stimulus. Input-specificity of LTP is the ability to cause specific changes only in the set of synapses that was stimulated with no LTP occurring elsewhere (Bi and Poo, 2001). The ability to selectively learn specific items of interest is the behavioural correlate of this cellular phenomenon. Temporal persistence describes how both LTP and behavioural learning persist over time. Induced LTP can persist for hours in *in vitro* preparations and can even last up to months in *in vivo* experiments (Abraham and

Williams, 2003). If memories can persist for a long time, then long-lasting changes must also occur in the brain to reflect the acquired memory.

The perforant path and Schaeffer collateral pathway are conventional sites to study synaptic plasticity. LTP is typically induced by repetitive high-frequency trains of stimulation (100 Hz for 1s); this is referred to as high-frequency stimulation (HFS). However, the long train of stimulation pulses delivered during HFS is not physiologically relevant because it does not resemble any known neuronal firing pattern (Connors and Gutnick, 1990). Neurons in the hippocampus typically fire in short bursts, known as complex spiking, with an interburst interval in the theta (3-12 Hz) range (Fox and Ranck, 1975). Therefore, theta-frequency stimulation was developed in an attempt to find a more physiologically relevant means of inducing LTP. Delivering shorter trains (4-5 pulses) of stimulation at the theta frequency has also been found to be an effective means of inducing LTP (Staubli and Lynch, 1987; Leung and Shen, 1995).

During excitatory transmission, glutamate is released from presynaptic vesicles and binds to AMPA and NMDA receptors postsynaptically. AMPA receptors allow the movement of Na^+ and K^+ through its channel, predominantly contributing to excitatory post synaptic potential (EPSP). NMDA receptors contribute little to the EPSP at rest, but they play a crucial role in synaptic plasticity. At resting membrane potential, the ion channel is blocked by Mg^{2+}; however with sufficient depolarization, Mg^{2+} dissociates and allows for Na^+ and Ca^{2+} to flow into the cell. NMDA receptors act as coincidence detectors because they require postsynaptic binding of glutamate and membrane depolarization to be activated. Activation of the NMDA receptor is believed to be required for inducing LTP. Application of an NMDA receptor antagonist 2-amino-phosphonopropionic acid (AP5)

completely blocks LTP in most hippocampal synapses (Collingridge et al., 1983; Zalutsky and Nicoll, 1990; Hanse and Gustafsson, 1992). Deletion of the NMDAR1 gene in mice subsequently impaired LTP at CA1 synapses and spatial memory (Tsien et al., 1996). Non-NMDA receptor-dependent forms of LTP have also been observed at various hippocampal synapses. This type of LTP may be mediated by voltage-gated Ca^{2+} channels (Johnston et al., 1992).

Ca^{2+} entry through the NMDA receptor is essential for LTP. Ca^{2+} chelators that block the rise in postsynaptic Ca^{2+} also block the induction of LTP. Furthermore, increasing the amount of postsynaptic Ca^{2+} by photolysis of caged Ca^{2+} can mimic LTP (Lynch, 1983; Malenka et al., 1988). α-calcium-calmodulin-dependent protein kinase II (CaMKII) is believed to mediate the downstream signaling effects of Ca^{2+}. Inhibiting or deleting CaMKII interferes with the ability to generate LTP. One underlying mechanism of LTP is proposed to be the phosphorylation of AMPA receptor subunit GluR1 by CaMKII as deletion of the GluR1 subunit prevents induction of LTP in CA1. Phosphorylation of AMPA receptors subsequently leads an increase in the single-channel conductance of homomeric GluR1 AMPA receptors, leading to the expression of LTP (Benke et al., 1998; Malenka and Bear, 2004; Soderling and Derkach, 2000). Increasing the number of AMPA receptors in the postsynaptic membrane through activity dependent changes in AMPA receptor trafficking also leads to the expression of LTP (Bredt and Nicoll, 2003; Derkach et al., 2007; Malinow and Malenka, 2002; Song and Huganir, 2002).

An increase in the EPSP is referred to as LTP if the potentiated response is maintained for greater than 30-60 minutes without returning to baseline levels. Different types of LTP have been defined according to the temporal persistence of the potentiated EPSP:

LTP1, LTP2 and LTP3 (Abraham and Otani, 1991). LTP1 is rapidly-decaying and independent of protein synthesis, involving post translational modification of synaptic proteins. LTP1 requires activation of the NMDA receptor and ryanodine receptor-mediated Ca^{2+} release. LTP2 is a more robust form that is dependent on protein synthesis, but does not implicate gene transcription. This type of LTP is also NMDA receptor-dependent and is uniquely sensitive to blockade of the $Ins(1,4,5)P_3$ receptor. LTP3 is long-lasting and depends upon changes in transcription and translation. Characteristically, LTP3 is distinguished by a voltage-gated Ca^{2+} channel-sensitive component, and is completely independent of store-mediated Ca^{2+} release. Therefore, temporal persistence of LTP is associated with different cellular sources of Ca^{2+} (Raymond, 2007).The average decay time constant of LTP 1, 2 and 3 is 2.5 hours, 3.5 days, and 20.3 days, respectively (Abraham, 2003).

Although the apical dendrites of CA1 have been the conventional site to assess LTP in the hippocampus, Schaeffer-collaterals also project from CA3 to CA1 via basal dendritic synapses. Compared to apical dendritic synapses, basal dendritic synapses are more susceptible to LTP induced by theta burst stimulation, and show a greater magnitude of potentiation following tetanus delivery (Capocchi et al., 1992; Leung and Shen, 1995). In contrast, HFS is more successful than theta burst stimulation when attempting to elicit LTP at the apical dendritic synapses (Leung and Shen, 1995). These findings suggest that different synapses on CA1 pyramidal cells may have different roles in encoding information: basal dendrites may be activated by theta-frequency inputs, whereas apical dendrites may be activated by long, high-frequency inputs.

1.4.3 Long-term depression (LTD)

In contrast to LTP, LTD is a persistent decrease in excitatory synaptic signaling, following some sort of intervention. LTD is most commonly induced by a low-frequency stimulation (LFS) protocol. LFS involves delivering many pulses (usually 900 pulses) at a low-frequency (0.5-3Hz). LTD can be observed at various hippocampal synapses; it was first discovered in the dentate gyrus *in vivo* and has only recently been demonstrated in CA1, through the Schaeffer collateral pathway. Two types of LTD have been observed: heterosynaptic and homosynaptic. Heterosynaptic LTD is when the strength of inactive synapses is depressed; whereas homosynaptic LTD is the depression in strength of active synapses. Homosynaptic LTD is typically of interest because it is input-specific and correlates to behavioural features of learning. Although LTD is proposed to play a significant role in learning and memory, the evidence for LTD is controversial due to difficulties in reproducing the phenomenon (reviewed by Bear and Abraham, 1996).

LTD induced by LFS is usually NMDA receptor-dependent as NMDA receptor antagonists can reversibly block LTD (Dudek and Bear, 1992; Mulkey and Malenka, 1992). The magnitude of induced LTD is age-dependent. Two-week-old rats show a decrease in EPSP that is double of what is observed in five-week-old rats, following the same tetanus protocol (Dudek and Bear, 1992). LTD is saturable and can be reversed by applying an LTP induction protocol. Similarly, LTP can be reversed by applying an LTD induction protocol (Mulkey and Malenka, 1992). This possible bidirectional change in synaptic strength with limits in the magnitude of induced LTP and LTD agrees with the model of synaptic plasticity proposed by BCM theory.

The reversal of LTP is referred to as depotentiation and there has been debate regarding whether LTD and depotentiation are actually the same phenomenon. Depotentiation is different from LTD in that it is a decrease in synaptic strength from a previously potentiated state. However, LTD and depotentiation are induced in similar ways and share many similar biochemical properties, leading researchers to believe they may be the same phenomenon. Both LTD and depotentiation are NMDA receptor-dependent, pathway specific (homosynaptic), and sensitive to phosphatase inhibitors. However, evidence that metabotropic glutamate receptor (mGluR) antagonists can inhibit depotentiation (Wexler and Stanton, 1993; Bashir et al., 1993; Bashir and Collingridge, 1994) has not been reported in LFS-induced LTD studies. Many reports of successful LTD induction involved using hippocampal slices from young rats (< 30 days old), whereas LTD is more difficult to achieve with mature rats (Mulkey and Malenka, 1992; Wagner and Alger, 1995). Therefore, LTD exhibits age dependence, whereas depotentiation can be observed in all preparations regardless of age. Activation of GABA receptors may play a role in distinguishing LTD from depotentiation. NMDA receptor-mediated postsynaptic responses are often truncated by $GABA_A$ inhibitory post synaptic potentials (IPSPs). $GABA_A$ IPSPs are reduced during LFS due to autoinhibition by presynaptic $GABA_B$ receptors. Because LTD and depotentiation are both NMDA receptor-dependent, GABA receptors may mediate LTD and depotentiation by acting on the NMDA receptor. $GABA_B$ receptor antagonism increases the $GABA_A$ IPSP; thus preventing LTD by LFS in young slices (Wagner and Alger, 1995).However, the induction of depotentiation was not significantly affected by $GABA_B$ antagonism. Therefore, priming stimulation achieved through an LTP protocol may have altered the

role of $GABA_B$ receptors in depotentiation. Furthermore, in mature slices where LTD was difficult to achieve, $GABA_A$ antagonists facilitated the induction of LTD, whereas in young slices, bicuculline did not affect LTD (Wagner and Alger, 1995). Therefore, GABAergic neurons may behave differently at different developmental stages. It is proposed that in young animals, $GABA_A$ inhibition is relatively weak; thus allowing autoinhibition by $GABA_B$ during LFS to be sufficient in inducing LTD. However, in mature animals, $GABA_A$ inhibition of the NMDA receptor is stronger; thus making it more difficult to achieve NMDA receptor activation through $GABA_B$autoinhibition. LTD is dependent on NMDA receptor activation; therefore LTD is less frequently observed in mature animals. However, depotentiation is still observed in mature animals because priming stimulation used to induce LTP relieves GABAergic inhibition, making it more likely for sufficient NMDA receptor activation to be achieved (Wagner and Alger, 1996).

1.5 Extracellular Field Potentials

Synaptic plasticity can be assessed in a variety of ways. In vivo and hippocampal slice preparations are common and both have their own advantages and disadvantages. Although the hippocampal slice retains intrinsic connections, basal brain projections are severed; thus neuromodulatory effects from projecting afferents are not considered. In vivo preparations offer an advantage where the whole brain is kept intact and only local damage to tissue by electrodes has to be taken into account (Holscher, 1999). Electrodes inserted into the extracellular space can measure field potentials. Field potentials are not localized to a small space, but are distributed across a conductive medium known as a volume conductor. Thus, they act as indirect measures of electrical activity produced by a

single neuron or a group of neurons. The extracellular space is a conductive medium allowing ion flow, and as such can act as a volume conductor.

The hippocampus is an ideal structure for examining extracellular current flow due to its laminar organization. Pyramidal cells are lined up in palisades (parallel) and synchronous activation during an evoked potential or spontaneous EEG will summate field potentials from individual neurons to generate a large signal. Field potentials generated by EPSPs at a population of dendrites can be referred to as the population EPSP (pEPSP), and if stimulation intensity is sufficiently strong, synchronous action potentials may be generated resulting in a population spike.

Basal and apical dendrites project into different strata of the hippocampal layer; therefore current flow can be localized into different compartments depending on the synapses activated. Current flows in a closed-loop along an axon, generating areas of transient negativity and positivity; thus creating dipole fields. Opening of AMPA ionchannels allows for net positive charge to flow into the cell. This leads to an intracellular increase in positive charge and membrane potential, while the extracellular space is relatively negative. Thus a current sink is the local volume where current (positive charge) flows from the extracellular to intracellular medium. Because current flows in a closed loop to maintain electrical neutrality within intracellular and extracellular medium, and currents flow from positive to negative potential, a current source is the local volume where current flows from the intracellular to extracellular medium(Leung, 2010). In summary, a current sink represents current flowing into the cell, whereas a current source represents current flowing out of the cell. Therefore, a current sink corresponds to relative

membrane depolarization while a current source corresponds to relative membrane hyperpolarization or less depolarization.

Excitation of distal apical dendritic synapses generates a distal dipole field **(Fig. 2A)**: a current sink is formed at the distal dendrites and a current source is formed at the proximal apical dendrites (Leung et al., 1995). Excitation of proximal apical dendritic synapses generates a proximal dipole field **(Fig. 2B)**: a current sink is formed at the proximal dendrites and a current source is formed at the basal dendrites. Excitation of basal dendritic synapses generates a basal dipole field **(Fig. 2C)**: a current sink is formed at the basal dendrites and a current source is formed at the soma (Kloosterman et al., 2001). These distinct profiles obtained from stimulation at different sites allows for studying properties of different hippocampal pathways.

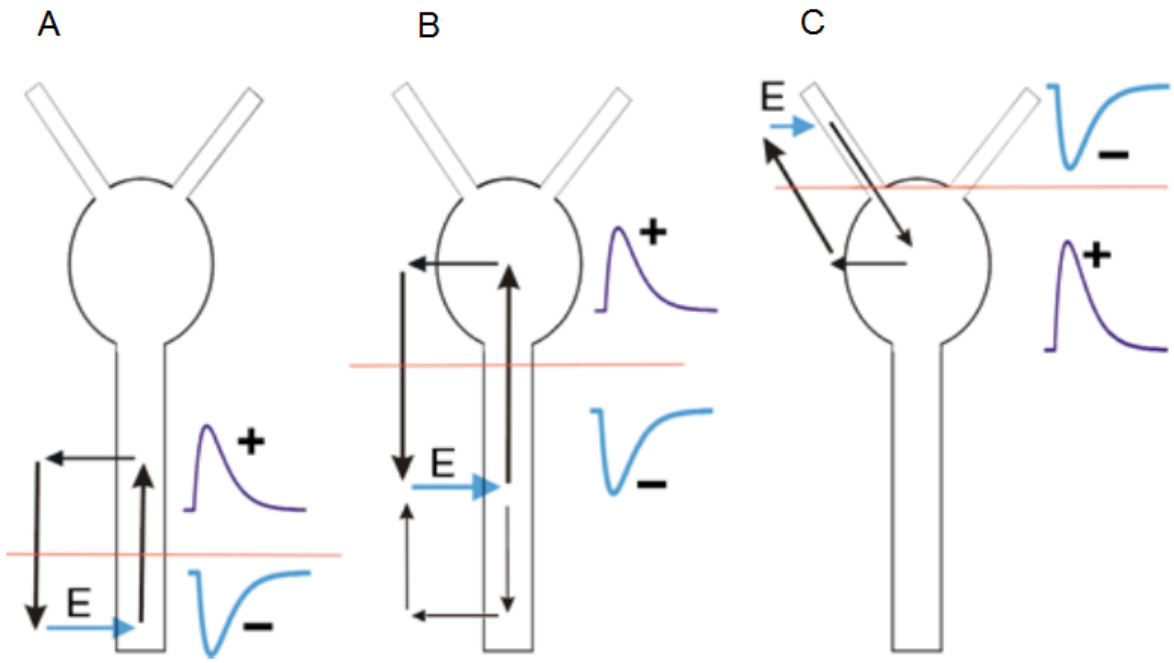

Figure 2. Evoked field potentials at different dendritic synapses of the CA1 pyramidal cell. "E" indicates where the excitation is occurring. Current flows in a closed loop creating areas of transient positivity and negativity. **(A)** Excitation of the distal apical dendrites generates a current sink at the distal dendrites and a current source at the proximal apical dendrites. **(B)** Excitation of the proximal apical dendrites generates a current sink at the proximal dendrites and a current source at the basal dendrites. **(C)** Excitation of the basal dendrites generates a current sink at the basal dendrites and a current source at the cell body (originally illustrated by Leung, 2010).

1.6 Hippocampal theta rhythm

Physiological regulators of synaptic plasticity remain unknown, but hippocampal theta rhythm is a proposed candidate. The hippocampal theta rhythm represents a rhythmic oscillation in membrane potential ranging from 3-10 Hz. The significance of theta rhythm originates from its association with active behaviors in rodents such as walking, rearing, and spatial exploration (Leung, 1998; Vanderwolf, 1969). During awake-immobility and slow-wave sleep, irregular slow activity (ISA) with delta and slow oscillations predominate the EEG (Leung et al., 1982; Wolansky et al., 2006). Theta rhythm can be broadly classified into two categories: Type I (atropine-resistant) and Type II (atropine-sensitive). Type I or movement theta occurs during certain kinds of movements (e.g., walking, head movements, jumping, swimming, and other voluntary movements). It also occurs during phasic periods of REM sleep and is distinguished by its ability to be unaffected by large doses of atropine. Type II or immobility theta occurs during certain motionless behaviours, where the animal's attention is engaged, and is abolished by large doses of atropine. Atropine-sensitive theta rhythm is also present during urethane-anaesthesia and can either be spontaneous or induced using a strong sensory stimuli. Atropine-sensitive theta typically has a lower frequency than atropine-resistant theta.

1.6.1 Significance of theta rhythm

Association between theta rhythm and active behaviors suggests that theta rhythm may facilitate information processing, and subsequently, memory formation. Lesions that attenuate theta rhythm impair performance of tasks requiring reversal of prior learning in rodents (Numan, 1978; M'Harzi et al., 1983; Whishaw and Tomie, 1997). Place cell

firing shows phase precession in relation to the theta rhythm, suggesting that different phases of theta rhythm may be implicated in encoding information (O'Keefe and Recce, 1993). Activity during the peak of hippocampal fissure theta is proposed to favour retrieval of information, whereas activity during the trough favours encoding of information. During the retrieval phase, LTP of CA3 synapses is reduced to prevent encoding of retrieval activity, and LTD during this phase allows for reversal of previously learned associations. LTP is enhanced during the encoding phase to form associations between sensory events (Hasselmo et al., 2002). Therefore, LTP may be favoured during the trough, while LTD is favoured during the peak.

1.6.2 Generation of theta rhythm

The medial septum and vertical band of the diagonal band of Broca serve as rhythm generators of theta-frequency oscillations in the hippocampus (Petsche et al., 1962; Stewart and Fox, 1990). Lesioning or inactivating the medial septum-diagonal band of Broca abolishes theta rhythm in all cortical targets. The nucleus pontisoralis (PnO) is directly involved in generation of theta rhythm. Stimulation of the PnO elicits theta rhythm in CA1 and brainstem injections of carbachol in the PnO produces theta almost instantaneously in the hippocampal formation, suggesting that a cholinergic input modulates the putative brainstem source for generation of theta rhythm (Petsche et al., 1965; Vertes et al., 1993). The medial septum is reciprocally connected to the supramammillary nucleus (SUM) (Borhegyi and Freund, 1998; Leranth et al., 1999); thus the supramammillary nucleus (SUM) may act as a relay center for PnO projections to the medial septum and CA1. Discharge of SUM cells in the urethane-anaesthetized rat is

rhythmic and in phase with hippocampal theta rhythm (Kirk and McNaughton, 1991; Kocsis and Vertes, 1992). Injection of procaine into the SUM attenuated the frequency and amplitude of theta, whereas procaine injections into the medial septum only attenuated amplitude (Kirk et al., 1992; Kirk and McNaughton, 1993). These results suggest that theta frequency may not be controlled by the medial septum, but rather the SUM. However, lesioning the SUM failed to produce any significant changes to theta in behaving animals, suggesting that multiple brainstem sites may be involved with the generation of theta rhythm (Thinschmidt et al., 1995). The main current generators of extracellular theta rhythm are the coherent membrane potential oscillations from pyramidal cells and granule cells.

Cholinergic inputs play an important role in generating theta rhythm. The medial septum sends cholinergic projections to principal cells and interneurons of the hippocampus (Léránthand Frotscher, 1987). Theta in anaesthetized animals consists of only an atropine-sensitive component, whereas theta in behaving animals consists of both atropine-sensitive and atropine-resistant components. The atropine-sensitive component is likely mediated by cholinergic input from the medial septum, while the atropine-resistant component may be mediated by serotonergic afferents from the raphe (Vanderwolf and Baker, 1986). Theta in the urethane-anaesthetized rat is predominantly caused by a rhythmic IPSP input on CA1 pyramidal cells (Leung and Yim, 1985).

Due to different driving components, atropine-resistant and atropine-sensitive theta show different properties in their phase profiles **(Fig. 3)**. Under anaesthesia, theta rhythm shows amplitude peaks at the level of stratum oriens and stratum radiatum, with an abrupt phase reversal (180°) at the pyramidal cell layer (Winson, 1976). Theta in the behaving

rat shows gradual phase reversal (180°) across the stratum radiatum (Winson, 1974). The gradual phase shift observed in atropine-resistant theta is believed to result from an additional excitatory input from the entorhinal cortex at the distal apical dendrites (Leung, 1984). Shifting of the extracellular theta rhythm poses a challenge for any experiment studying theta rhythm. Thus, the reference theta rhythm is usually taken at the level of the hippocampal fissure or alveus, where phase shift is least likely to occur. Theta rhythm is largest in amplitude and most regular in frequency at the level of the stratum lacunosummoleculare in hippocampal CA1 (Bullock et al., 1990).

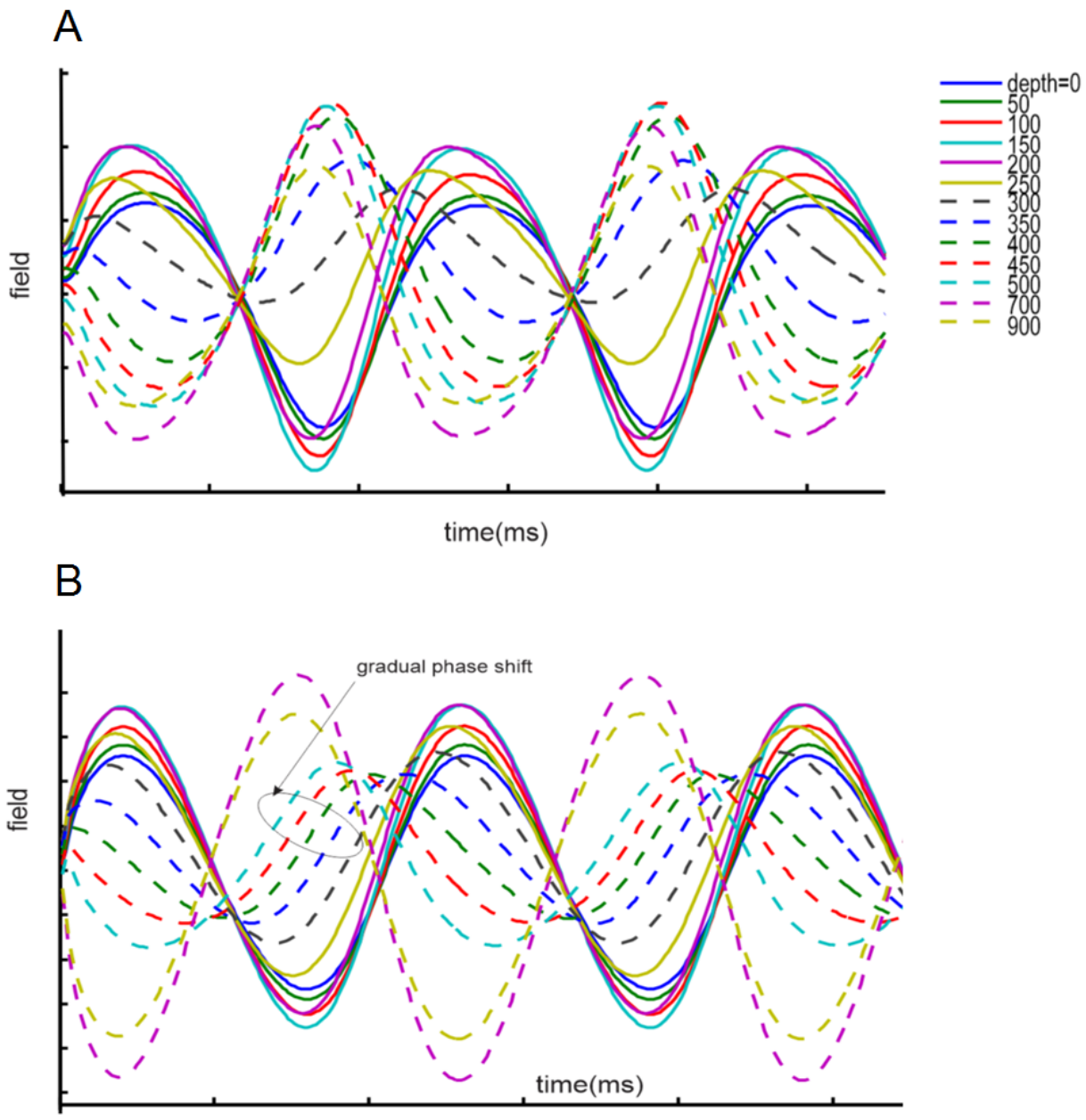

Figure 3. A model of theta rhythm generation after (Leung, 1984) predicts extracellular theta rhythm profile across different depths of pyramidal cell layer in **(A)** urethane-anaesthetized rats and **(B)**behaving rats. Behaving rats show a gradual phase shift in stratum radiatum layer (250-600 µm), whereas urethane-anaesthetized rats show an abrupt phase shift. The stratum radiatum layer is where proximal apical dendrites synapse onto CA1 pyramidal cells and is the most common site for examining synaptic plasticity. In the stratum oriens layer (50-200 µm), where basal dendrites synapse, the phase of extracellular theta rhythm is relatively constant and not predicted to shift.

1.7 Theta rhythm and synaptic plasticity

Numerous studies have tried to examine whether membrane potential fluctuations during theta rhythm may be a physiological modulator of synaptic plasticity. Theta phase modulation of synaptic plasticity was first demonstrated in the medial perforant path (EC to DG) in urethane-anaesthetized rats. Stimulation at the peak of extracellularly-recorded theta rhythm at the stratum radiatum resulted in small, but significant LTP, while stimulation at the trough resulted in no LTP or LTD (Pavlides et al., 1988). Similar results were found for the Schaeffer-collateral pathway (CA3 to CA1). In carbachol induced theta oscillations in vitro, bursts delivered to the peak and trough resulted in LTP and depotentiation, respectively. In behaving rats, three bursts (5 pulses at 400 Hz) delivered to the peak resulted in LTP, while three bursts delivered to the trough resulted in LTD (Hyman et al., 2003). In urethane-anaesthetized rats, burst stimulation to the peak resulted in LTP, while stimulation to the trough resulted in depotentiation, but not LTD (Holscher et al., 1997). Therefore, a controversy exists as to whether LTD or depotentiation results from trough stimulation. Depotentiation differs from genuine LTD in that depotentiation is a decrease from a previously potentiated state, whereas LTD is a decrease from the baseline response. Ultimately, this controversy indicates that fundamental mechanisms responsible for theta phase-dependent synaptic plasticity still remain elusive.

1.8 Rationale and objectives

Conventional techniques to induce LTP and LTD have been questioned mainly due to their physiological relevance and ability to be reproduced consistently (Bear & Abraham, 1996; Hölscher, 1999). The search for physiological means of memory modulation has led scientists to examine synaptic plasticity in relation to hippocampal theta rhythm.

Fluctuations in membrane depolarization during different phases of theta rhythm may provide the appropriate dynamics for inducing LTP and LTD. Although two studies have reported theta phase-dependent synaptic plasticity in the Schaeffer-collateral pathway *in vivo* (Holscher et al., 1997; Hyman et al., 2003), their focus was on plasticity at the proximal apical dendritic synapses. Schaeffer-collaterals are also known to project to basal dendritic synapses on CA1 pyramidal cells. LTP at the basal dendrites has different properties than apical dendritic LTP. These different properties between basal and apical LTP provide heterogeneity in LTP threshold and optimal conditions for LTP during the appropriate behaviours. Leung and Shen (1995)proposed that basal LTP is optimal during theta behaviours (e.g., REM sleep, voluntary movement), whereas apical LTP is optimal during non-theta behaviours (e.g., immobility, slow-wave sleep). Furthermore, Holscher et al. (1997) studied urethane-anaesthetized rats, whereas Hyman et al. (2003) studied behaving rats. Theta rhythm in behaving and urethane-anaesthetized rats is known to differ in frequency and method of generation. All previous studies examining synaptic plasticity in relation to theta rhythm used a qualitative assessment of the phase of theta rhythm where stimulation was delivered. This qualitative assessment may be inconsistent and does not allow for further discrimination of different phases during the theta rhythm. Therefore, a quantitative assessment of theta phase and synaptic plasticity is required.

1.8.1 Aim 1: Synaptic plasticity at basal and apical dendrites is modulated by a single burst delivered to different phases of the theta rhythm

Holscher et al. (1997) found that a single burst of five pulses delivered to the apical dendritic synapses during the peak of theta rhythm was able to induce stable LTP. However, they did not examine the effects of delivering a single burst during other

phases of theta rhythm. It is unlikely that stimulation has to occur strictly at the peak to induce LTP. Stimulation during positive phases of theta rhythm may also have the ability to induce LTP and the optimal phase of theta rhythm for inducing LTP still remains unknown. Therefore, we sought to investigate how a single burst of five pulses delivered to the apical dendritic synapses during different phases of theta rhythm can affect synaptic plasticity. No study to date has examined the same objective at the basal dendritic synapses. Therefore, we also examined how the basal dendritic synapses were affected by a single burst of electrical pulses during different phases of hippocampal theta rhythm.

1.8.2 Aim 2: Multiple bursts delivered to basal dendrites during different phases of theta rhythm results in a continuum of synaptic modification

Previous studies attempted theta phase stimulation by delivering bursts of electrical pulses at either the peak or trough of hippocampal theta rhythm. Although these bursts consistently land on the same phase, the effect of delivering multiple bursts to different phases of theta rhythm has not been examined. During urethane anaesthesia, the maximum firing probability for CA3 pyramidal cells is widely distributed across all phases of the theta rhythm (Fox et al., 1986). Furthermore, controversy exists as to whether LTD or depotentiation occurs when stimulating bursts land at the trough (Holscher et al., 1997; Hyman et al., 2003). Stimulation at the trough may ultimately serve to offset potentiation induced by peak stimulation; thereby providing a bidirectional modulatory component of theta rhythm dependent plasticity. To best examine this modulatory effect, stimulating bursts should be delivered to different phases of theta rhythm. Therefore, one objective was to test how electrical bursts given during different

phases of theta rhythm will affect synaptic plasticity at the basal dendritic synapses. We hypothesize that inducing bursts interact with each other to create a continuum of synaptic modification: greater net activity in the positive phase will favour LTP, whereas greater net activity in the negative phase will favour LTD.

1.8.3 Aim 3: Evoked spike excitability is modulated by different phases of the theta rhythm

The exact cellular mechanisms leading to LTP and LTD still remain unknown. However, induction of LTP and LTD is believed to depend upon varying levels of intracellular depolarization. High levels of depolarization during stimulation favours LTP, whereas lower, yet still elevated, levels of depolarization favour LTD (Cummings et al., 1996). Therefore, preferential induction of LTP and LTD during different phases of theta rhythm is believed to depend upon the fluctuation levels of membrane potential that occur during theta rhythm. A population spike is an increasing function of the number of discharging cells and can thus be used as a measure to the extent to which an afferent volley discharges a cell population (Andersen, 1971). Thus, a larger population spike corresponds to when a greater number of cells have reached the threshold for action potential firing.Rudell and Fox (1984) found that population spike excitability in CA1 is modulated by different phases of theta rhythm; however they evoked population spikes from stimulating the ventral hippocampal commissure and their theta reference was in the dentate moleculare layer. CA1 pyramidal cell firing has a maximal probability around the positive peak of dentate theta during urethane anaesthesia (Fox et al., 1986). The largest CA1 evoked potentials from CA3 apical stimulation occur 18° after the positive peak of the dentate fissure theta (Wyble et al., 2000). Therefore, the positive phase of dentate theta may correspond to when CA1 pyramidal cell excitability is at its maximum. To

determine how the fluctuating levels of membrane depolarization contribute to synaptic excitability, we evoked population spikes by single-pulse stimulation of basal and apical dendritic synapses during different phases of theta rhythm. Examining the magnitude of these evoked population spikes should allow us to determine which phases of the extracellularly-recorded theta rhythm correspond to different levels of membrane depolarization. Because previous studies have found that LTP preferentially occurs at the peak of extracellularly-recorded theta rhythm at the level of stratum radiatum (Holscher et al., 1997; Hyman et al., 2003), this phase may represent the time at which membrane depolarization is at its greatest. Therefore, we hypothesize that evoked population spikes at the basal and apical dendritic synapses will have maximal amplitude when delivered to the peak, and minimal amplitude when delivered to the trough. Furthermore, bursts of stimulating pulses may result in a significant phase difference between the initial and final pulse. Thus, determining the exact phase where stimulation occurs becomes a difficult task. Using a single stimulating pulse will allow for more accurate determination of theta phase contributions to synaptic excitability.

1.8.4 Aim 4: Evoked spike excitability is modulated by the presence of theta rhythm

Leung and Peloquin (2008) demonstrated that synaptic excitability at the basal and apical dendrites is modulated differently by the presence of theta rhythm. This observation may be due to differences in excitability at the dendritic synapses during theta versus non-theta activity. Theta rhythm suppresses the EPSP slope from stimulation at the apical dendrites, and slope values were consistently larger during periods of slow-oscillation compared with periods of theta (Wyble et al., 2000; Schall et al., 2008). However, excitability as a measure of population spike amplitude was not determined. In addition,

the effect of theta rhythm on excitability from basal dendritic stimulation has not been examined. Therefore, our objective was to compare how excitability at the basal and apical dendrites is affected by the theta rhythm. Lower suppression of excitability by theta rhythm may be more conducive for inducing LTP since it allows a greater likelihood for membrane potential to reach a threshold for NMDA-receptor activation. We hypothesize that CA1 pyramidal cell excitability is affected by the presence of theta rhythm.

2. METHODS

2.1 Animals

Adult male Long-Evans rats, weighing between 200g and 350g, were used (Charles River Laboratories). Rats were housed in standard cages in a temperature-regulated environment in a 12:12h light/dark cycle commencing at 7am, and had ad-lib access to food and water. A maximum of three rats were allowed to inhabit a single cage. Typically, rats were kept in the animal facility for no longer than two weeks since they first arrived. Experiments were conducted during the day (10am -7pm).

2.2 Electrode implantation

2.2.1 Stimulating and recording electrodes

Stimulating electrodes were constructed out of stainless steel wire, 0.005inches in diameter, insulated with Teflon except at the tips. Silicon recording probes were purchased from NeuroNexus, Ann Arbor, MI. The probes had 16 recording sites spaced 50 µm apart on a vertical shank (Model #: A1x16-5mm-100-177-CM16LP).

2.2.2 Surgery

Rats were anaesthetized using 30% urethane anaesthesia (1.5g/kg solution, i.p.) and placed in a stereotaxic surgery apparatus. Atropine methyl nitrate was administered (5 mg/kg i.p.) to reduce airway secretions throughout the experiment. Animal body temperature was maintained between 36.5°C and 37°C via feedback-controlled heating pad connected to a rectal thermometer. The skull surface was exposed and oriented such that lambda and bregma were in a horizontal plane, and burr holes were drilled to prepare for implantation. Stimulating electrodes were lowered into CA3b (P3.2, L3.2) and CA3a (P3.2, L2.2) relative to bregma (Paxinos and Watson, 1986) to stimulate Schaeffer

collaterals projecting from hippocampal area CA3 to CA1. The 16-channel silicon probe was lowered into area CA1 of the hippocampus at P3.8, L2.0 (Paxinos and Watson, 1986) to record evoked field excitatory post-synaptic potentials (fEPSPs). The exact electrode depth varied between animals; therefore depth of electrode placement was determined using electrophysiological criteria (Kloosterman et al., 2001). The recording electrode was lowered to a depth of ~3.0 mm to record both basal and apical evoked responses, while also being able to record EEG at the level of the stratum lacunosummoleculare**(Fig. 4)**. The CA3a electrode was lowered to a depth of ~3.0 mm into the stratum radiatum to activate CA1 apical dendrites and the CA3b electrode was lowered to a depth of ~ 2.5 mm into the stratum oriens to activate CA1 basal dendrites **(Fig. 4)**. The ventral coordinates were calculated relative to skull surface. Two screws were secured in the skull over the cerebellum and frontal cortex to serve as the stimulus anode or recording ground.

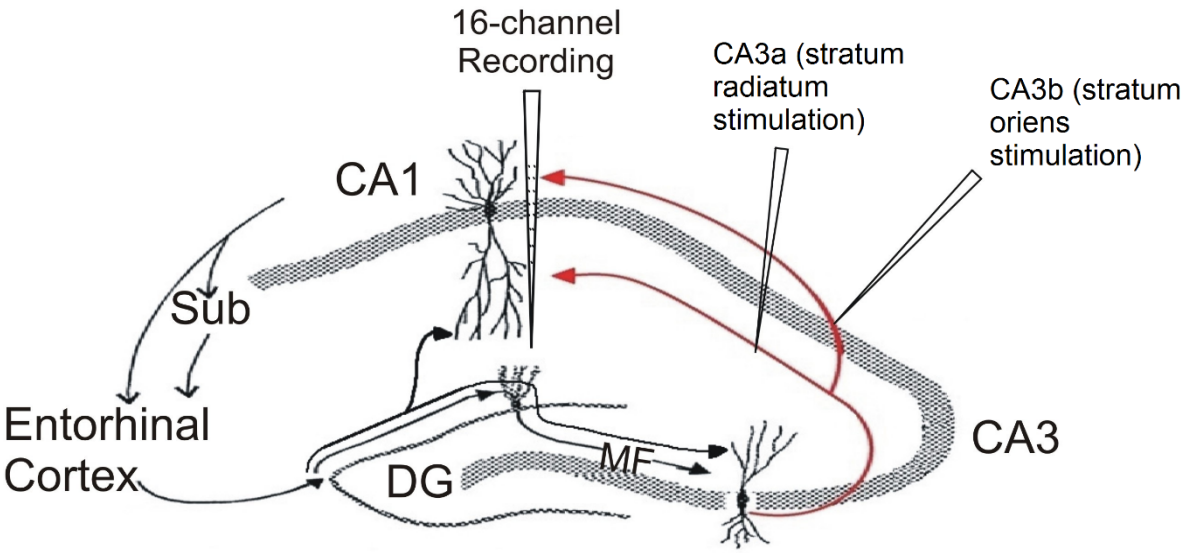

Figure 4. A coronal section of the rat hippocampus illustrating the position of recording and stimulating electrodes. Stimulation of CA3a activated stratum radiatum afferents to CA1 apical dendritic synapses. Stimulation of CA3b activated stratum oriens afferents to CA1 basal dendritic synapses. The 16-channel recording probe was inserted to a depth such that responses from stratum oriens to stratum lacunosummoleculare of CA1 can be recorded.

2.3 Experimental Paradigm

2.3.1 Electrophysiology

Signals from the 16-channel recording probe were amplified 200-1000x by a TDT (Tucker-Davis Tech, TDT) headstage, a 16-channel Medusa preamplifier and fed by optic fibres to TDT digital processors (RA16 Base Station). Signals were digitized at 6.1-24.4 kHz by TDT real-time processors and custom-made software by our lab. Stimulus pulses (0.2 ms duration) were delivered through a photo-isolated stimulation unit (PSIU6, AstroMed/Grass Instrument).

2.3.2 Single burst experiments

The basal and apical dendrites were stimulated at different intensities to construct an input-output curve. Baseline evoked responses were monitored at 1.5-2 x threshold intensity at a sampling rate of 24.4 kHz for 4096 samples. Four sweeps were taken at 0.1 Hz and averaged to generate an averaged evoked potential for a particular time point. Sampling time points occurred at an interval of 2.5 minutes. Synaptic and action currents spread due to volume conduction; therefore a technique known as current-source density (CSD) analysis can be used to remove the effects of volume conduction and identify the macroscopic locations of current sources and sinks (**Fig. 6**). A one-dimensional CSD was calculated from the field potential. CSD(z,t) as a function of depth z and time t was calculated by a second-order differencing formula:

$$CSD(z, t) = \sigma [2 \Phi(z, t) - \Phi(z + \Delta z, t) - \Phi(z - \Delta z, t)] / (\Delta z)^2 \qquad \text{(Equation 1)}$$

Where $\Phi(z, t)$ is the potential at depth z and time t, Δz is the spacing (50 μm) between

adjacent electrodes on the 16-channel probe. The conductivity σ was assumed to be constant and the CSDs were reported in units of V/mm^2.

CSD analysis in this study used an effective step size of 100 µm, i.e. n=2 in equation 1, which was equivalent to CSD obtained by n=1 formula followed by 1-2-1 spatial smoothing (Freeman and Nicholson, 1975; Leung, 2010). The maximal slope (of 1 ms duration) during the rise of the maximum excitatory sink was used to assess the magnitude of the evoked potential **(Fig. 5B)**. Slope measurements of the excitatory sink were chosen instead of amplitude because the former correlate directly with strength of synaptic transmission and are less susceptible to spurious field artifacts (Johnston and Wu, 1995) that may include the slower inhibitory synaptic potentials, or polysynaptic postsynaptic potentials. After a stable baseline was obtained for 30 minutes (coefficient of variation (SEM/mean) of the sink slopes <0.05), induction of synaptic plasticity at a particular phase of theta was attempted.CSD analysis using 100 µm step size was used to determine the location of current sources and sinks. The maximal slope (of 1 ms duration) during the rise of the maximum excitatory sink was used for LTP assessment **(Fig. 5B)**. After a stable baseline was obtained for 30 minutes (coefficient of variation (SEM/mean) of the sink slopes <0.05), induction of synaptic at a particular phase of theta was attempted. A single burst consisting of 5 electrical pulses with an interpulse frequency of 200 Hz at 3-3.5 x the threshold intensity was delivered to the basal or apical dendrites during different phases of hippocampal theta rhythm. Previous studies used a stimulation intensity that elicited 90% of the maximum EPSP (Hyman et al., 2003; Holscher et al., 1997), which can range from 4-6 x the threshold intensity in our preparations. However, stimulating at 90% maximum EPSP has a high likelihood of

inducing seizure activity, represented by synchronous afterdischarges at the level of the cell body following tetanus delivery. Therefore, the stimulation intensity used in our experiments was lower compared to other in vivo experiments. Post-tetanic responses were recordedfor 120 minutes at the initial intensity used for monitoring baseline and normalized by the baseline average.

2.3.3 Multiple bursts during theta activity

The recording procedures followed those used for single burst stimulation, except only the basal dendrites were stimulated. The basal dendrites were stimulated at different intensities to construct an input-output curve. Baseline evoked responses were monitored at 1.5-2 x threshold intensity at a sampling rate of 24.4 kHz for 4096 samples. Four sweeps were taken at 0.1 Hz and averaged to generate an averaged evoked potential for a particular time point. Sampling time points occurred at an interval of 5 minutes. Bursts consisting of 4-6 electrical pulses with an interpulse frequency of 200 Hz at 2.5-3 x the threshold intensity were delivered to the basal dendrites during different phases of hippocampal theta rhythm. Electrical bursts for all experiments were delivered within a 4 minute time period, and consecutive bursts had a minimum interburst interval of 4 seconds to avoid seizure induction. Post-tetanic responses were recorded for 90 minutes at the initial intensity used for monitoring baseline and normalized by the baseline average. EEG was recorded before and after burst delivery.

Theta rhythm was either spontaneously present or induced by pinching the base of the rat's tail. Theta phase stimulation was achieved using custom-programmed RPvdsEX software (Tucker-Davis Tech, TDT). An extracellular signal was extracted from one of

the 16 channels and digitally filtered, without phase distortion, between 3 to 8 Hz. Delivery of the bursts depended on detection of frequency peaks at 3-5 Hz, and the time of the bursts depended on an amplitude threshold. By adjusting the amplitude threshold and delay, stimulation at a particular phase could theoretically be achieved. However, detection was not perfect, and bursts may be delivered to different phases of a theta rhythm, or sometimes during non-theta activity when analyzed posthoc. Therefore, the total number of bursts delivered during theta rhythm differed for some experiments because bursts may have occasionally landed during non-theta activity.

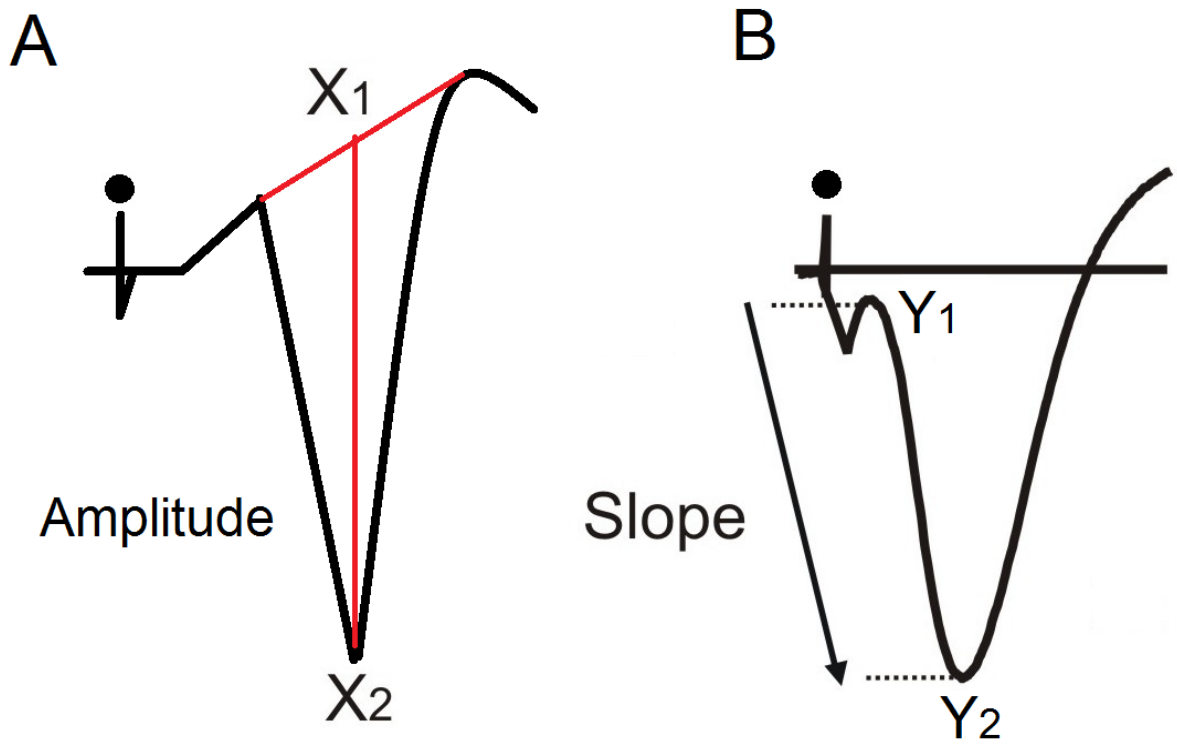

Figure 5. Slope and amplitude measurements taken from CSD analyzed averaged evoked potentials. For experiments involving single high-intensity evoked potentials, the magnitude of the population spike was calculated by taking the amplitude from X1 to X2 **(A)**. For LTP experiments, the slope of the excitatory sink was calculated at 1 ms intervals for the whole duration of the rising phase of the excitatory sink (Y1 to Y2), and the value of the maximal magnitude of the slope was taken as the estimate of the slope **(B)**. The filled circle indicates the shock artifact.

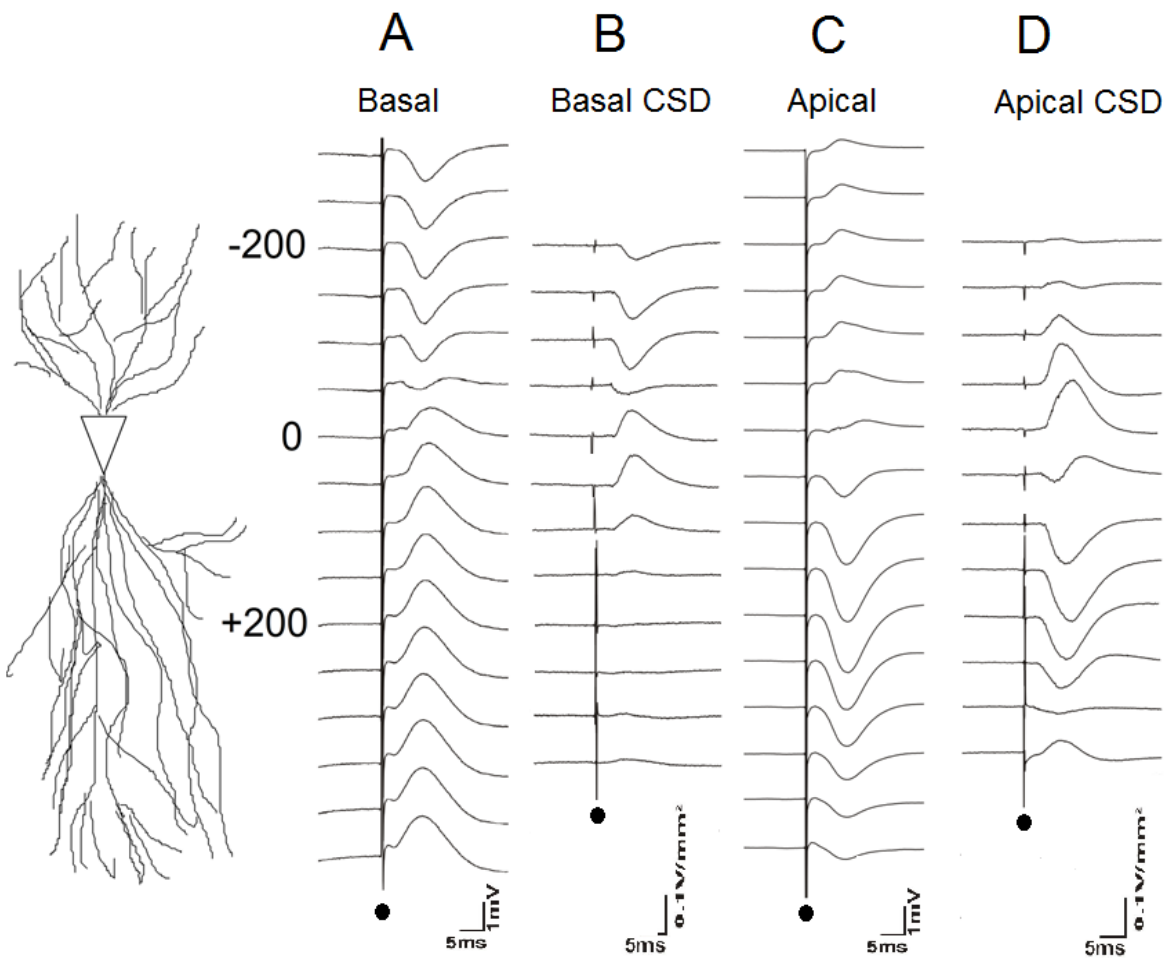

Figure 6. Average evoked potentials (AEPs: **A** and **C**) and current source density (CSD: **B** and **D**) transients in CA1 of a representative rat (CL087) following basal orthodromic (**A** and **B**) or apical orthodromic excitation (**C** and **D**). Potentials were recorded simultaneously by a 16-channel electrode silicon probe with 50 µm interval between electrodes. Depths are indicated by the schematic CA1 pyramidal cell drawn and by the distance (in µm) away from the cell body layer (+ toward the apical dendrites and – toward the basal dendrites). **(A)** AEPs (average of 4 sweeps) following stimulation of the CA3 stratum oriens at 60 µA (1.5 times threshold). **(B)** CSD profiles derived from AEPs shown in **(A)**. Stimulation of the CA3 stratum oriens generated a current sink (negative deflection) in the CA1 basal dendrites. **(C)** Apical dendritic response as a result of CA3 stratum radiatum low intensity stimulation at 45 µA (1.5 times threshold). **(D)** CSD profiles derived from the AEPs shown in **(C)**. Stimulation of the CA3 stratum radiatum generated a current sink in the CA1 apical dendrites. Artifacts are indicated by the solid circle underneath.

2.3.4 Evoked potential during theta and non-theta activity

The basal and apical dendrites were stimulated at different intensities to generate an input-output curve. A single high intensity electrical stimulus was delivered to either the basal or apical dendrites to evoke a population spike with a magnitude of approximately 1.5 x the spiking threshold. Electrical pulses were delivered at a frequency of 0.05 Hz and traces were sampled at 12 kHz for 16384 samples. The stimulus was delayed for 1s following initiation of sampling so that an adequate period of spontaneous EEG activity can be assessed prior to the stimulus. The spontaneous background EEG activity cycled between periods of theta and non-theta activity. EEG activity preceding the stimulus was determined to be theta or non-theta based on power spectral analysis **(Fig. 7)**. If the peak occurred at a frequency between 3-5 Hz, it was considered theta activity. Non-theta slow activity in this study was classified by having peak power occurring at 1-2 Hz, outside of 3-5 Hz. Sum of theta (3-5 Hz) power and sum of low delta (1-2 Hz) power were calculated, and the ratio of integrated theta to integrated delta power, or theta/delta power was also calculated. Population spike amplitude was measured from the current-source density (CSD) analysis at the cell body level by drawing a tangent line between the first and second positive peaks, and the spike amplitude was measured by the height of the vertical line connecting the negative spike peak to the tangent line **(Fig. 5A)**.

2.3.5 Evoked potential during different phases of theta rhythm

Hippocampal EEG was monitored for the onset of spontaneous theta rhythm. When theta rhythm was present, a single high-intensity stimulating pulse was delivered to either the basal or apical dendrites at approximately 1.5 x spiking threshold intensity. Pulses were

delivered at a frequency of 0.05 Hz and delayed for 1s after sampling initiated so that there was sufficient theta EEG preceding the pulse to be analyzed. Population spike amplitude was measured as explained above **(Fig. 5A)**.

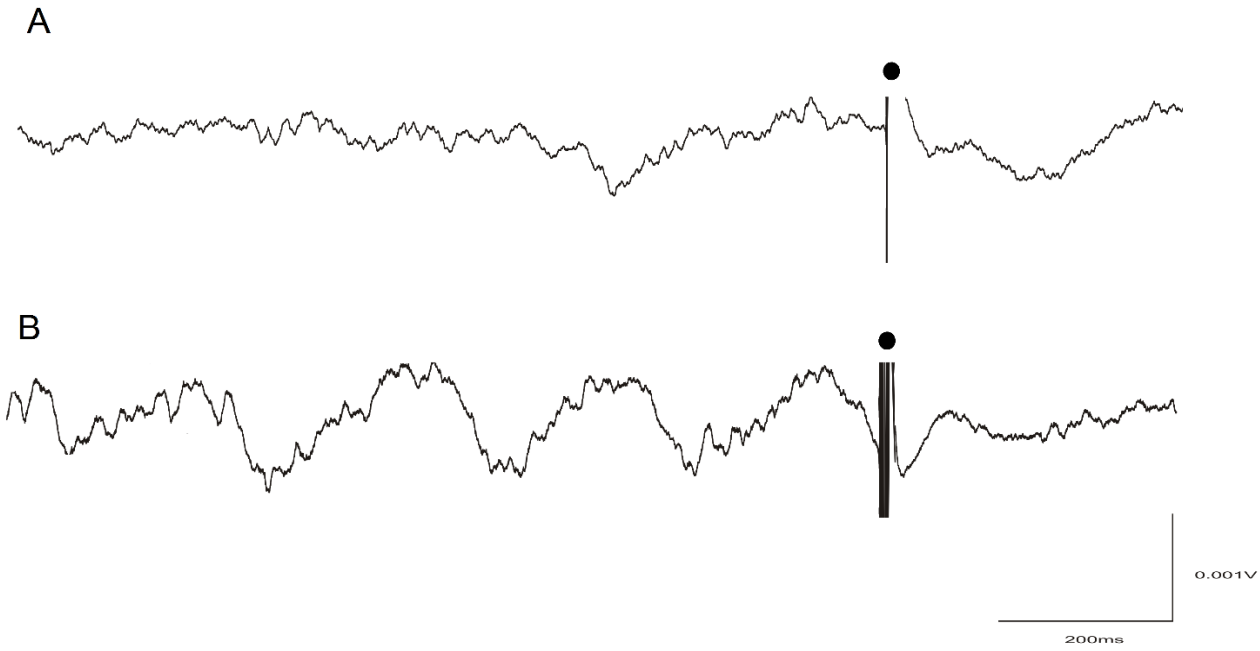

Figure 7. Representative traces of high-intensity stimulation being delivered during background theta and non-theta activity. Single high intensity pulses were delivered during background **(A)** non-theta activity or **(B)** theta activity. Stimulus was delayed for 1s after the start of sampling so that EEG activity preceding the stimulus can be analyzed. Displayed traces were recorded at the level of the stratum lacunosummoleculare, where theta amplitude is greatest. The filled circle indicates the shock artifact.

2.4 Inclusion Criteria

The criteria for inclusion of experiments in the analysis was consistent among all experiments and include pre-tetanus, during tetanus, and post-tetanus standards. Measurements of slope were taken from all levels of the basal and apical sinks. If the baseline of a specific measure was unstable, the baseline recording was run for longer until 30 minutes of stable baseline was achieved. The entire duration of tetanus delivery was monitored closely to make sure there were no epileptiform or spontaneous population spike discharges.

The area underneath apical and basal sinks at all 16-channels was monitored at different time points throughout an experiment to ensure no shifting of the 16-channel probe occurred. If the sink versus depth profile shifted at all, the basal or apical excitatory sink would not be consistent. Therefore, these experiments where channel shifting occurred were not included in the group analysis.

2.5 Confirmation of Electrode Location

2.5.1 Perfusion

After an experiment, the sites of the stimulating electrodes were lesioned by passing a 0.5 mA current for 0.5 s duration, repeated three times. The rat was then intracardially perfused with 50 ml of saline followed by 50 ml of 4% formaldehyde solution. The brain was removed from the cranium and placed in a 4% formaldehyde solution for a minimum of 24 hours prior to sectioning.

2.5.2 Histology and Staining

Brains were frozen on a freezing microtome and sliced into 40 µm thick coronal sections. Brain slices were mounted onto slides and later stained with thionin. The stimulus and recording electrode locations were identified and confirmed using a light microscope (**Fig. 8**).

2.6 Analysis and Statistics

2.6.1 Phase analysis

To determine posthoc whether bursts landed during hippocampal theta rhythm, a custom-made MATLAB program (MathWorks) Fourier-transformed EEG traces at the level of stratum lacunosummoleculare (Ch. 15) to determine the dominant frequency of EEG in the 0.67 second period (4096 points sampled at 6.103 kHz) immediately preceding burst delivery. If the dominant frequency was between 3-6 Hz, the bursts were considered to be delivered during hippocampal theta rhythm. The phase of theta rhythm where stimulation occurred was determined by comparing the time of stimulation onset in relation to the peaks of the digitally filtered signal immediately before the bursts **(Fig. 9)**. Theta rhythm was modeled after a sine wave starting at phase 0°, with positive peak at 90°, and trough (negative peak) at 270°. One cycle of the sine wave is 360° **(Fig. 10)**.

2.6.2 Phase referencing to stratum oriens or alveus

Phase of theta rhythm where stimulation occurred was predicted from local theta at the level of stratum lacunosummoleculare. However, recording probe depth may not have been consistent with every experiment and extracellular theta at the apical dendrites was

subject to phase shifting. Therefore, to obtain a more consistent phase reference between individual experiments, the phase of theta rhythm where stimulation occurred was also determined with reference to the level of stratum oriens or alveus. A spectral analysis was performed for EEG traces sampled at 6.103 kHz for 16384 points. Only traces with peak power at the theta frequency (3-5 Hz) were chosen for analysis. The phase shift that occurred from Channel 4 to Channel 15 of the 16-channel recording probe was calculated for each individual experiment. Channel 15 was typically at the distal apical dendritic level, while Channel 4 was at the basal dendrites or alveus. Phase of stimulation onset was not directly predicted from local theta at stratum oriens/alveus because theta amplitude was lower compared to stratum lacunosummoleculare theta, making peak to peak prediction less accurate.

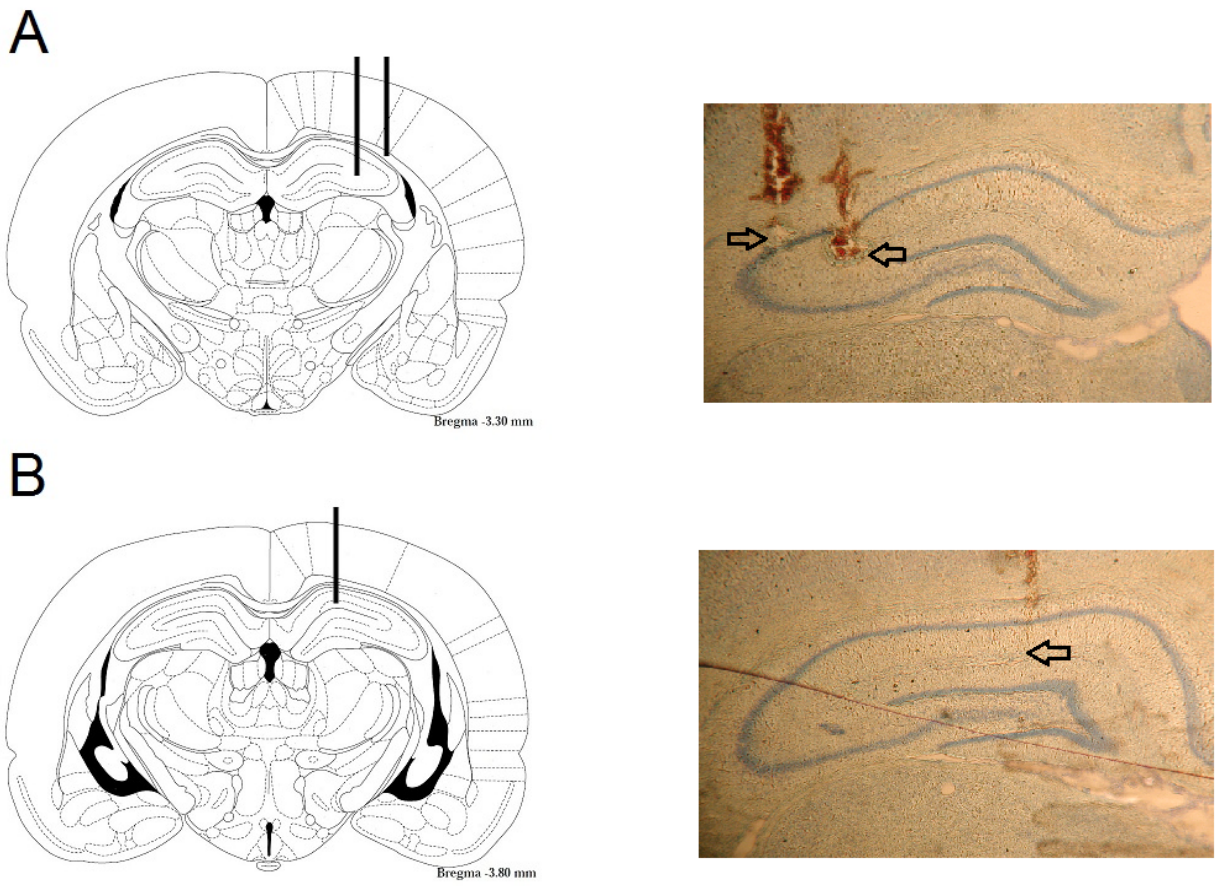

Figure 8. Coronal hippocampal slices indicating electrode location. Locations were based on coordinates taken from Paxinos and Watson (1986). Schematic hippocampal slices on left illustrating stimulating and recoding electrode locations (designated by solid line) and examples of corresponding thionin stained sections on right from one representative animal (CL057). **A:** Placement of the two stimulating electrodes in CA3 with the stratum oriens coordinate at (P3.2, L3.2) and stratum radiatum coordinate at (P3.2, L2.2). Lesions made through the stimulating electrode tips are marked with arrows. The ventral coordinates varied between animals and averaged 2.7 mm below the skull surface for the stratum oriens stimulating electrode and 3 mm for the stratum radiatum stimulating electrode. **B:** Placement of the CA1 recording electrode at coordinate (P3.8, L1.8). The arrow marks the most ventral location of the track made by the recording electrode, at approximately 3 mm below the skull surface.

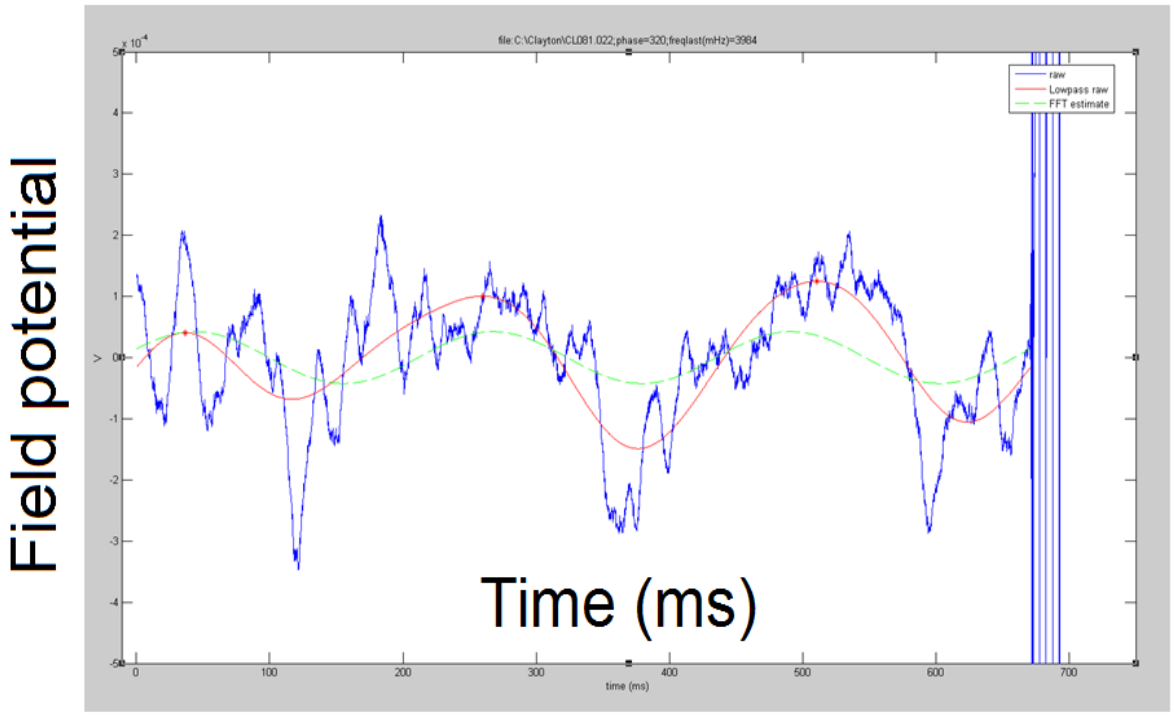

Figure 9. Estimating the phase at which burst stimulation occurred. The phase of theta rhythm at which the first pulse of a burst of stimulation occurred was estimated using a custom-made MATLAB program, as shown for a representative rat (CL081). The raw theta EEG recorded at stratum lacunosummoleculare is shown in blue. Digitally filtered (3-8 Hz) EEG is shown as a red trace, from which frequency was estimated by the inverse of the interval between the last two peaks, and the theta phase was estimated by ((time from last peak to first pulse of the burst)/ (interval between two peaks) * 360° + 90°).

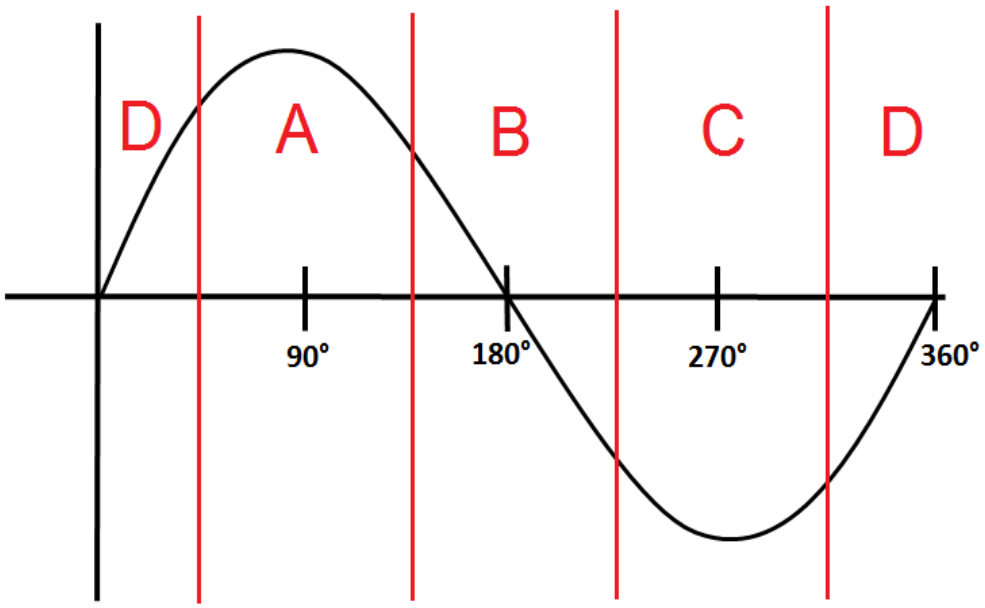

Figure 10. The different phases of a sinusoidal oscillation. Because theta rhythm is an oscillation, it can be represented by a sine wave. One full cycle is 360°. The absolute peak is at 90° and the absolute trough is at 270°. The sine wave can be divided into four main phases for easier conceptualization: **(A)** Peak (45°-135°), **(B)** Falling phase (135°-225°), **(C)** Trough (225°-315°), and **(D)** Rising phase (315°-45°).

2.6.3 Multiple burst analysis

In this experiment, multiple bursts of pulses were delivered during the induction of LTP. Since not all bursts were delivered to at same phase, a method was needed to quantify the combined phase of all bursts. To quantify the combined phase of all bursts, the phase of each burst was sine transformed using the equation: $x = \sin(\theta)$, where θ is defined as the phase of theta rhythm in degrees) where stimulation occurred. The values of this transformation ranged from +1 (alignment with the absolute peak: 90°) to -1 (alignment with the absolute trough: 270°), and were summed to obtain a Combined Phase Index (CPI). CPI values were then divided by the total number of stimulating bursts given for that particular experiment. Therefore, PPI values will have a maximum value of 1 (indicating that all bursts landed during the absolute peak), and a minimum value of -1 (indicating that all bursts landed during the absolute trough).

A separate measure of phase activity called the Positive Phase Index (PPI) was established to account for the scenario where negative phase stimulation does not contribute to synaptic plasticity. PPI only takes into account positive values obtained from sine transformation. The PPI is a sum of all the positive sine-transformed phase values for all the stimulating bursts, divided by the total number of stimulating bursts. Therefore, PPI values will have a maximum value of 1 (indicating that all bursts landed during the absolute peak), and a minimum value of 0 (indicating that no bursts landed during the positive phase).

2.6.4 Statistics

To determine post-hoc whether theta and non-theta traces were significantly different, a Wilcoxon matched-pairs signed rank test was used to compare the ratio of theta power/delta (1-2 Hz) power between two groups. The amplitude of evoked population spikes at the basal and apical dendrites were compared during theta and non-theta activity using a Wilcoxon matched-pairs signed rank test. $p < 0.05$ was considered statistically significant.

For experiments assessing LTP, repeated measures analysis of variance (ANOVA) was used for statistical analysis of the normalized data at different times. If a significant main or interaction effect was found, Newman-Keuls post-hoc test was applied. $p < 0.05$ was considered statistically significant. Correlation between phase and LTP was assessed using linear regression analysis. Data points were phase shifted until an optimal correlation was observed.

To determine the optimal phase of theta rhythm for inducing maximal LTP using a single burst, 4 consecutive data points with respect to phase were grouped together. A running average was taken with respect to phase and LTP. These separate groups were compared using one-way ANOVA to determine whether LTP was significantly different for groups at different phases. $p < 0.05$ was considered statistically significant.

Evoked population spikes were triggered during different phases of theta rhythm at the basal and apical dendrites. Eight phase bins, each with a range of 40°, were defined in order to allow for grouped comparison: 0°-40°, 40°-80°, 80°-120°, 120°-160°, 160°-200°, 200°-240°, 240°-280°,280°-320°, 320°-360°. Amplitude of evoked population spikes

were averaged within each phase bin, then averaged across all eight phase bins to obtain a representative normal excitatory baseline for the entire theta rhythm. Averages for each phase bin were normalized to the baseline to determine which phases showed an increase or decrease in excitability. Two-way ANOVA was used to compare between phase groups and between apical and basal dendrites. $p < 0.05$ was considered statistically significant.

3. RESULTS

3.1 Single bursts delivered to basal and apical dendrites during different phases of theta rhythm

The multiple burst experiments were designed to examine the interaction between stimulating bursts occurring at different phases of hippocampal theta rhythm. However, the optimal phase for inducing LTP could not be identified from these experiments. Therefore, delivering a single burst to different phases of theta rhythm was performed in order to identify the optimal phase of theta rhythm for inducing synaptic changes.

3.1.1 Single burst delivered to apical dendrites

A single burst delivered to the apical dendrites showed phase preference for LTP. The normalized excitatory sink slopes were averaged from 0-120 minutes post-tetanus. These average values were then compared to the phase of theta rhythm where stimulation occurred, constructing a correlation plot between the magnitude of LTP and phase **(Fig. 12A)**. The phase of theta rhythm where stimulation occurred and the magnitude of induced LTP does not appear to be correlated (R^2=0.06; p=0.21). However, linear correlation is biased by the magnitude of LTP at extreme ends of the phase plot, and maximal correlation could occur if the peak LTP occurred at phase 0°, which is defined as the onset phase of a sine-wave cycle. This assumption, however, is incorrect because phase preference for LTP or LTD is unknown a priori. Therefore, the data set was phase shifted across a full theta cycle (360°) in order to determine where the optimal correlation would occur. A phase shift of 18°-26° resulted in the optimal linear correlation **(Fig. 12B)**. From the phase shifted correlation plot, the phase of theta rhythm where

stimulation occurred and the magnitude of induced LTP is significantly correlated (R^2=0.33; p<0.01). Fluctuations in the evoked potential may occur post-tetanus; therefore, it was important to assess correlation at shorter time intervals. The averaged response from 0-30 minutes post-tetanus was not significantly correlated to phase (R^2=0.09; p=0.13, **Fig. 13A**). However, the averaged response from 30-60 min (R^2=0.38; p<0.01, **Fig. 13B**), 60-90 min (R^2=0.24; p<0.05, **Fig. 13C**), and 90-120 min (R^2=0.34; p<0.01, **Fig. 13D**) post-tetanus was significantly correlated to phase.

The magnitude of induced LTP and phase of theta rhythm where stimulation occurred showed a significant linear correlation **(Fig. 12B)**; however a linear correlation may not be the optimal method to define the relationship between these two variables. Because the fluctuation of membrane potential resembles a sinusoidal wave, using a sine correlation may better model the data points **(Supplementary Fig. 1)**. The sine wave correlation yielded a greater correlation coefficient (R^2=0.75) compared to linear correlation methods (R^2=0.33). However, the linear correlation was performed using raw data, whereas the sine wave was modeled after the running averages plot, which may reduce variation between data points. The best-fitting sine wave appeared to undergo approximately two cycles of oscillatory activity. Modelling the data after one cycle of a sine wave did not yield a high correlation coefficient.

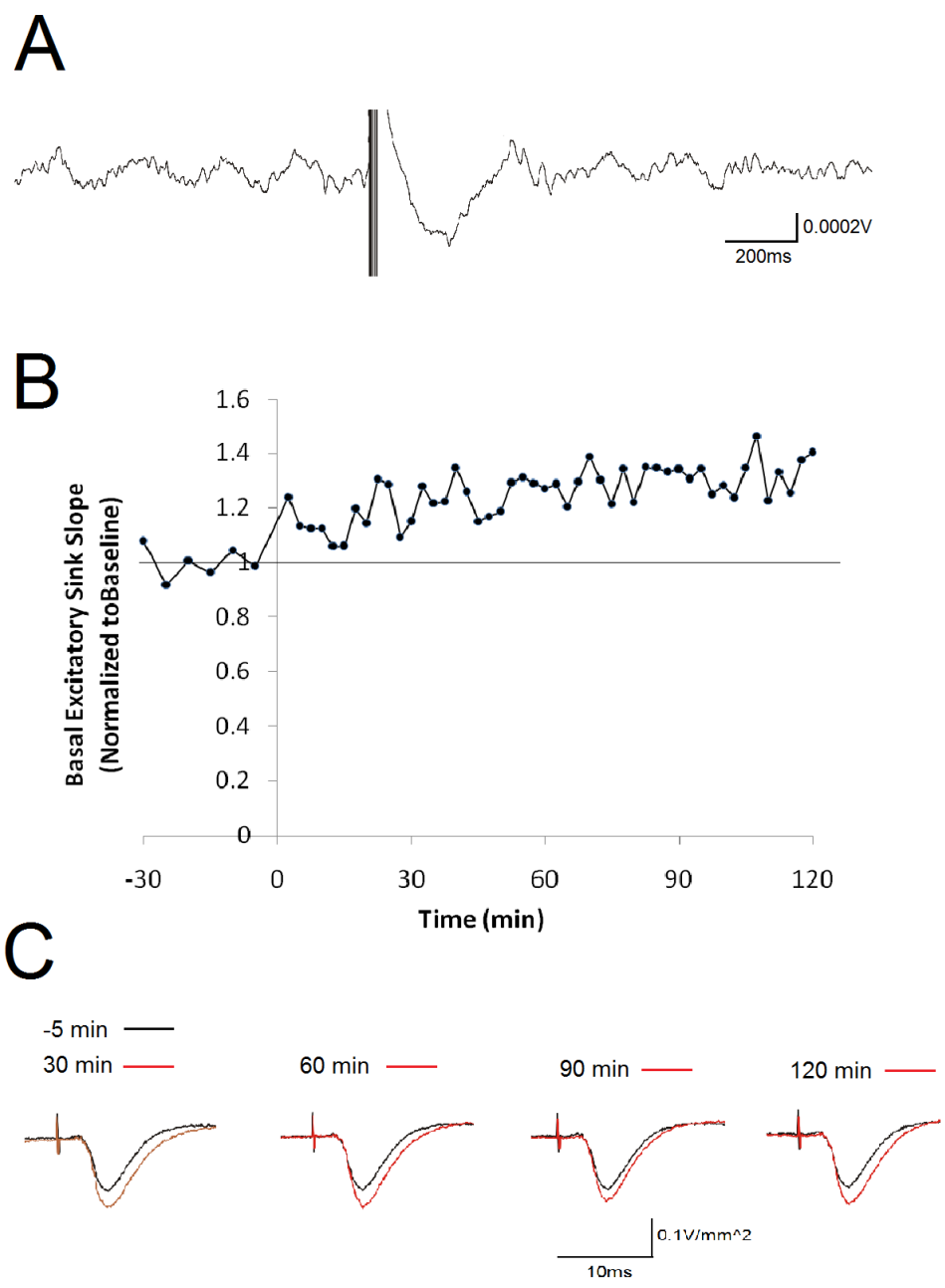

Figure 11. Basal tetanus during the rising phase of theta rhythm leading to LTP for a representative rat (CL081). **(A)** A burst of stimulation was delivered to the basal dendrites during the rising phase of theta rhythm (estimated phase = 20°). **(B)** An average evoked potential (n=4 sweeps) was recorded every 2.5 minutes and the basal dendritic sink was analyzed and normalized by the 30 min baseline average. Tetanus was delivered at t=0.**(C)** Basal excitatory sinks are illustrated at 30, 60, 90, and 120 minutes post-tetanus, compared to the last baseline point (-5 min). The potentiation at all 4 time points is robust.

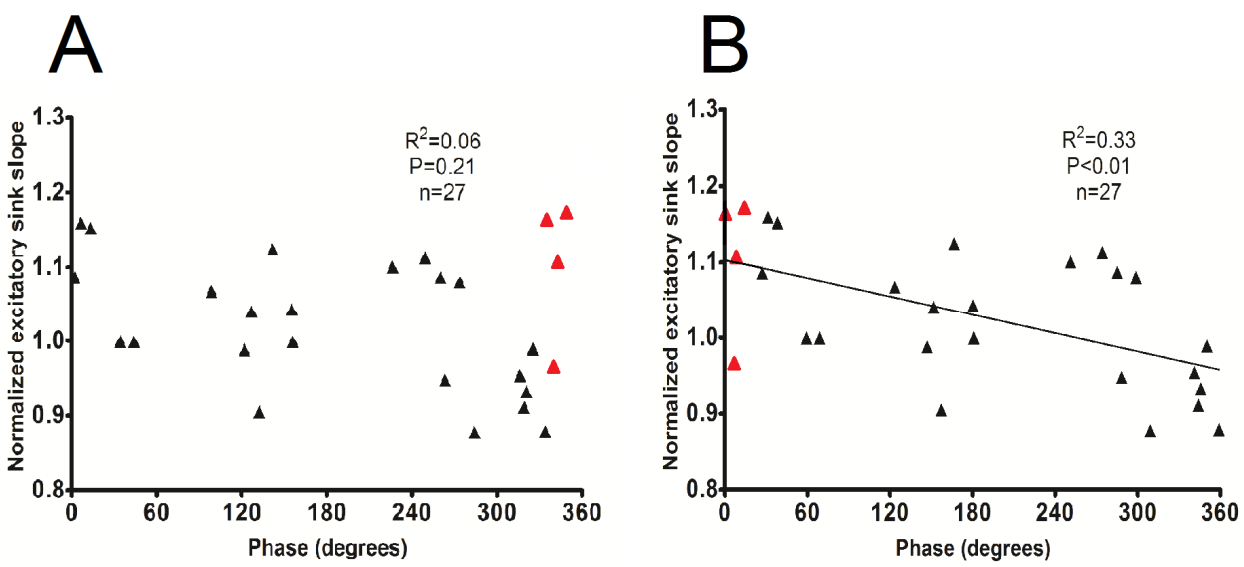

Figure 12. Raw and phase shifted correlation between magnitude of LTP and phase of theta rhythm at the apical dendrites. Following single burst delivery (5 pulses at 200 Hz) to the apical dendrites, the averaged normalized excitatory sink from 0-120 minutes post-tetanus was compared to the phase of theta rhythm where stimulation occurred **(A)**. A phase shift of 18°-26° yielded optimal correlation between phase and LTP; thus the figure shows all data points shifted 26° **(B)**. Points that were phase shifted past 360° are shown in red. The extracellular theta rhythm reference was at the level of stratum lacunosummoleculare.

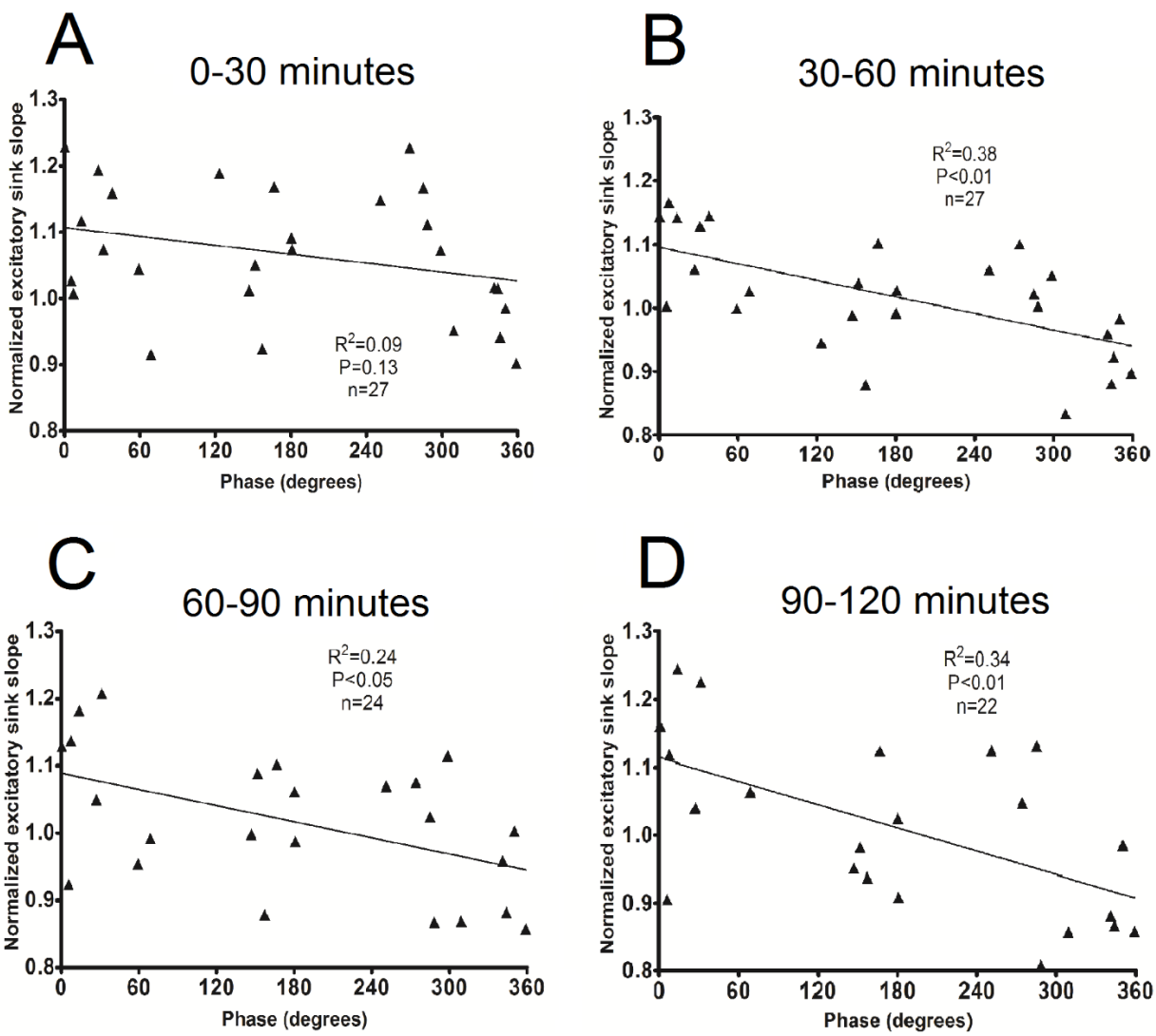

Figure 13. Correlation between magnitude of LTP and phase of theta rhythm at 30 minute intervals at the apical dendrites. Following single burst delivery (5 pulses at 200 Hz) to the apical dendrites, the averaged normalized excitatory sink slope at A) 0-30, B) 30-60, C) 60-90 and D) 90-120 minutes post-tetanus was compared to the phase of theta rhythm where stimulation occurred. All data points were phase shifted by adding 26°to the actual phase of stimulation. The extracellular theta rhythm reference was at the level of stratum lacunosummoleculare.

Because a phase shift of 18°-26° yielded optimal correlation, this suggests that stimulation during the rising phase of theta rhythm may be optimal for inducing LTP at the apical dendrites. An alternate procedure was to use the running average of 4 consecutive phase points to obtain the phase of maximal and minimal LTP **(Fig. 14)**. The maximum apical excitatory sink slope with running average was 114.4 ± 1.9% (n=4) of the baseline, occurring at an average phase of 354.92°.The minimum apical excitatory sink slope was 94 ± 0.7% (n=4) of the baseline, occurring at an average phase of 284.17°. The running averages of normalized LTP were significantly different from each other ($p<0.01$; One-way ANOVA) and Newman-Keuls post-hoc analysis revealed that LTP averages during the rising phase (315°**-**45°) had significantly ($p<0.05$) greater LTP than LTP averages during the trough (225°**-**315°). This was confirmed for the full time course of the LTP – experiments where burst tetanus landed on the rising phase show significantly greater LTP for the full 120 minutes post-tetanus compared to experiments where the burst landed on the trough **(Fig. 15)**. The slope of the apical excitatory sink for the rising phase experiments increased to a maximum of 126.7 ± 4% (n=4) of the baseline at 75 minutes, and the 0-120 minute post-tetanus average was 115 ± 3% (n=4) of the baseline. The slope of the apical excitatory sink for the trough experiments increased to a maximum of 108.1 ± 7.6% (n=4) at 30 minutes, and decreased to a minimum of 82.4 ± 5% (n=4) at 120 minutes. The 0-120 minute post-tetanus average was 93.8 ± 4.9% (n=4) of the baseline. A comparison of the two groups, at the rising phase and at the trough, revealed a significant group effect ($F(1,180) = 165.84$, $p<0.01$), a non-significant time effect ($F(29,180) = 1.24$, $p=0.197$), and a significant group x time interaction effect ($F(29,180) = 2.63$, $p<0.01$). A post-hoc Newman-Keuls multiple comparison test showed

a significant difference between groups at time points 45, 55, 75, 80, 90, 100, 105, 110, 115, and 120 minutes post-tetanus ($p < 0.05$). The potentiation induced during the rising phase was persistent over time, while potentiation induced during the trough showed a steady decline over time. t-tests revealed a significant difference in the evoked potential slopes after tetanus compared to baseline for both rising phase ($t=7.150$; $p<0.0001$; $df=28$; $n=4$) and trough ($t=2.192$; $p<0.05$; $df=28$; $n=4$) stimulation. Therefore, tetanus of the apical dendrites during the rising phase of theta rhythm induced significant LTP compared to baseline, whereas trough stimulation induced significant LTD.

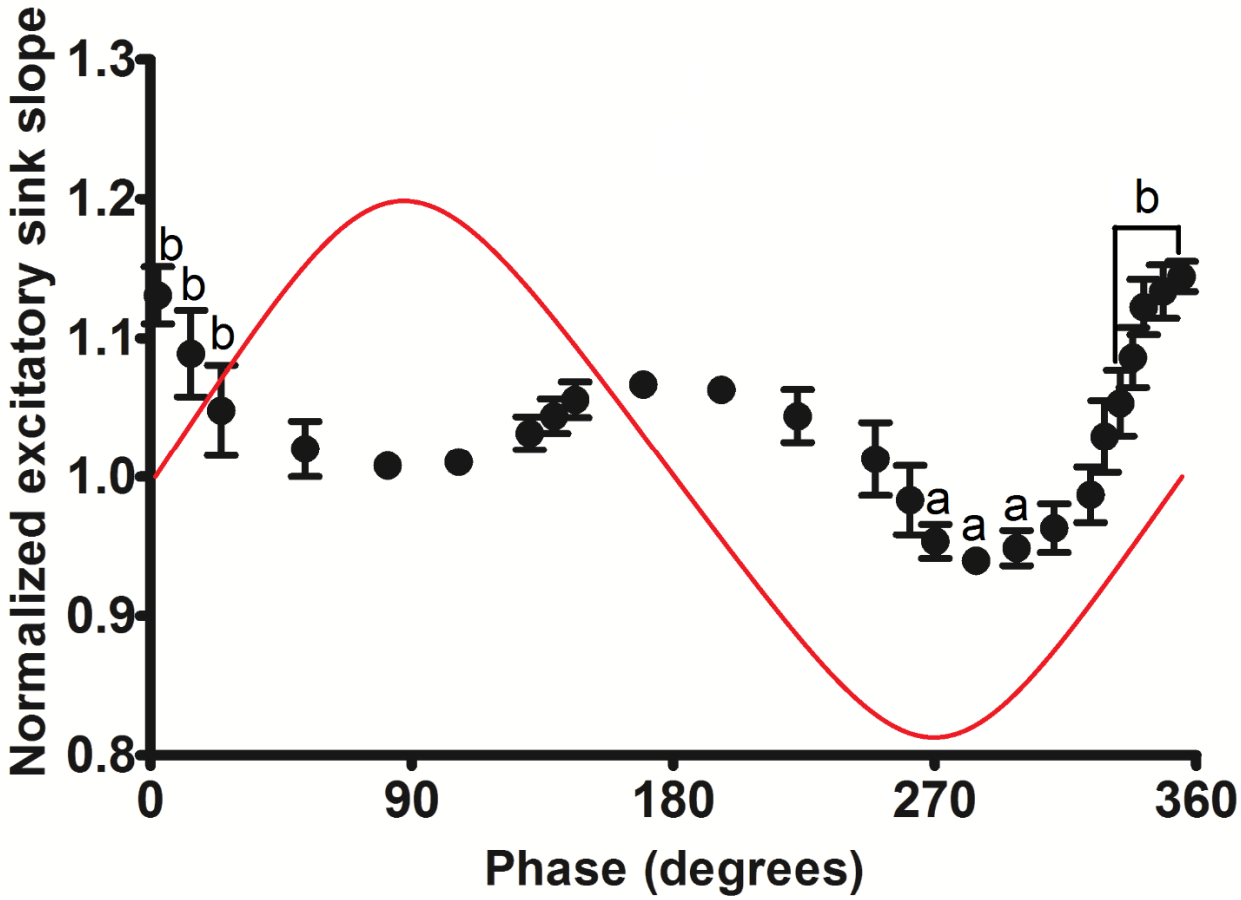

Figure 14. Plot of running average of 4 consecutive phase values and the normalized excitatory sink slope, with data shown in **Fig. 12A**. This allowed 27 individual running averages to be formed, each consisting of 4 experiments. The superimposed sinusoidal red waveform represents one cycle of sine wave, representing the theta rhythm at stratum lacunosummoleculare. One-way ANOVA analysis revealed significant differences between groups indicated by different lower-case alphabet characters (a and b). $P<0.05$ was considered to be statistically significant.

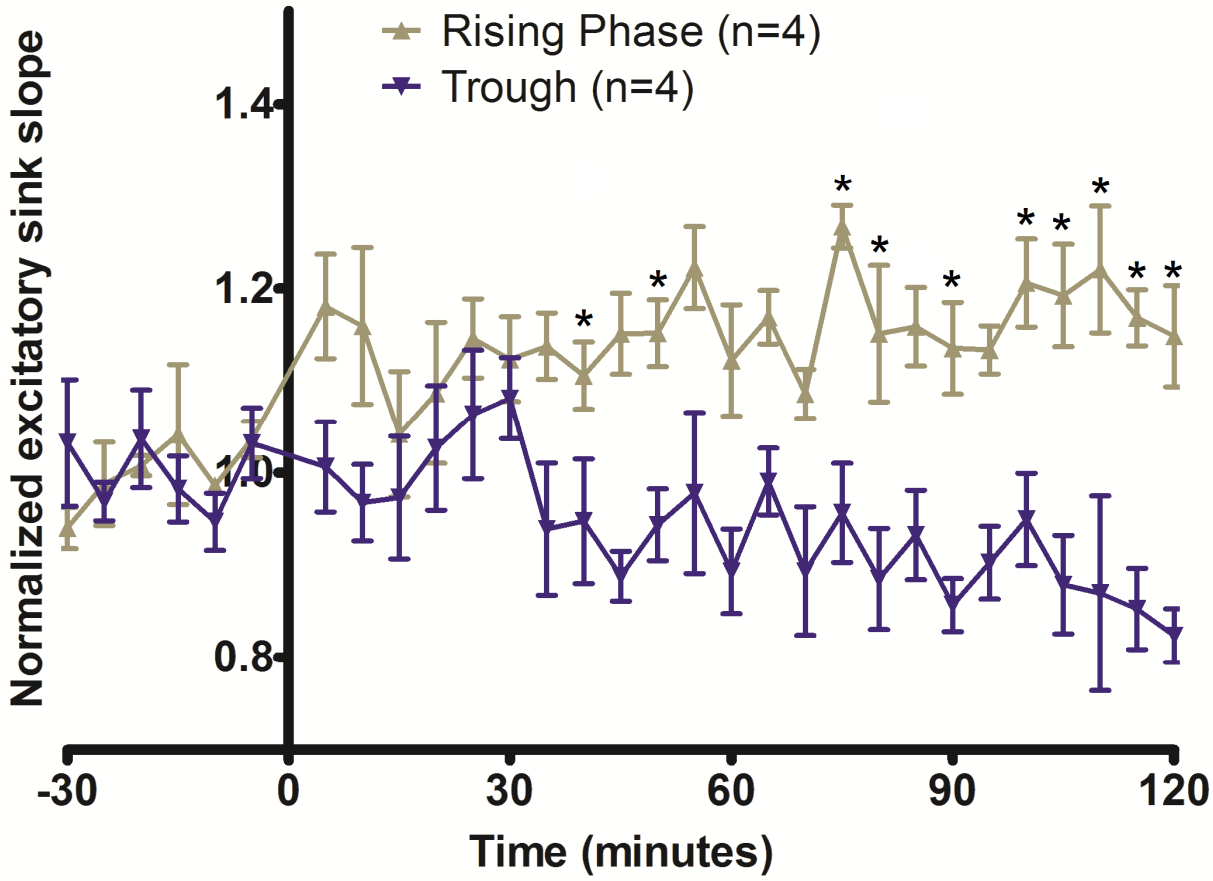

Figure 15. Average LTP time profile for experiments where stimulation was delivered during the rising phase versus that in which stimulation was delivered during the trough. A stable baseline was established for 30 minutes prior to tetanus delivery at time t=0. Tetanus was a single burst consisting of 5 electrical stimulus pulses with an interpulse frequency of 200 Hz. Only the apical dendrites were tetanized. Evoked responses were monitored for 120 minutes following tetanus delivery. Significant differences between groups are indicated by the asterisk: *P<0.05.

3.1.2 Single burst delivered to basal dendrites

A single burst delivered to the basal dendrites showed phase preference for LTP. A representative experiment is shown in **Figure 11**.The normalized excitatory sink slopes were averaged from 0-120 minutes post-tetanus. These average values were then compared to the phase of theta rhythm where stimulation occurred, constructing a correlation plot between the magnitude of LTP and phase **(Fig. 16A)**. The phase of theta rhythm where stimulation occurred and the magnitude of induced LTP does not appear to be correlated (R^2=0.03; p=0.41). As was done for the apical dendritic LTP data (Section 3.1.1), the data set was phase shifted in order to determine where the optimal correlation would occur, and a phase shift of 45°-80° resulted in the optimal linear correlation **(Fig. 16B)**. From the phase shifted correlation plot, the phase of theta rhythm where stimulation occurred and the magnitude of induced LTP is significantly correlated (R^2=0.29; p<0.01). When correlation of LTP over shorter time intervals was performed, the averaged normalized response was significantly correlated to phase for response averaged from 0-30 min (R^2=0.22; p<0.05, **Fig. 17A**). 30-60 min (R^2=0.30; p<0.01, **Fig. 17B**), and 60-90 min post-tetanus (R^2=0.26; p<0.01, **Fig. 17C**). However, the response averaged from 90-120 minutes post-tetanus (R^2=0.13; p=0.08, **Fig. 17D**) was not significantly correlated to phase.

The magnitude of induced LTP and phase of theta rhythm where stimulation occurred showed a significant linear correlation **(Fig. 16B)**; however a linear correlation may not be the optimal method to define the relationship between these two variables. Because the fluctuation of membrane potential resembles a sinusoidal wave, using a sine correlation may better model the data points **(Supplementary Fig. 2)**. The sine wave correlation

yielded a greater correlation coefficient (R^2=0.5974) compared to linear correlation methods (R^2=0.29). However, the linear correlation was performed using raw data, whereas the sine wave was modeled after the running averages plot, which may reduce variation between data points.

A phase shift of 45°-80° yielded optimal correlation, suggesting that stimulation during the rising phase of theta rhythm may induce the largest LTP at the basal dendrites. The phase for optimal LTP was evaluated by taking the running average of 4 consecutive phase points **(Fig. 18)**. The maximal basal LTP was 118.4 ± 1.7% (n=4) of the baseline, occurring at a phase average of 354.1°. The minimum basal LTP of 104.5 ± 0.8% (n=4) of the baseline was found at an average phase of 230.6°. The differences among the running averages were statistically significant ($p<0.01$; One-way ANOVA) and Newman-Keuls post-hoc analysis revealed that the average LTP induced during the rising phase (315°**-**45°) was significantly ($p<0.05$) greater than the average LTP induced during the trough (225°**-**315°). The time course of LTP in experiments in which burst stimulation (induction) landed on the rising phase was significantly higher than the LTP time course in which induction landed on the trough **(Fig. 19)**. The slope of the basal excitatory sink for the rising phase experiments increased to a maximum of 134.7 ± 6.6% (n=3) at 115 minutes post-tetanus, and the 0-120 minute post-tetanus average was 122.7 ± 2.4% (n=4) of the baseline. The slope of the basal excitatory sink for the trough experiments increased to a maximum of 107.8 ± 7.3% (n=4) at 40 minutes, and decreased to a minimum of 89 ± 4.1% (n=3) at 120 minutes. The 0-120 minute post-tetanus average was 102.3 ± 3.5% (n=4) of the baseline. A comparison of the two groups with LTP induced at rising phase and near the trough revealed a significant group effect ($F(1,173) = 310$,

$p<0.01$), a significant time factor ($F(29,173) = 5.574$, $p<0.01$), and a significant group x time interaction factor ($F(29,173) = 5.360$, $p<0.01$). Post-hoc Newman-Keuls multiple comparison tests showed significant differences between LTP of the groups at time points 55-120 minutes post-tetanus ($p<0.05$). The potentiation observed in rising phase experiments is persistent over time, and negative phase experiments show little change in the evoked response post-tetanus. t-tests revealed a significant difference in the evoked potential slopes after tetanus compared to baseline for only rising phase stimulation ($t=7.516$; $p<0.0001$; $df=28$; $n=4$). There was no significant difference in the post-tetanus evoked potential slopes for trough stimulation compared to baseline ($t=1.139$; $p=0.26$; $df=28$; $n=4$). Therefore, tetanus of the basal dendrites during the rising phase of theta rhythm induced significant LTP compared to baseline, whereas trough stimulation induced neither LTP nor LTD.

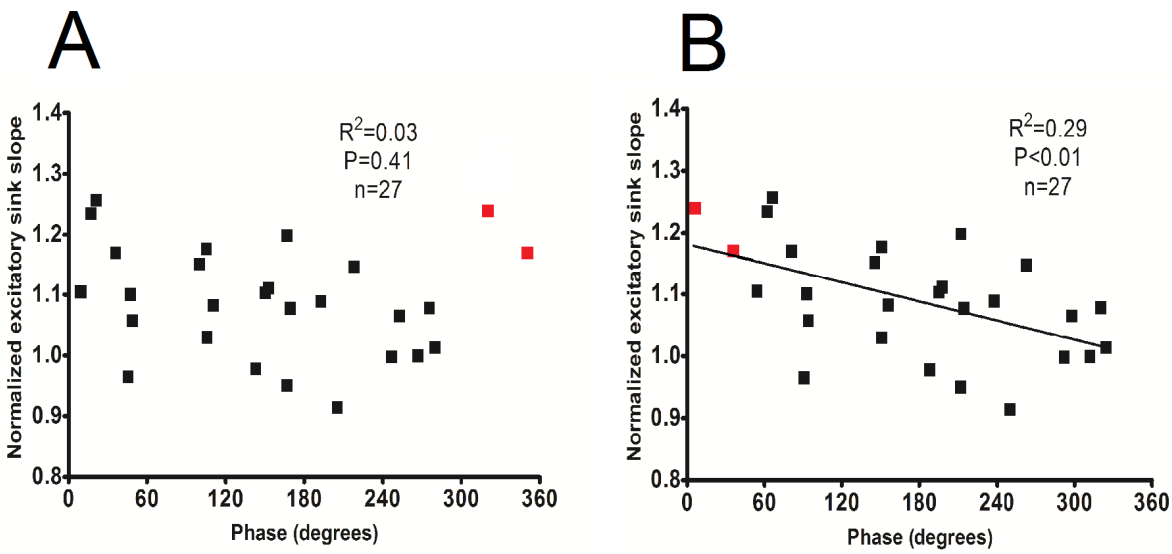

Figure 16. Raw and phase shifted correlation between magnitude of LTP and phase of theta rhythm at the basal dendrites. Following single burst delivery (5 pulses at 200 Hz) to the basal dendrites, the averaged normalized excitatory sink from 0-120 minutes post-tetanus was compared to the phase of theta rhythm where stimulation occurred **(A)**. A phase shift of 45°-80° yielded optimal correlation between phase and LTP; thus the figure shows all data points shifted 45° **(B)**. Points that were phase shifted past 360° are shown in red. The extracellular theta rhythm reference was at the level of stratum lacunosummoleculare.

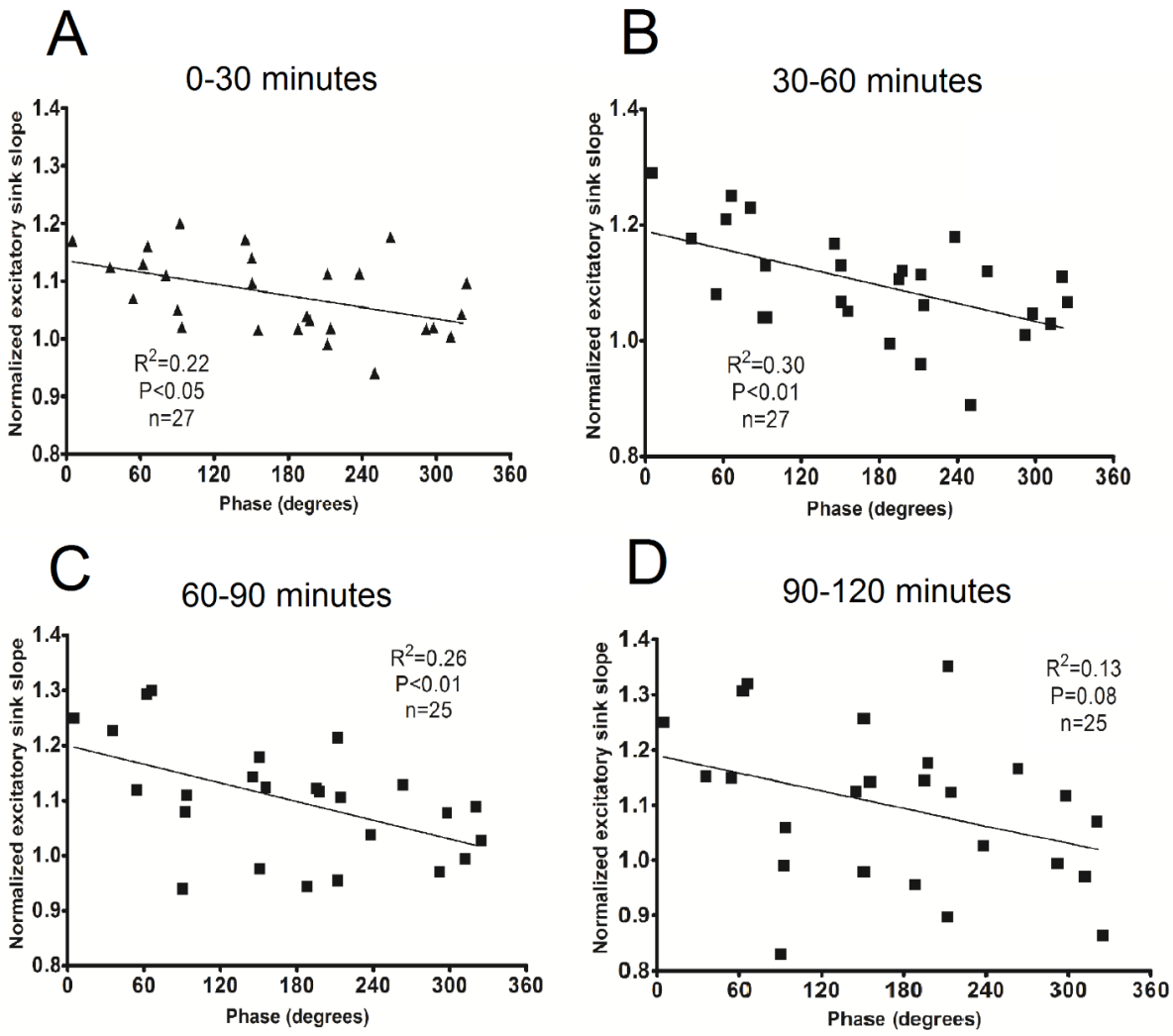

Figure 17. Correlation between magnitude of LTP and phase of theta rhythm at 30 minute intervals at the basal dendrites. Following single burst delivery (5 pulses at 200 Hz) to the basal dendrites, the averaged normalized excitatory sink slope at A) 0-30, B) 30-60, C) 60-90 and D) 90-120 minutes was compared to the phase of theta rhythm where stimulation occurred. All data points were phase shifted by adding 45° to the actual phase of stimulation. The extracellular theta rhythm reference was at the level of stratum lacunosummoleculare.

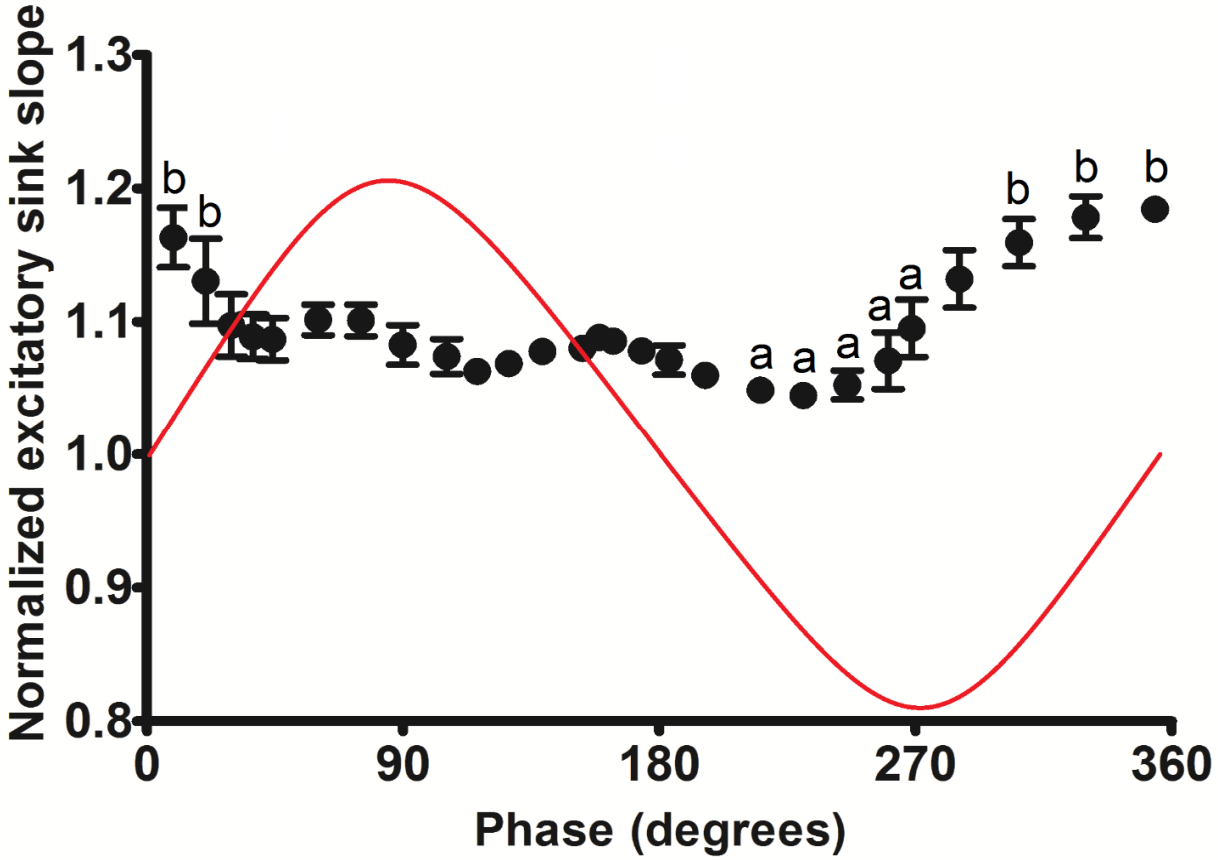

Figure 18. Plot of running average of 4 consecutive phase values and the normalized excitatory sink slope, with data shown in **Fig. 16A**. This allowed 27 individual running averages to be formed, each consisting of 4 experiments. The superimposed sinusoidal red waveform represents one cycle of sine wave, representing the theta rhythm at stratum lacunosummoleculare. One-way ANOVA analysis revealed significant differences between groups indicated by different lower-case alphabet characters (a and b). $P<0.05$ was considered to be statistically significant.

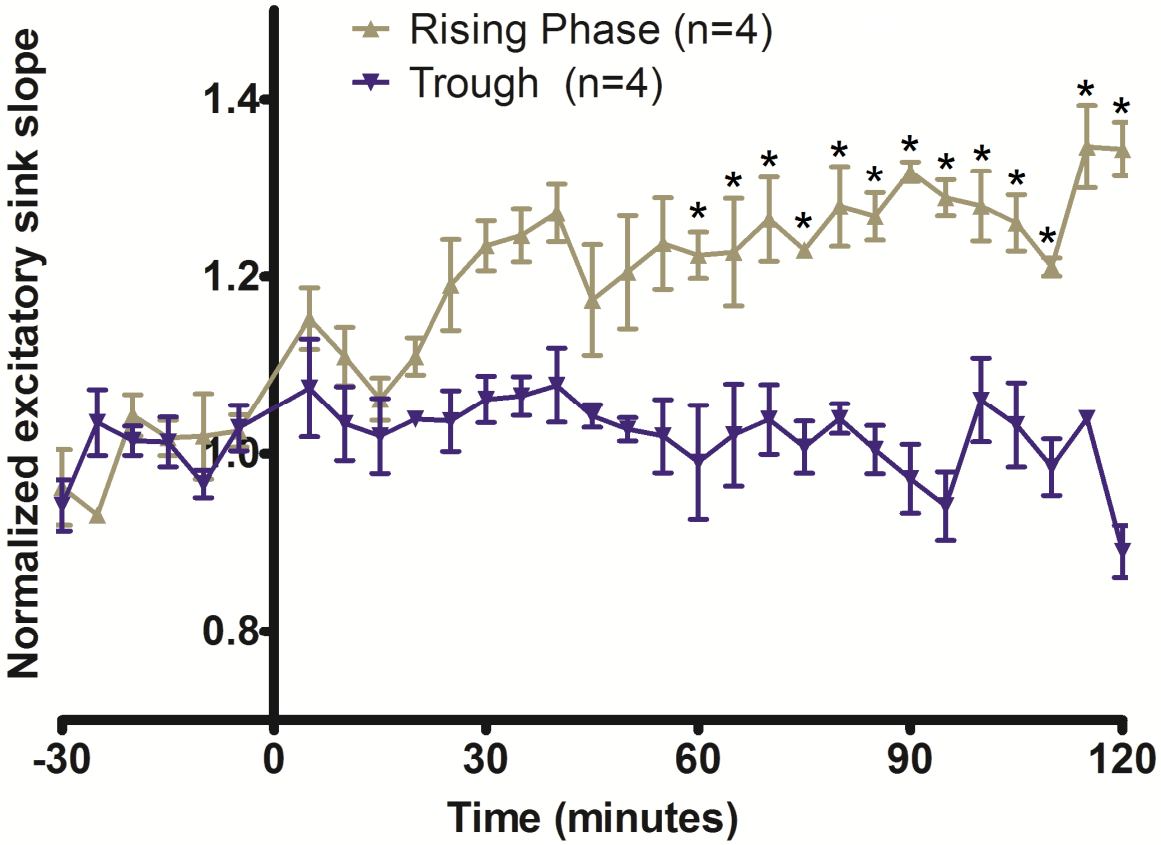

Figure 19.LTP time profile for experiments where stimulation was delivered during the rising phase versus the trough. A stable baseline was established for 30 minutes prior to tetanus delivery at time t=0. Tetanus was a single burst consisting of 5 electrical stimulus pulses with an interpulse frequency of 200 Hz. Only the basal dendrites were tetanized. Evoked responses were monitored for 120 minutes following tetanus delivery. Significant differences between groups are indicated by the asterisk: *P<0.05.

The reference theta at the level of stratum lacunosummoleculare may experience some phase shifting, and the reference theta may not consistently be at the same depth for every experiment. Therefore, a more consistent reference theta may be advantageous for analysing single burst results. Based on spectral analysis of the theta profile, the least amount of phase shifting occurs at the level of the stratum oriens or alveus. Therefore, all phase calculations using an apical dendritic reference theta were phase shifted to a stratum oriens or alveus reference (typically -160° to -180° phase shift). As was done for the apical dendritic LTP data (Section 3.1.1), the data set was phase shifted in order to determine where the optimal correlation would occur. A phase shift of 226°-228° provided the optimal correlation for apical dendritic LTP data using the new reference **(Fig. 20)**. The correlation using a stratum oriens reference (R^2=0.53; $p<0.001$) is greater than that using a stratum lacunosummoleculare reference (R^2=0.33; $p<0.01$). Likewise, a phase shift of 243°-265° provided the optimal correlation for basal dendritic LTP data **(Fig. 21)**. Correlation using the new phase reference (R^2=0.30; $p<0.01$) was slightly greater than that using an apical dendritic reference (R^2=0.29; $p<0.01$). The phase shift for optimal correlation suggests that stimulation during the falling phase of the stratum oriens/alveus reference theta yields maximal LTP, and the phase shift needed to obtain optimal correlation for basal and apical dendrites was similar.

In summary, single burst stimulation of both the apical and basal dendrites induced maximal LTP at the rising phase of the theta rhythm. LTP was graded and not all-or-none, and lower LTP can be induced at other phases of the theta rhythm. Statistically significant LTD was shown for apical stimulation during the trough, whereas basal stimulation during the trough did not result in LTP nor LTD. Using a stratum

oriens/alveus reference provided better correlation for apical and basal LTP data compared to a distal apical dendritic reference.

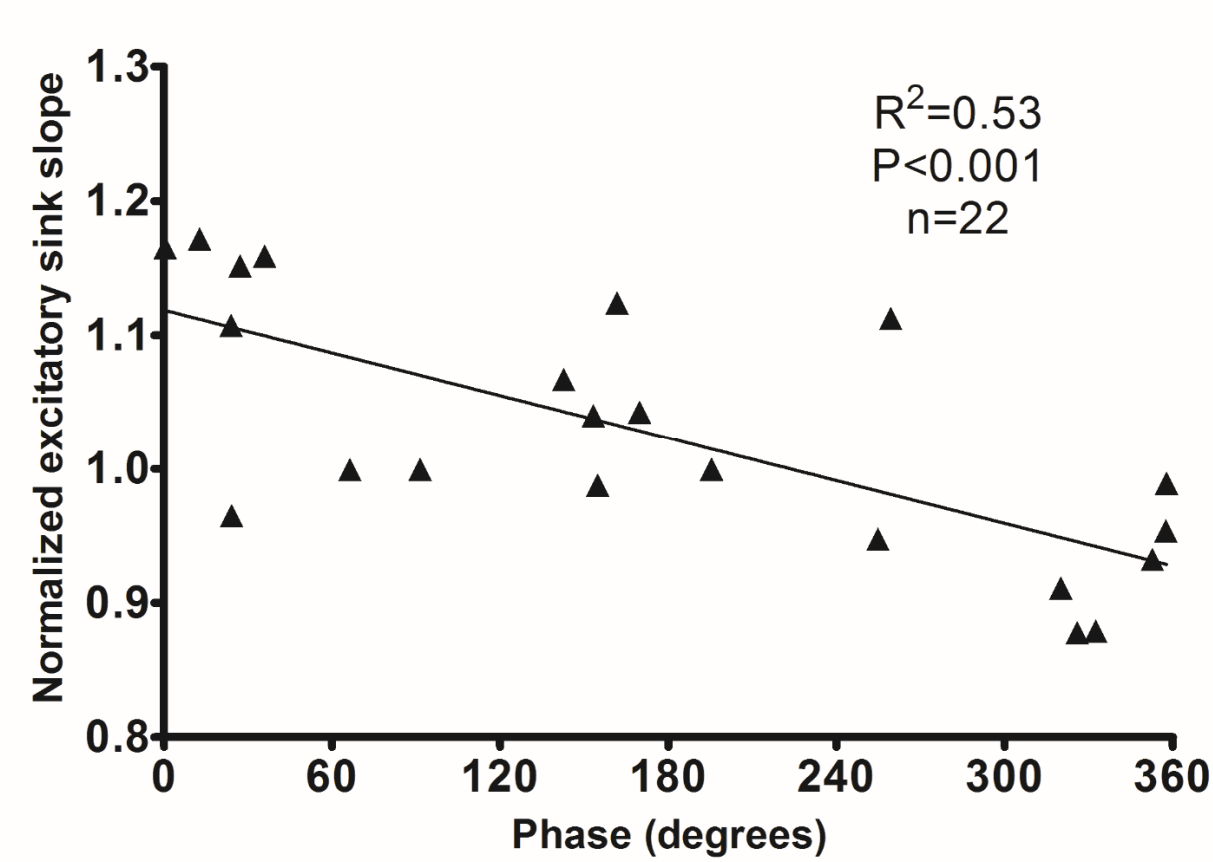

Figure 20. Phase shifted correlation between magnitude of LTP and phase of theta rhythm at the apical dendrites using a stratum oriens/alveus reference. Following single burst delivery (5 pulses at 200 Hz) to the apical dendrites. The averaged normalized excitatory sink from 0-120 minutes post-tetanus was compared to the phase of theta rhythm where stimulation occurred. A phase shift of 226°-228° yielded optimal correlation between phase and LTP; thus the figure shows all data points shifted 226°.

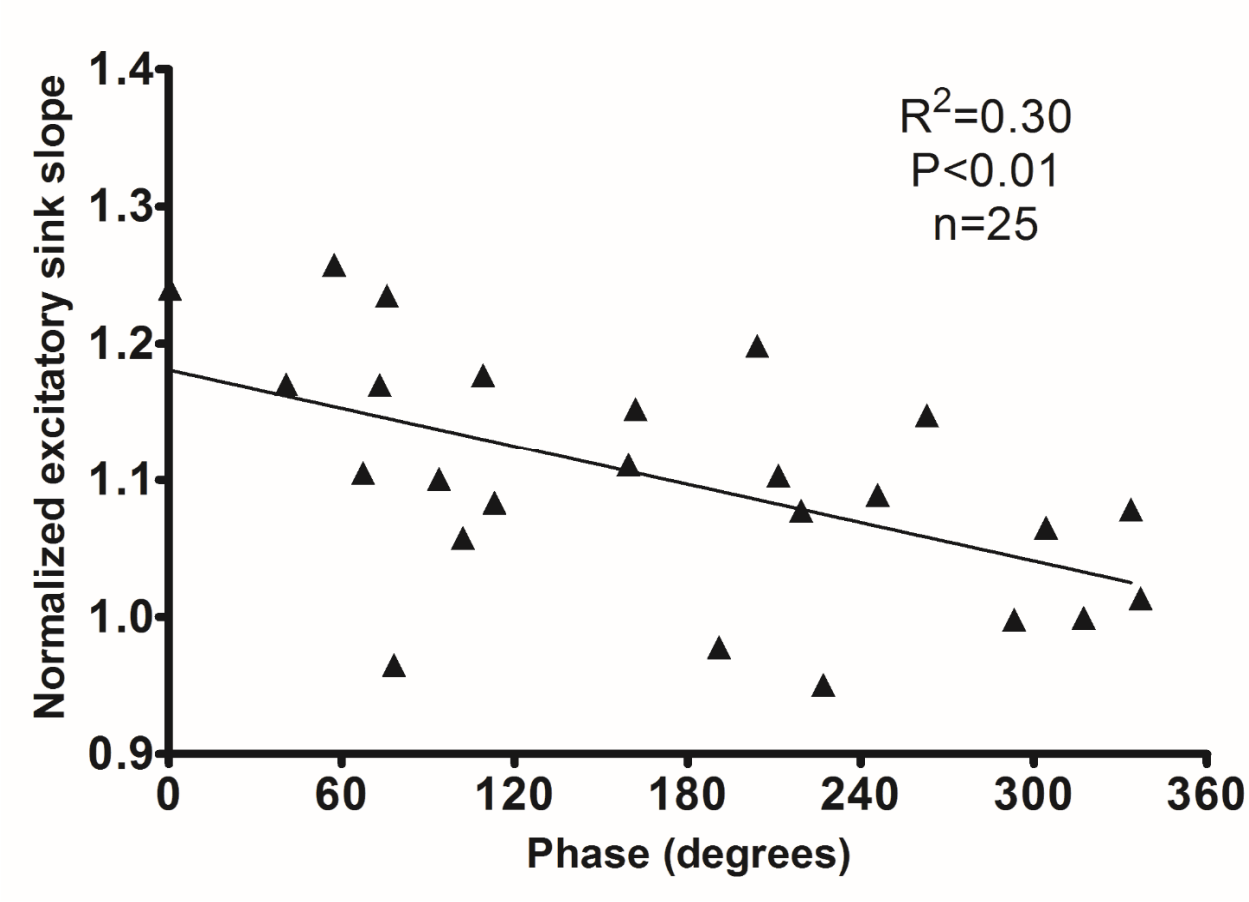

Figure 21. Phase shifted correlation between magnitude of LTP and phase of theta rhythm at the basal dendrites using a stratum oriens/alveus reference. Following single burst delivery (5 pulses at 200 Hz) to the apical dendrites. The averaged normalized excitatory sink from 0-120 minutes post-tetanus was compared to the phase of theta rhythm where stimulation occurred. A phase shift of 243°-265° yielded optimal correlation between phase and LTP; thus the figure shows all data points shifted 243°.

3.2 Multiple bursts delivered to the basal dendrites at different phases of theta rhythm

In order to study whether theta phase during burst stimulation affected LTP resulting from multiple burst stimulation, two combined phase indices were developed and calculated for individual experiments (Section 2.6.3).

The averaged normalized excitatory sink slope from 0-120 minutes post-tetanus was positively correlated to the calculated combined phase index **(Fig. 22A)**, but this correlation was not statistically significant (R^2=0.2896, p=0.0578). This may be due to fluctuations in the evoked response over time. Therefore, it was important to assess correlation with LTP values over smaller time intervals. From 0-30 minutes post-tetanus **(Fig. 22B)**, the averaged normalized excitatory sink slope was significantly correlated to the combined phase index (R^2=0.4792, p<0.01). LTP averaged from 30-60 minutes (R^2=0.2803, p=0.0628), 60-90 minutes (R^2=0.0839, p=0.3876), and 90-120 minutes post-tetanus (R^2=0.0671, p=0.5009) was not significantly correlated to the combined phase index. Some experiments showed immediate potentiation following tetanus, and potentiation was stable over time **(Fig. 23)**. In experiments where there was no immediate potentiation following tetanus, the evoked response may show gradual change over the course of 120 minutes.

To determine whether changes occurring at the basal dendrites were input specific, we compared the potentiated basal response from experiments that showed LTP to their respective control apical pathway **(Fig. 24)**. There was a significant group effect ($F(1,159) = 99.67$; $p<0.01$), a significant time effect ($F(22,159) = 3.072$; $p<0.01$) and a significant interaction effect ($F(22,159) = 1.968$; $p<0.01$). The averaged apical response

from 0-120 minutes post-tetanus was not significantly different from baseline ($t(21) = 1.329$; $p=0.20$). These results indicate that potentiation at the basal dendritic synapses was input specific, showing no concurrent potentiation at the apical dendritic synapses.

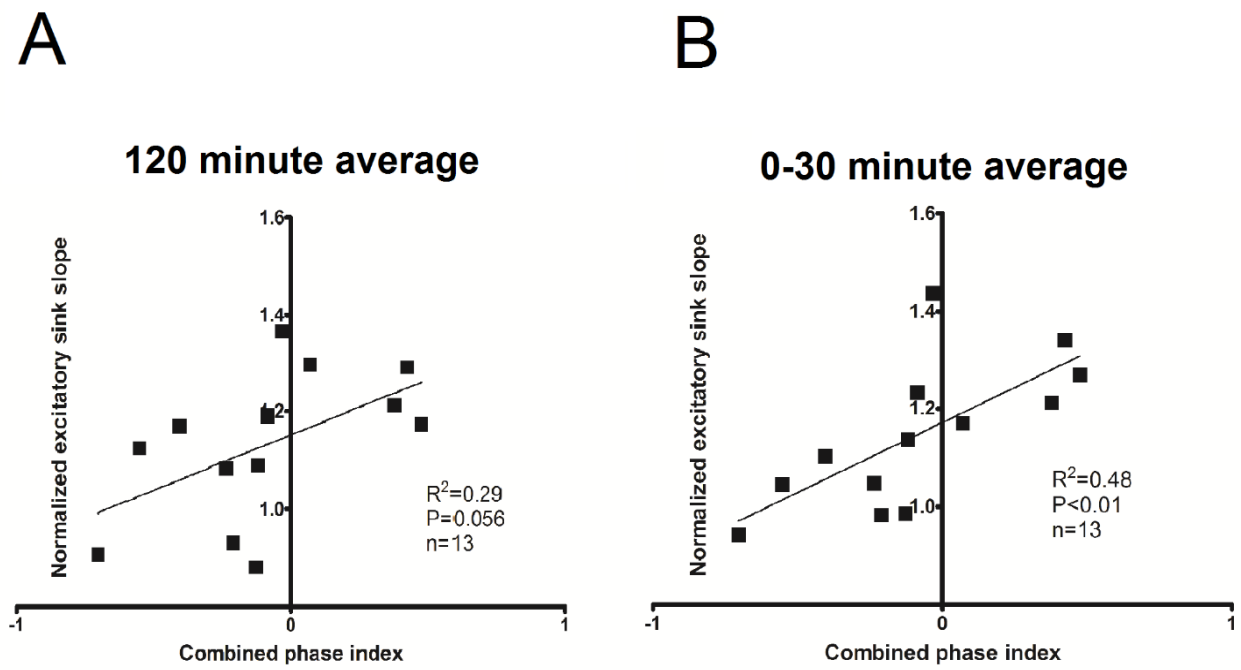

Figure 22. Normalized excitatory sink slope values averaged from 0-120 minutes **(A)** and 0-30 minutes **(B)** post-tetanus compared to the combined phase index. Each point represents a different experiment (n=13). The theoretical maximum combined phase index for a particular experiment is +1 (all bursts landed on the absolute peak) and the theoretical minimum is -1 (all bursts landed on the absolute trough).

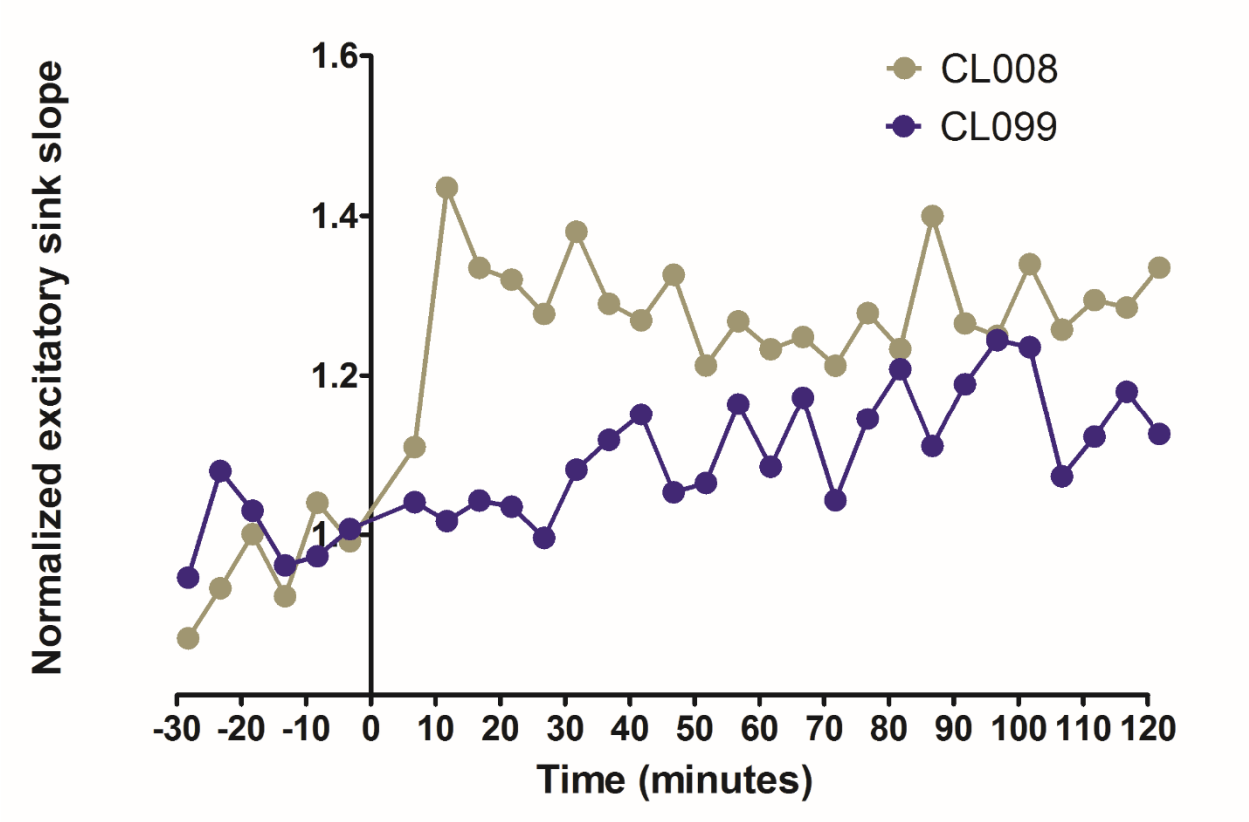

Figure 23. Normalized excitatory response (LTP) profile comparing two representative experiments with high and low combined phase index (CPI) (CL008 and CL099). The CPI for CL009 was 0.423, whereas the CPI for CL099 was -0.554.The former rat illustrates an example of robust LTP, showing immediate potentiation following tetanus, and this potentiation persisted over time. CL099 did not show immediate potentiation following tetanus, but the evoked response slowly increased over time. A stable baseline was established for 30 minutes prior to tetanus delivery at time t=0.Tetanus contained 3-6 bursts consisting of 4-6 electrical stimulus pulses with an interpulse frequency of 200 Hz. Evoked responses were monitored for 120 minutes following tetanus delivery.

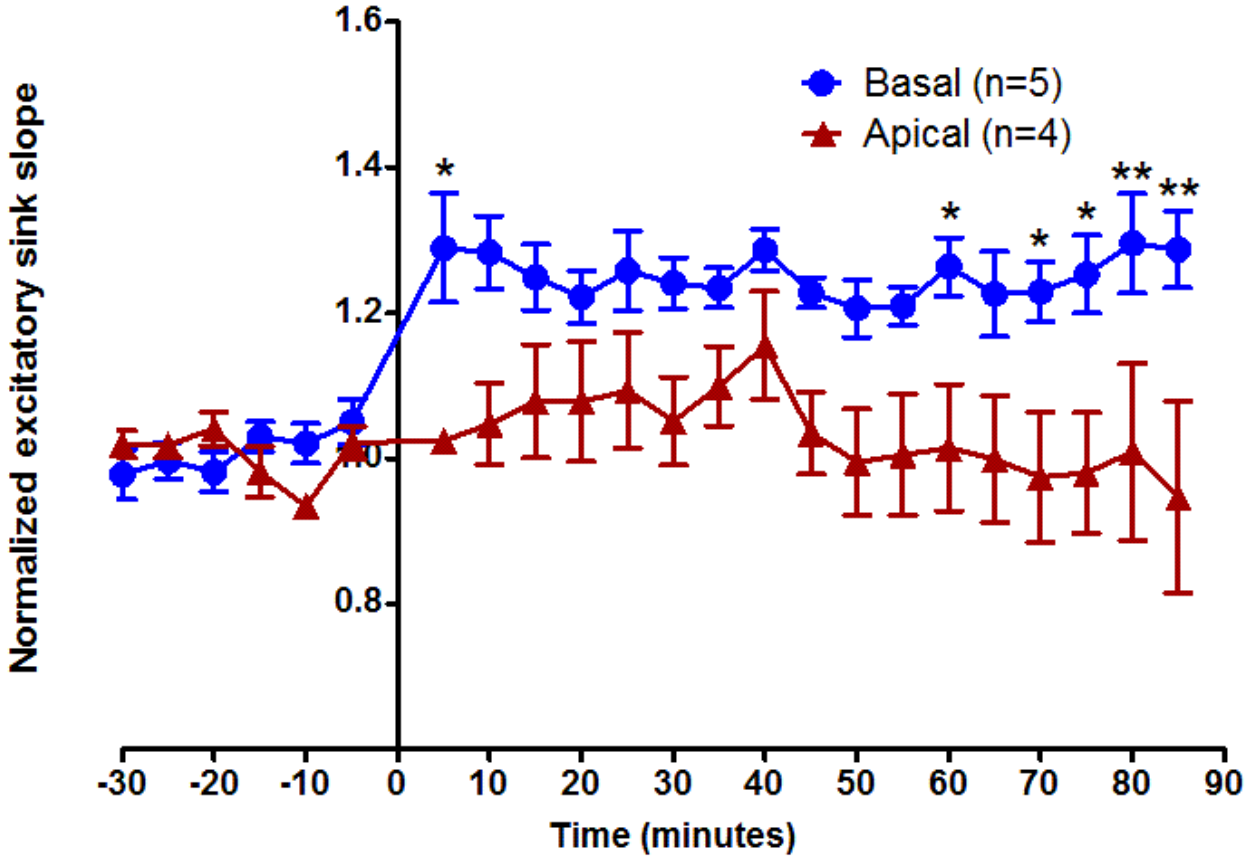

Figure 24. Time profile for CPI experiments that showed LTP and their corresponding non-tetanized apical control pathway. A stable baseline was established for 30 minutes prior to tetanus delivery at time t=0. Tetanus contained 3-6 bursts consisting of 4-6 electrical stimulus pulses with an interpulse frequency of 200 Hz, delivered only to the basal dendrites. Evoked responses were monitored for 85 minutes following tetanus delivery. Significant differences between groups are indicated using the asterisk: *P<0.05, **P<0.01.

The combined phase index was not significantly correlated to the degree of observed LTP, but a general trend could be observed **(Fig. 22A)**. The combined phase index assumes that stimulation during both the positive and negative phase of theta rhythm contributes to the modulation of synaptic plasticity. Therefore we developed another index, the "positive phase index", to calculate the contribution of burst stimulation only during the positive phase, and exclude burst stimulation during negative theta phase. The correlation between the positive phase index and LTP averaged from 0-120 minutes post-tetanus was significant (R^2=0.5042, p<0.01, **Fig. 25A**). Because the evoked potentials post-tetanus may fluctuate, it was important to evaluate correlation with LTP values over smaller time intervals. The correlation is significant for LTP values averaged from 0-30 minutes (R^2=0.6873, p<0.01, **Fig. 25B**) and 30-60 minutes post-tetanus (R^2=0.5501, p<0.01, **Fig. 25C**).However, the correlation was not significant from LTP averaged from 60-90 minutes (R^2=0.3027, p=0.0795) and 90-120 minutes post-tetanus (R^2=0.009, p=0.8077). Correlation using the positive phase index was greater than correlation using the combined phase index. Some experiments showed immediate potentiation following tetanus, and potentiation was stable over time **(Fig. 26)**. In experiments where there was no immediate potentiation following tetanus, the evoked response may show gradual change over the course of 120 minutes. To determine whether changes occurring at the basal dendrites were input specific, we compared the experiments that had a potentiated basal response to their respective non-tetanized apical control pathway **(Fig. 27)**. There was a significant group effect (F(1,228) =121.6; p<0.01), a significant time effect (F(22,228) =2.894; p<0.01) and a significant interaction effect (F(22,228) =2.229; p<0.01). The averaged apical response from 0-120 minutes post-tetanus was not

significantly different from baseline ($t(21) = 1.198$; $p=0.24$).These results indicate that potentiation at the basal dendritic synapses was input specific, showing no concurrent potentiation at the apical dendritic synapses.

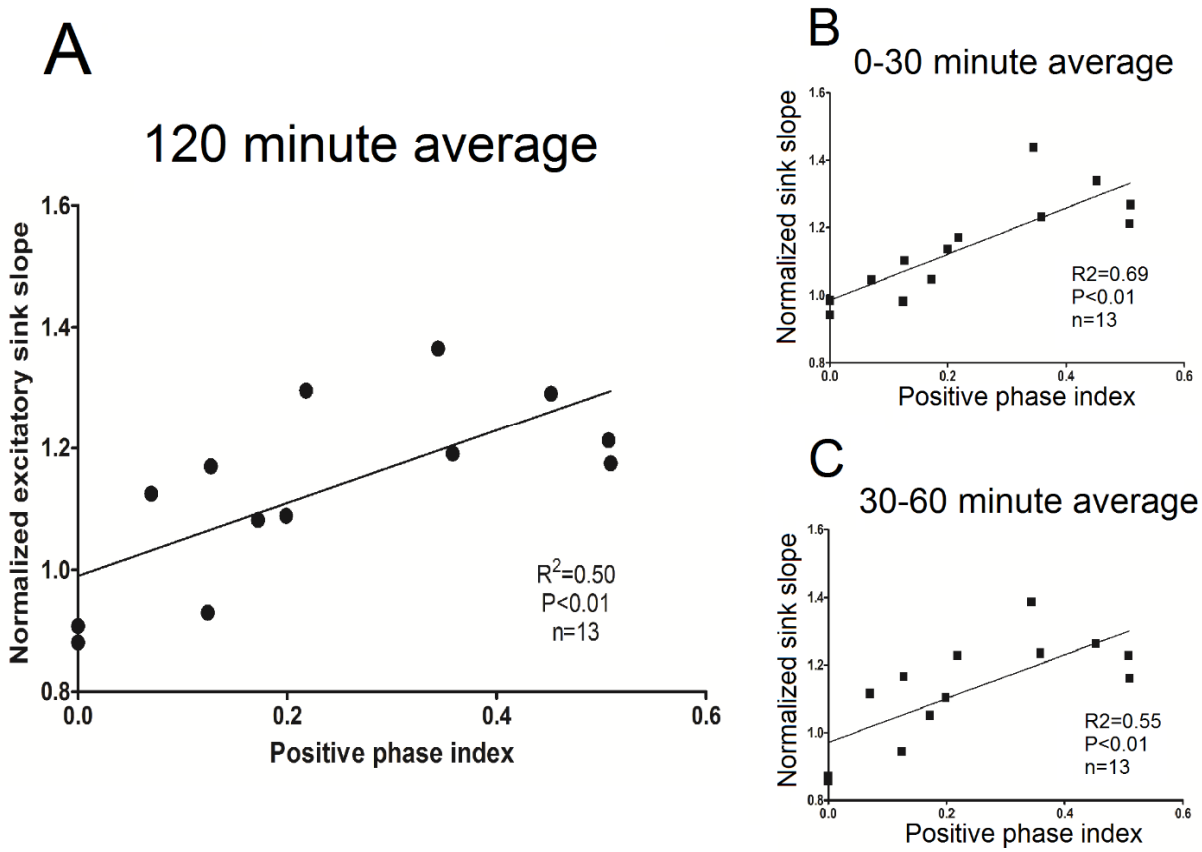

Figure 25. Normalized excitatory sink slope values averaged from 0-120 minutes **(A)**, 0-30 minutes **(B)**, and 30-60 minutes **(C)** post-tetanus compared to the positive combined phase index. Each point represents a different experiment (n=13). The theoretical maximum of the combined phase index for a particular experiment is 1 (indicating all burst landed on the absolute peak), and the theoretical minimum is 0 (meaning no bursts were delivered during the positive phase).

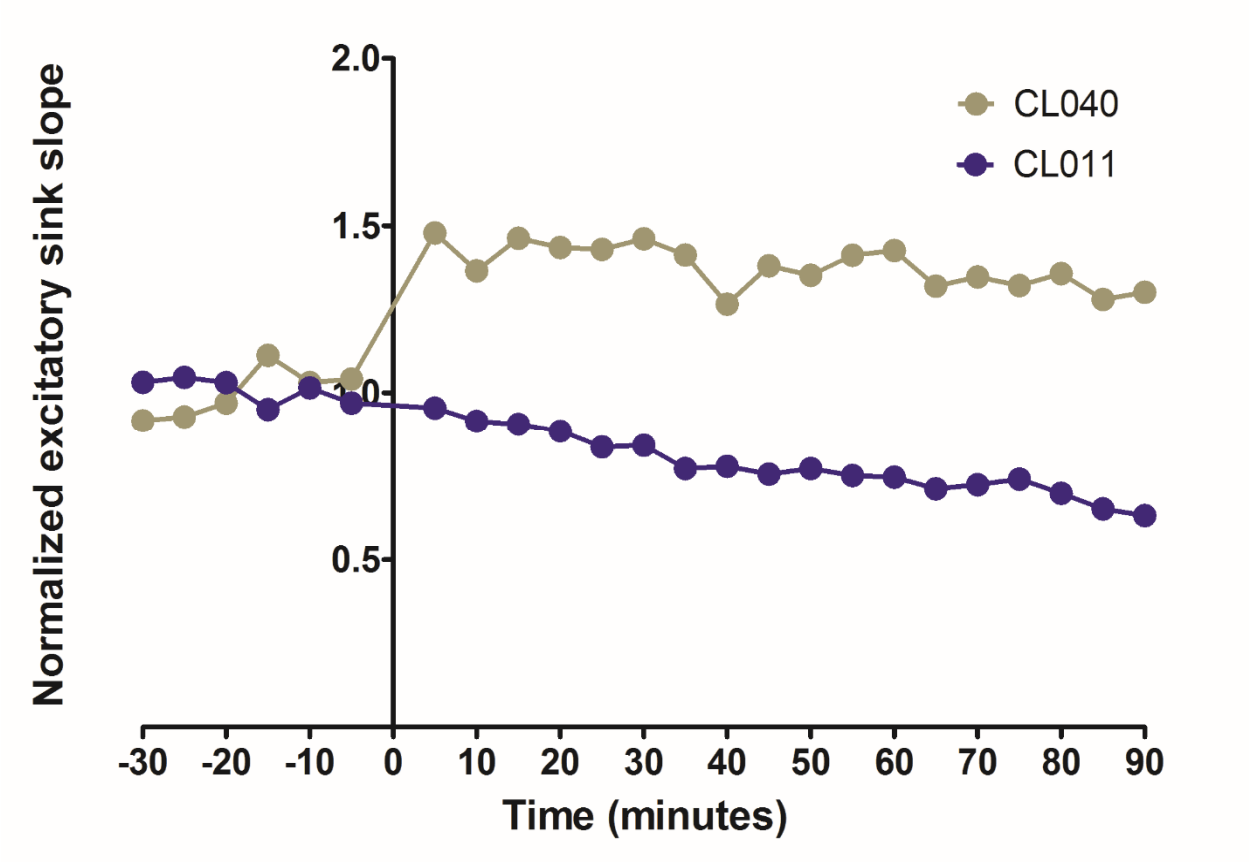

Figure 26. Normalized excitatory response (LTP) profile comparing two representative experiments with high and low "positive combined phase index" (CL040 and CL011). The positive combined phase index for CL040 was 0.344, whereas that for CL099 was 0.124. The former rat illustrates an experiment with robust LTP, showing immediate potentiation following the tetanus, and this potentiation persisted over time. CL011 did not show LTP, and the evoked response slowly decreased over time. A stable baseline was established for 30 minutes prior to tetanus delivery at time t=0.Tetanus contained 3-6 bursts consisting of 4-6 electrical stimulus pulses with an interpulse frequency of 200 Hz. Evoked responses were monitored for 90 minutes following tetanus delivery.

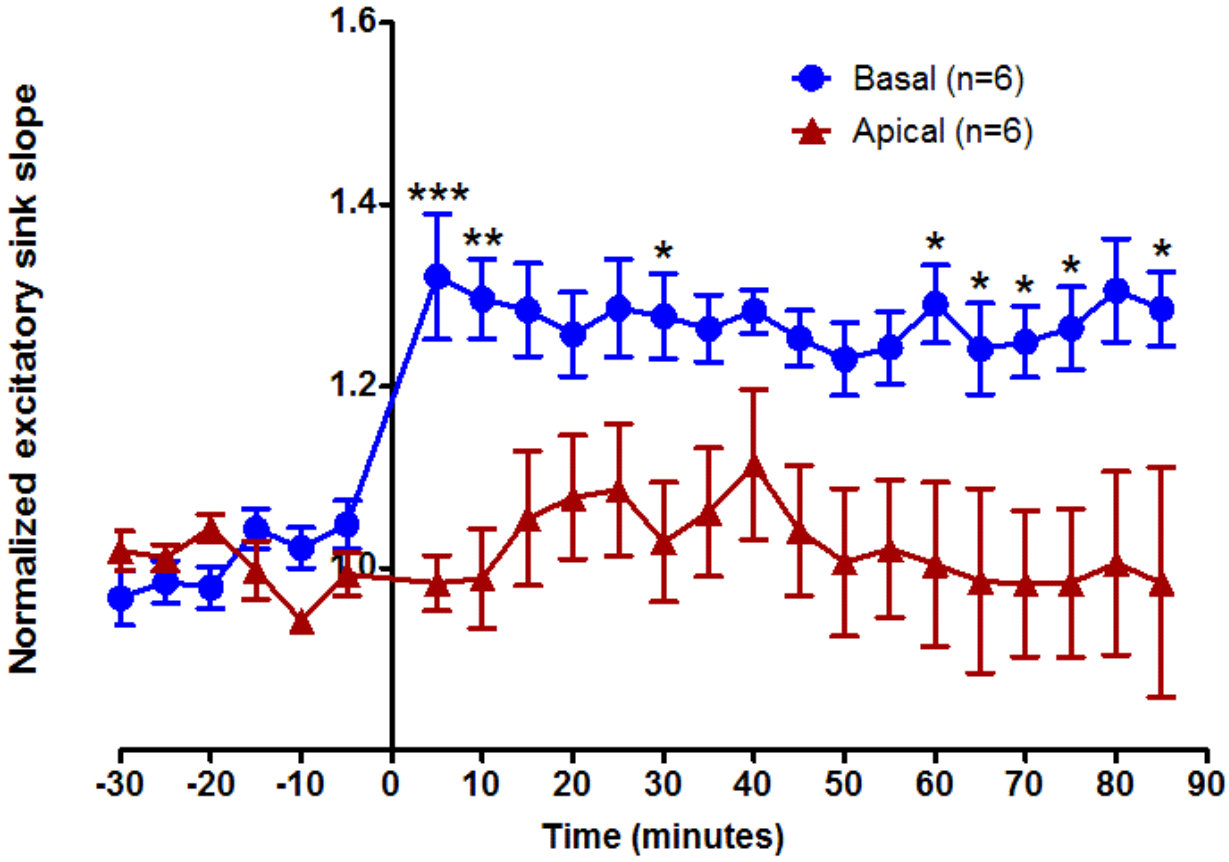

Figure 27. Average time profiles of the normalized excitatory sink slope response for experiments with positive combined phase index (n=6) shown for the tetanized (basal dendritic) pathway, and their corresponding apical dendritic control pathway. A stable baseline was established for 30 minutes prior to tetanus delivery at time t=0. Tetanus contained 3-6 bursts consisting of 4-6 electrical stimulus pulses with an interpulse frequency of 200 Hz, delivered only to the basal dendrites. Evoked responses were monitored for 85 minutes following tetanus delivery. Significant differences between groups are indicated using the asterisk: *P<0.05, **P<0.01, ***P<0.001.

3.3 Population spike excitability during different phases of hippocampal theta rhythm

Population spikes were evoked in CA1 apical and basal dendrites during background theta activity to elucidate how different phases of the theta rhythm modulate excitability at CA1 pyramidal cell synapses.

A single high-intensity stimulus delivered to the apical dendrites evoked an apical dendritic population spike at 1.5 x spiking threshold intensity **(Fig. 31C)**. The amplitude of this population spike appeared to be affected by the phase of theta rhythm where stimulation occurred, showing preference for the falling phase **(Fig. 28)**. To determine whether this was actually a significant effect, different groups were formed, each spanning a range of 40° phase and the normalized population spike amplitude was calculated and compared between groups **(Fig. 30)**. The maximum apical normalized population spike amplitude of 112 ± 6.1% (n=14) of the overall average (average across the entire theta cycle) occurred at a phase of 120°-160°.The minimum apical normalized population spike amplitude was 92.2± 8.4% (n=14) of the overall average, and this occurred at 280°-320°.

The amplitude of the population spike evoked by high intensity (1.5 x population spike threshold) stimulation of the basal dendrites **(Fig. 31A)**also showed a maximal amplitude when stimulated during the falling phase **(Fig. 29)**.The maximum basal normalized population spike amplitude was 114.5± 7.2% (n=9) of the overall average, and this was found at 120°-160° phase **(Fig. 30)**. The minimum basal normalized population spike amplitude of 88.4± 6.6% (n=9) of the overall average was found at320°-360° phase.

When the population spike excitability across theta phase was compared between apical and basal dendritic stimulation, two-way (group x phase) ANOVA analysis revealed a significant phase effect ($F(8,179) = 19.99$; $p<0.01$), a non-significant group(basal and apical dendritic stimulation) effect ($F(1,179) = 0.6107$; $p=0.435$), and a non-significant interaction effect ($F(8,179) = 1.816$; $p=0.077$). Both apical and basal profiles show a gradual increase in excitability near the falling phase (120°-160° for both stimulation of the basal and apical dendrites), and a gradual decrease in excitability near the rising phase, at 280°-320° for the apical dendrites, and 320°-360° for the basal dendrites.

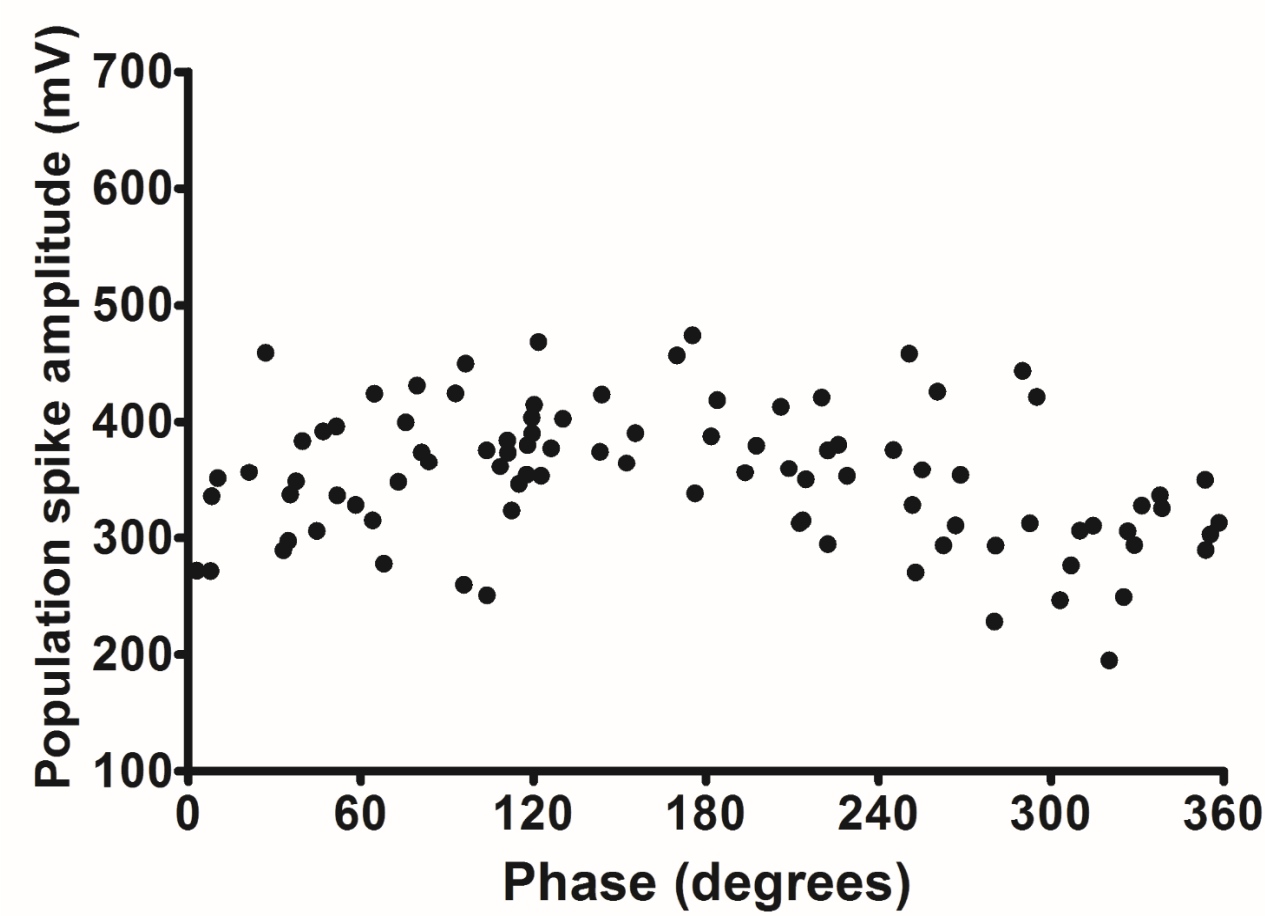

Figure 28. Population spike amplitude varied with the phase of hippocampal theta rhythm, shown in a representative rat (CL112). A single high intensity stimulating pulse (~1.5 x population spike threshold) was delivered to the apical dendrites, and phase was referenced to the extracellular theta rhythm at CA1 stratum lacunosummoleculare. Stimulating pulses were delivered at a frequency of 0.05 Hz and the population spike amplitude was measured from the cell body layer.

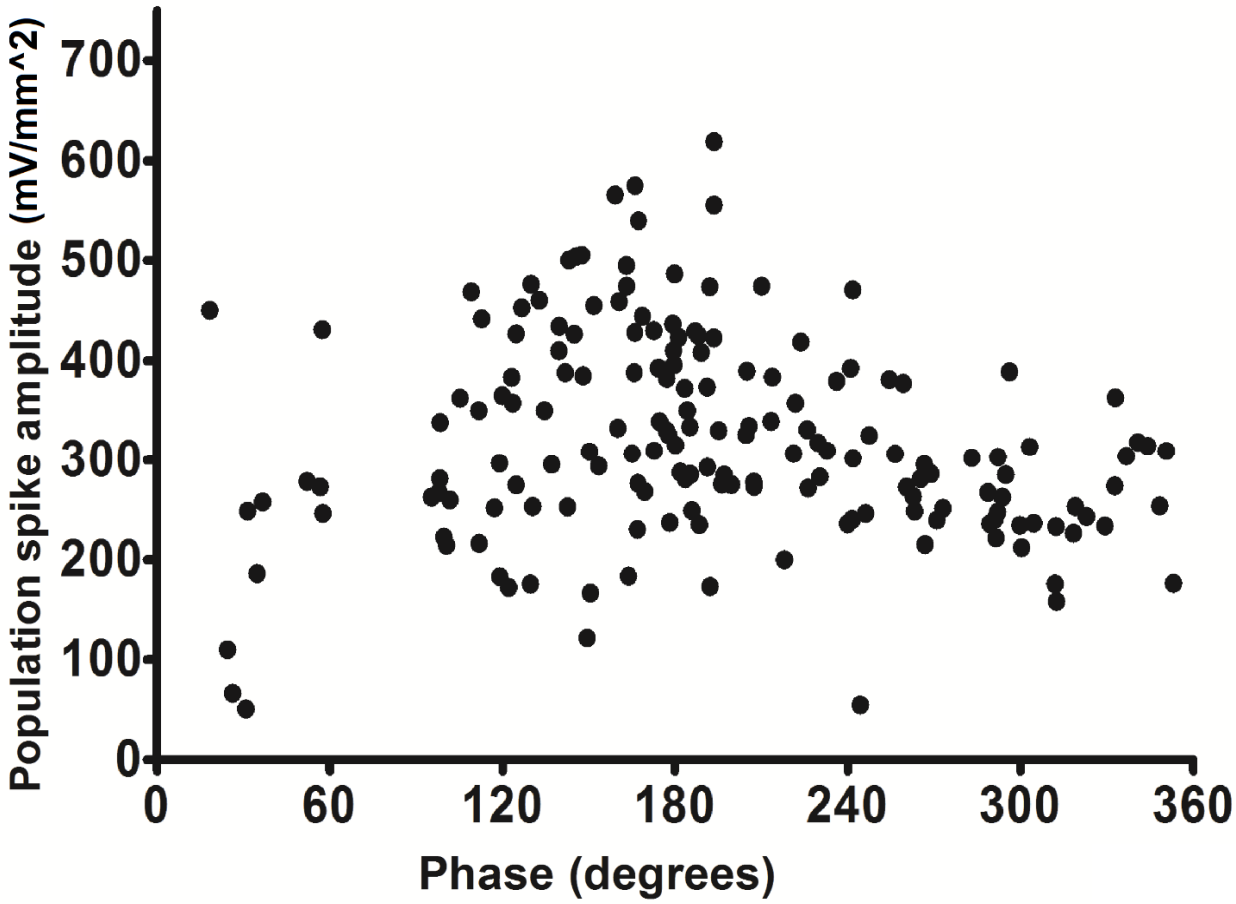

Figure 29. Population spike amplitude varied with the phase of hippocampal theta rhythm, shown in a representative rat (CL124). A single high intensity stimulating pulse (~1.5 x population spike threshold) was delivered to the basal dendrites, and phase was referenced to the extracellular theta rhythm at CA1 stratum lacunosummoleculare. Stimulating pulses were delivered at a frequency of 0.05 Hz and the population spike amplitude was measured from the cell body layer.

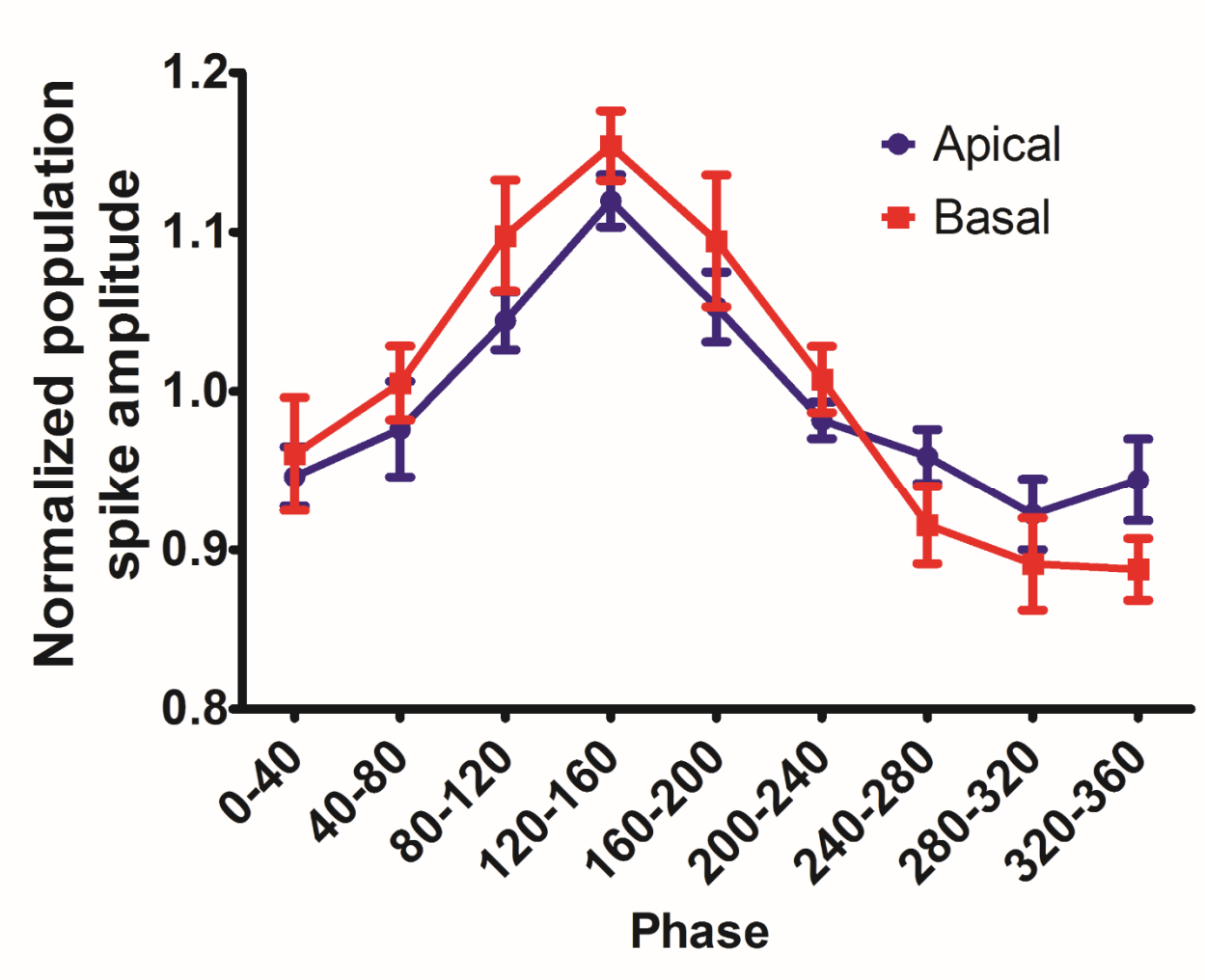

Figure 30. Grouped normalized CA1 population spike amplitudes show maximal excitability at the falling phase of theta rhythm recorded at the stratum lacunosummoleculare. The average normalized population spike amplitude of 25 rats was determined at each of the nine phase intervals of 40° range. Stimulation of either the basal (n=11) or apical (n=14) dendrites resulted in maximal excitability at 120°-160° phase (corresponding to the falling phase) and minimal excitability at 240°-360° (rising phase). Two-way ANOVA analysis showed a significant phase effect but no significant stimulation (basal versus apical) group effect.

3.4 Evoked population spikes during theta and non-theta activity

Population spikes were evoked in CA1 apical and basal dendrites during background theta and non-theta activity to elucidate how theta rhythm modulates excitability at different CA1 pyramidal cell synapses.

Single pulse high-intensity stimulation of the stratum oriens in CA3 evoked characteristic population spike profiles recorded by the 16-channel probe in CA1. The spike propagated from the basal dendrites through the cell body and into the apical dendrites **(Fig. 31A,B)**. Single pulse high-intensity stimulation of the stratum radiatum evoked characteristic population spike profiles in CA1 pyramidal cells, with the spike propagating from the proximal apical dendrites through the cell body and into the basal dendrites **(Fig. 31C,D)**.

From stimulating the apical dendrites, the amplitude of the population spike sink measured at the cell body was larger during non-theta activity compared to theta activity ($n=13$; $p < 0.001$; **Fig. 32A**). The mean amplitude of the evoked population spike sink during theta activity was 499.39 ± 320.08 mV/mm^2 compared to a mean amplitude of 780.57 ± 410.46 mV/mm^2 during non-theta activity. To confirm post-hoc that theta activity is distinct from non-theta activity, the ratio of theta to delta (integrated 1-2 Hz power) power was compared between theta and non-theta groups **(Fig. 32B)**. There was a significant difference in theta to delta ratio between theta and non-theta groups ($n=13$; $p < 0.001$).

From stimulating the basal dendrites, the population spike sink amplitude measured at the cell body was larger during theta activity compared to non-theta activity ($n=12$; $p < 0.001$; **Fig. 33A**). The mean amplitude of the evoked population spike sink during theta

activity was 246.55 ± 91 mV/mm^2 compared to a mean amplitude of 192.08 ± 65.46 mV/mm^2 during non-theta activity. To confirm post-hoc that theta activity is distinct from non-theta activity, the ratio of theta to delta (integrated 1-2 Hz power) power was compared between theta and non-theta groups **(Fig. 33B)**. There was a significant difference in theta to delta ratio between theta and non-theta groups ($n=12$; $p < 0.001$).

Overall, the amplitude of evoked population spikes was larger for apical stimulation compared to basal stimulation during both theta and non-theta activity ($p<0.05$ and $p<0.001$, respectively). Both groups showed a modulation of population spike amplitude by hippocampal theta rhythm: the amplitude of the population spike evoked from basal dendritic stimulation was greater during theta activity compared to non-theta activity, while the amplitude of the population spike evoked from apical dendritic stimulation was greater during non-theta activity compared to theta activity.

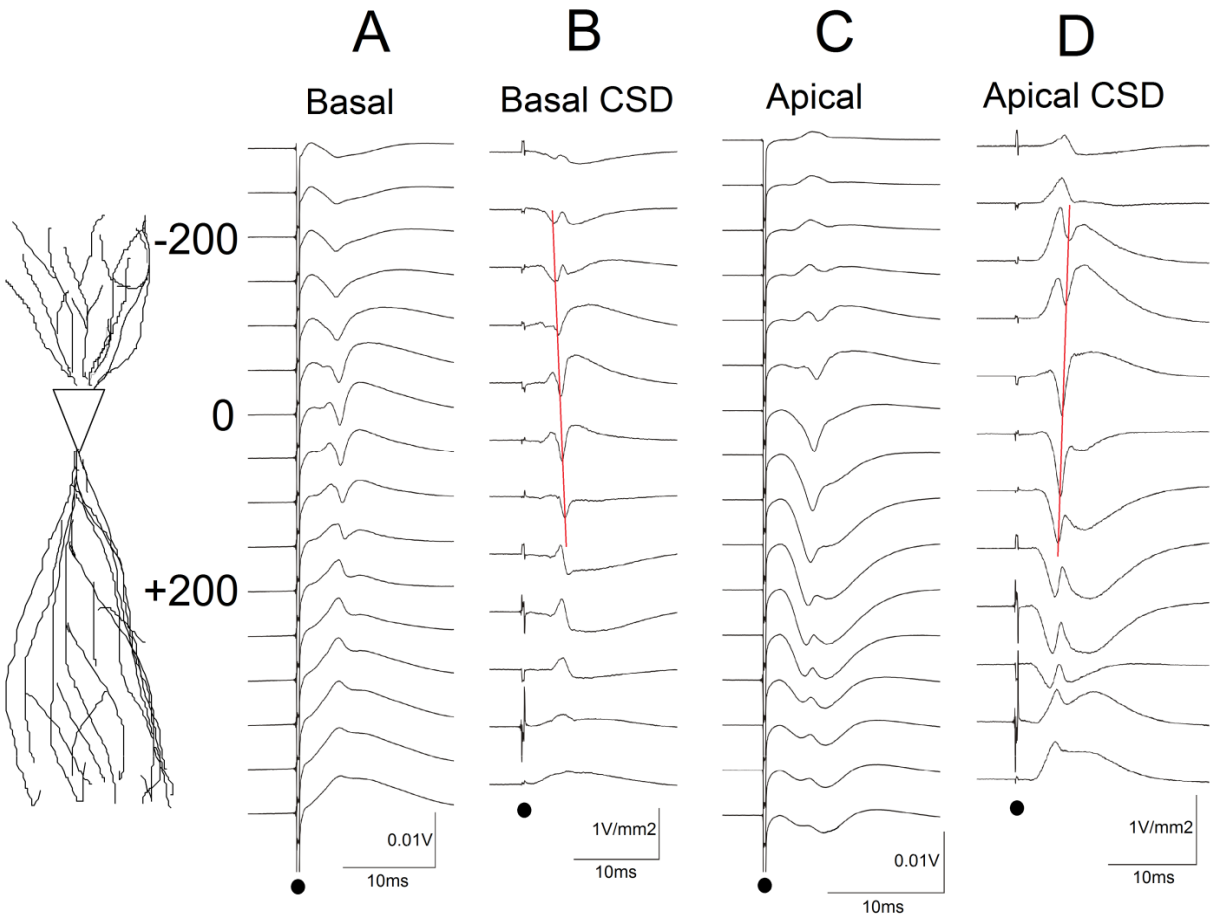

Figure 31. Average evoked potentials (AEPs: **A** and **C**) and current source density (CSD: **B** and **D**) transients in CA1 of representative rats following basal orthodromic excitation (CL122) and apical orthodromic excitation (CL097) at high intensity, evoking a population spike. Potentials were recorded simultaneously by a 16-channel electrode silicon probe with 50 µm interval between electrodes. Depths are indicated by the schematic CA1 pyramidal cell drawn and by the distance (in µm) away from the cell body layer (+ toward the apical dendrites; - toward the basal dendrites). Population spike peaks are linked with a red line, indicating propagation direction. **A:** Stimulation of CA3 stratum oriens at 450 µA (~1.5 x spiking threshold). **B:** CSD profiles derived from the AEPs shown in *A*. Stimulation of the stratum oriens in CA3 generated a basal dendritic spike in CA1 that propagated into the cell bodies and then into the apical dendrites. **C:** Stimulation of CA3 stratum radiatum at 450 µA (~1.5 x spiking threshold). **D:** CSD profiles derived from the AEPs shown in *C*. Stimulation of the stratum radiatum in CA3 generated an apical dendritic spike in CA1 that propagated into the cell bodies and then into the basal dendrites. Stimulation artifacts are indicated by the solid circle underneath.

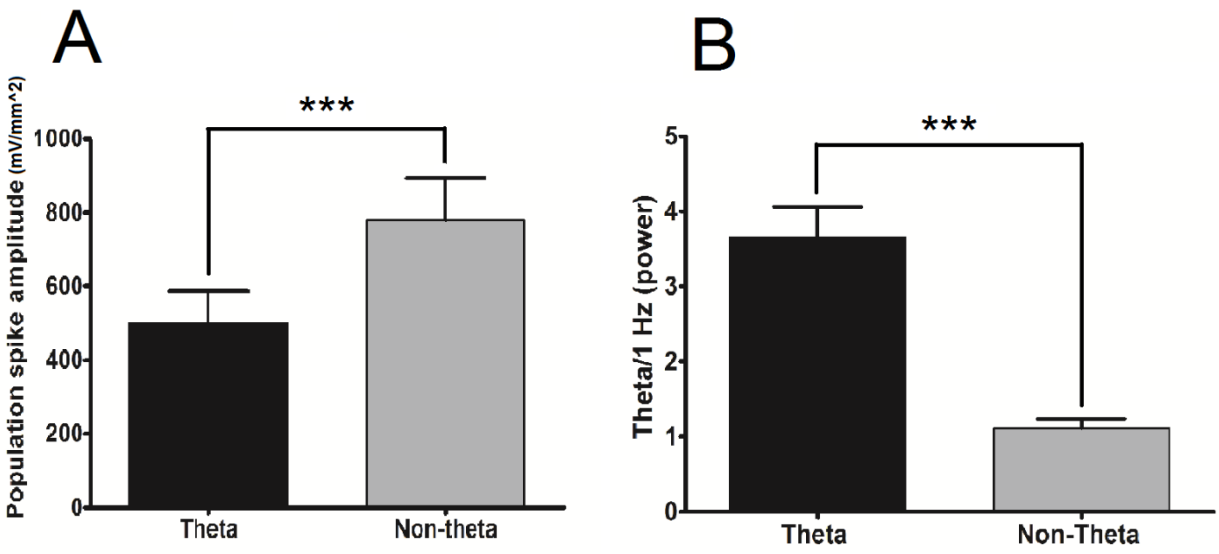

Figure 32. Excitability from apical dendritic stimulation during theta and non-theta activity. **(A)** Amplitude of the population spike evoked from apical dendritic stimulation during theta activity compared to non-theta activity (n=13). The amplitude of the population spike was measured at the cell body – typically channel 7/8 on the 16-channel probe.**(B)** Theta and non-theta groups were significantly different from each other by comparing the ratio of theta to delta power (n=13).*** P<0.001 difference, Wilcoxon matched-pairs rank sum test.

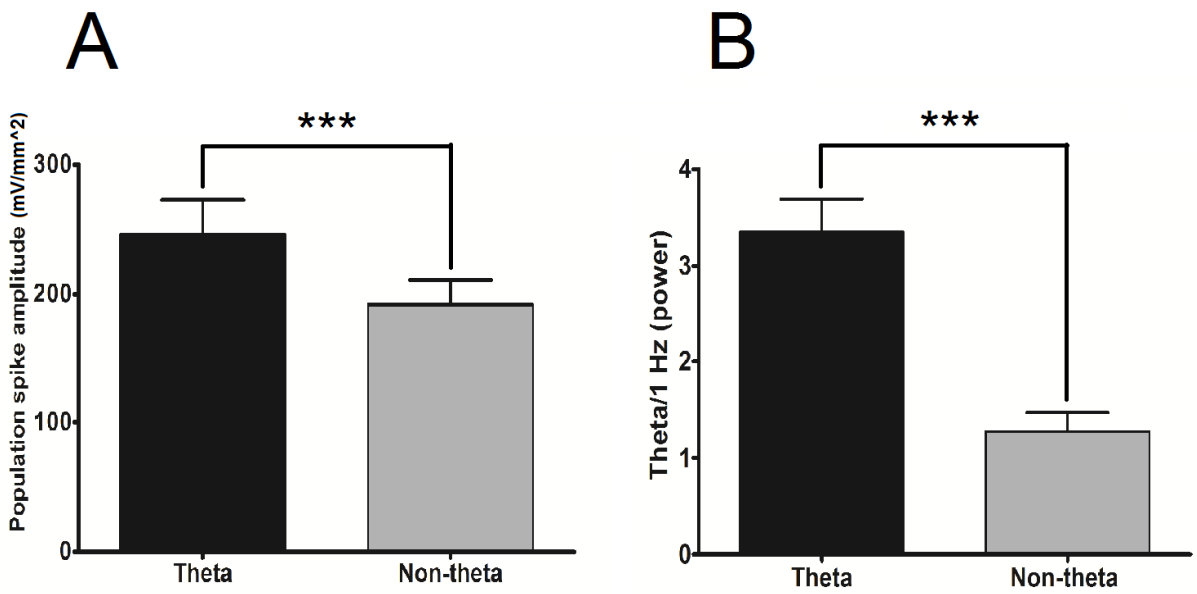

Figure 33. Excitability from basal dendritic stimulation during theta and non-theta activity. **(A)** Amplitude of the population spike evoked from basal dendritic stimulation during theta activity compared to non-theta activity (n=12). The amplitude of the population spike was measured at the cell body – typically channel 7/8 on the 16-channel probe. **(B)** Theta and non-theta groups were significantly different from each other by comparing the ratio of theta to delta power (n=12). *** P<0.001 difference, Wilcoxon matched-pairs rank sum test.

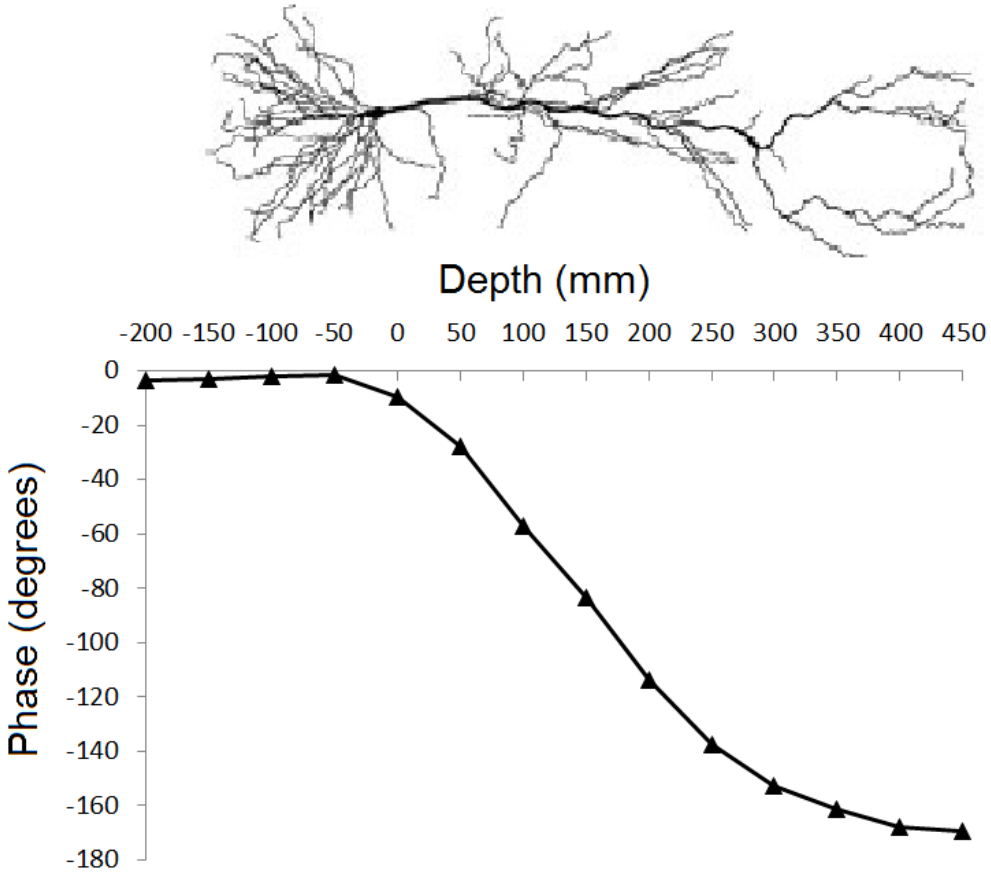

Figure 34. Phase profile of extracellular theta rhythm in the urethane-anaesthetized rat. Theta activity was simultaneously recorded from 16 sites in CA1 and averaged for 52 rats. Depth 0 indicates approximately the cell body layer. Negative depth is towards the basal dendrites, whereas positive depth is towards the apical dendrites. Phase shift from stratum oriens (-200 mm) to stratum lacunosummoleculare (450 mm) is almost 180°.

4. DISCUSSION

4.1 Confirmation of hypotheses

The results confirmed my four hypotheses. First, LTP at the basal and apical dendrites was maximal when the inducing burst stimulation was delivered during the rising phase of the theta rhythm recorded at stratum lacunosummoleculare (SLM), confirming my hypothesis that synaptic plasticity at the basal and apical dendrites is modulated by the theta rhythm. Second, when multiple bursts were delivered to the basal dendrites during different phases of theta rhythm, the magnitude of induced LTP was correlated to the degree to which bursts landed near the positive phase (reflected by the two combined phase indices), confirming my hypothesis that inducing bursts interact with each other to create a continuum of synaptic modification. Third, CA1 pyramidal cell excitability from basal and apical dendritic stimulation was maximal during the falling phase of theta rhythm, confirming my hypothesis that pyramidal cell excitability is modulated by different phases of the theta rhythm. Fourth, CA1 pyramidal cell excitability from apical stimulation was suppressed by theta rhythm, whereas excitability from basal stimulation was enhanced by theta rhythm, confirming my hypothesis that CA1 pyramidal cell excitability is affected by the occurrence of theta rhythm. These results will be further discussed as follows.

4.2 Theta-phase dependent LTP and LTD of the apical dendritic synapses by single burst stimulation induction

This study quantified the magnitude of apical LTP in relation to the phase of theta rhythm where stimulation occurred. My results provided a detailed dependence of apical LTP on

theta phase, which was not apparent in the literature. Holscher et al. (1997) only provided results of single burst stimulation at the peak of theta in urethane-anaesthetized rats, but did not quantify how close to the peak their burst stimulation occurred. I found LTD at the trough of theta rhythm with single burst stimulation, while they inferred only depotentiation of the previously potentiated response when multiple bursts were delivered to the trough. Similar to what Hyman et al. (2003) observed in the behaving rat, a single burst of stimulation to the apical dendrites during the negative phase of theta rhythm was sufficient to induce LTD. However, they used a theta reference at stratum radiatum, while I used a theta reference at SLM. Phase shift between stratum radiatum and SLM is minor (Ylinen et al., 1995); therefore our results can be comparable. My study used urethane-anaesthetized rats, and previous studies using urethane-anaesthetized rats only observed depotentiation from delivering 10 consecutive bursts of stimulation to the negative phase (Holscher et al., 1997). LTD may not have been observed in their study because there was no quantitative analysis of theta phase, and burst stimulation may have landed at any part of the negative phase. My study revealed that suppression of baseline fEPSPs occurred after single burst stimulation at the trough of the SLM theta rhythm (270°-298°). Since potentiation was not previously induced, the results should be interpreted as LTD, and not depotentiation. Depotentiation differs from genuine LTD in that depotentiation is a decrease in synaptic transmission from a previously potentiated state, whereas LTD is a decrease in synaptic transmission in naive synapses. Some studies argue that both phenomena may be closely related (Wagner and Alger, 1996). It is interesting that a single burst of stimulation was able to induce LTD at the apical dendritic synapses. A single burst of high frequency stimulation more resembles the

natural bursting activity of neurons in the hippocampus (Fox and Ranck, 1975). Therefore, my results provide a possible physiological mechanism by which LTD is induced in the hippocampus by brief high-frequency bursts.

A single burst of stimulation to the apical dendrites during the rising phase (334°-24°) of theta rhythm was able to induce LTP. LTP is most commonly induced through high-frequency, long-duration trains of stimulation. However, this type of stimulation also does not resemble physiological neuronal firing. One burst of stimulation was able to induce a 120% increase in the fEPSP slope compared to baseline (Holscher et al., 1997), whereas I observed a maximal increase of 126% in my study. The stimulation intensity used in my study was lower than that used by Holscher et al. (1997). Therefore, my study elicited relatively larger LTP with lower stimulus intensity. This discrepancy may be due to stimulation landing on different phases of the theta rhythm. Holscher et al. (1997) targeted the positive peak of theta rhythm, and although LTP was observed at that phase, it may not have been optimal for inducing maximal LTP. However, one burst of stimulation is unlikely to saturate LTP. LTP was saturated at 150% of the baseline response with either high-frequency tetanus or three bursts of stimulation delivered to the peak of theta rhythm (Holscher et al., 1997). Huerta and Lisman (1995) also reported LTP and LTD occurring from stimulating at different phases of the theta-frequency oscillation; however their experiments were performed on hippocampal slices in vitro, and theta oscillations were induced by carbachol. The in vitro condition may not mimic physiological conditions in vivo. Nonetheless, they found that LTP induced by phase stimulation was blocked by NMDA glutamate and muscarinic receptor antagonists at concentrations that inhibited theta. Therefore, theta phase-dependent synaptic plasticity

may be mediated by the NMDA receptor, consistent with what has been observed in area CA1 of the hippocampus (Collingridge et al., 1983; Zalutsky and Nicoll, 1990; Leung and Shen, 1999a).

4.3 Theta phase-dependent LTP of the basal dendritic synapses by single burst stimulation induction

A novel finding in my experiments was that synaptic plasticity at the basal dendrites was also modulated by hippocampal theta rhythm. Previous in vivo studies have only examined theta phase-dependent LTP at the apical dendritic synapses (Holscher et al., 1997; Hyman et al., 2003); however no study to date has examined the dependence of basal LTP on theta phase. Burst stimulation to the basal dendrites during the rising phase (306°-30°) of theta rhythm induced maximal LTP, whereas burst stimulation during the trough (215°-269°) of theta rhythm induced minimal LTP. As burst stimulation approached the rising phase of theta rhythm, the magnitude of induced LTP increased concomitantly. Therefore, synaptic plasticity at the basal dendrites is modulated by different phases of the theta rhythm. When burst stimulation was delivered to the rising phase of SLM theta, the basal excitatory sink slope increased by a maximum of 135% from baseline. This potentiation is similar to the 126% observed increase at the apical dendrites. It is worth noting that LTP was achieved by delivering only a single burst of inducing stimulation. Previous studies reporting basal LTP had to use either high-frequency tetanus or theta-primed burst protocols (Capocchi et al., 1992; Leung et al., 1992; Kaibara and Leung, 1993; Leung and Shen, 1995; Roth and Leung, 1995), which consist of more stimulating bursts or bursts of longer duration. Basal dendritic LTD was not observed after stimulation delivered at any phase of the theta rhythm. At the apical

dendrites, LTD can be induced when burst stimulation is delivered near the trough of the theta rhythm (Hyman et al., 2003).

4.4 Theta phase-dependent synaptic plasticity (differences between apical and basal dendrites)

The phase of theta rhythm for inducing maximal LTP at the basal and apical was the same (rising phase). Similarly, the least optimal phase for inducing LTP was found at the trough. However, only LTP occurred from stimulation at the basal dendrites, whereas apical dendritic stimulation could result in LTP or LTD. It appears that basal LTD cannot be elicited from stimulation at any phase of the theta rhythm. Previous studies have found that LTP is easier to induce at the basal dendritic synapses (Arai et al., 1994; Capocchi et al., 1992; Leung et al., 1992; Kaibara and Leung, 1993; Leung and Shen, 1995; Roth and Leung, 1995). Basal dendrites have a lower threshold for LTP in vivo. LTP can be readily induced with shorter duration theta-frequency bursts, and no LTD had been observed in previous studies in our laboratory (Leung et al., 1992, Kaibara and Leung, 1993; Leung and Shen, 1995; Roth and Leung, 1995; Leung and Shen, 1999). There may be several reasons for the lack of LTD from stimulating the basal dendrites. Basal dendrites are shorter and less branched (Ishizuka et al., 1995), which would allow for less electrotonic attenuation and higher depolarization levels for a given current (Henze et al., 1996). A higher depolarization would allow for stimulating bursts to open more NMDA receptor channels, leading to a greater influx of Ca^{2+}. The magnitude of rise in postsynaptic Ca^{2+} concentration determines whether LTP or LTD occurs, and LTP usually occurs when there is a greater rise in intracellular Ca^{2+} (Cummings et al., 1996; Nishiyama et al., 2000). It is also possible that theta phase-dependent synaptic plasticity has NMDA

receptor-dependent and NMDA receptor-independent components. Basal and apical dendrites of CA1 capable of expressing non-NMDA receptor dependent type of synaptic plasticity (Cavus and Teyler, 1998). NMDA receptor-independent plasticity still requires postsynaptic Ca^{2+} influx, activation of metabotropic glutamate receptors (mGluRs) and is blocked by L-type voltage-dependent calcium channel (VDCC) antagonists. A higher density of voltage dependent calcium channels (VDCCs) in the basal dendritic region compared to the apical dendritic region (Cavus and Teyler, 1998) can also contribute to greater Ca^{2+} influx at the basal dendrites; thus preferentially inducing LTP, as opposed to LTD.

There may be several reasons why LTD is preferred at the apical dendritic synapses compared to the basal dendritic synapses. Induction of LTD at homosynaptic sites requires functional ryanodine receptors (Nishiyama et al., 2000). The function of ryanodine receptors may differ at apical and basal compartments. Between burst hyperpolarization of the apical dendrites is greater than basal dendrites during theta burst stimulation, and long hyperpolarization after bursts due to activation of $GABA_B$ receptors is smaller with basal stimulation than apical. Blocking this hyperpolarization allowed apical LTP levels to reach that of basal dendrites (raised LTP ceiling). Later EPSPs in a stimulating burst are severely reduced by fast IPSPs generated by inhibitory interneurons and mediated by $GABA_A$ receptors (Larson and Lynch, 1986; Mott and Lewis, 1991). Fast IPSPs were smaller when equal sized EPSPs were generated by inputs to stratum oriens versus stratum radiatum (Arai et al., 1994). Immunocytochemically defined (calbindin containing) populations of GABA positive interneurons are present in higher numbers in apical dendritic field of CA1 than in basal regions (Toth and Freund, 1992).

Therefore, inhibitory signaling is different between apical and basal dendrites. However, the density of $GABA_A$ and $GABA_B$ receptors is not significantly different between stratum oriens and stratum radiatum (Chu et al., 1990). Therefore, differential postsynaptic response to interneuron activation is not likely to be a significant factor in shaping inhibitory responses to basal versus apical inputs. However, the number of interneurons stimulated by afferents when generating equivalent depolarization may be different, and this may be related to the morphology of dendritic trees. Apical dendrites have one or two main shafts from which emerge a collection of fine secondary and tertiary branches. Basal dendrites are composed of a number of primary dendrites, which may allow for better spatial summation. Thus fewer afferents would be needed to generate an equivalent depolarization sufficient to unblock NMDA receptors or activate larger number of L-type VDCCs at the basal dendrites, and fewer interneurons would also be activated. Distribution of inhibitory interneurons may also play a role. The proportion of inhibitory inputs on oriens dendrites is lower than radiatum dendrites (Megias et al., 2001). Greater inhibitory signaling at the apical dendrites may attenuate activation of NMDA receptors or L-type VDCCs; thus limiting the amount of postsynaptic Ca^{2+} influx, and allowing LTD to occur under the right conditions.

The role of NMDA receptors may also differ between basal and apical compartments. NMDA receptors in the brain are heterogeneous, and receptors with different subunits may have different affinity for glutamate and NMDA receptor antagonists (Monaghan et al., 1988; Monyer et al., 1994; McBain and Mayer; 1994). The NMDA receptor is composed of hetero-oligomer subunits (NR1, NR2 and occasionally NR3) (Cull-Candy et al., 2001). The structure requires two obligatory NR1 subunits and two regulatory

subunits that can be NR2 or NR3. Four distinct subtypes (NR2 A,B,C,D) exist in the NR2 family. NR2A and NR2B subunits mostly dominate the rat hippocampus (Watanabe et al., 1993; Monyer et al., 1994; Wenzel et al., 1995; Dunah et al., 1996; Fritschy et al., 1998). NMDA receptor subunits have been implicated in determining the direction of synaptic plasticity: NR2A is important for LTD, while NR2B is important for LTP (reviewed by Yashiro and Philpot, 2008). A ratio of NR2A:NR2B has been proposed to determine the direction of synaptic plasticity. Thus, synapses with a higher ratio would favour LTD, whereas synapses with a lower ratio would favour LTP. Apical LTP is more resistant than basal LTP to NMDA receptor antagonists (Leung and Shen, 1999b). It is possible that synergistic opening of both NMDA and high-threshold Ca^{2+} channels contribute to the critical amount of intracellular Ca^{2+} required for LTP and LTD.

Nitric oxide synthase (NOS) has also been implicated in the induction of LTP, particularly eNOS (endothelial form) and nNOS (neuronal form). Mice with double mutation of eNOS and nNOS show significantly reduced LTP, compared to mice with only a single isoform mutation. Distribution of eNOS is not uniform within the CA1 pyramidal cell, present in cell body and apical dendrites, but absent from basal dendrites. LTP induction in stratum radiatum synapses has NOS-dependent and NOS-independent components, whereas stratum oriens LTP is fully NOS-independent (Haley et al., 1996; Son et al., 1996). The involvement of NOS with LTD is controversial. Izumi and Zorumski (1993) reported that LTD was blocked by NOS inhibitors, whereas Cummings et al. (1994) reported that LTD was not blocked by NOS inhibitors. eNOS and nNOS double mutants show partially reduced LTD, but the effect was not significant (Son et al., 1996). Therefore, NOS may play some role in the induction of LTD, and the differential

distribution NOS isoforms at basal and apical compartments may explain observed differences in LTD induced by theta-phase dependent burst stimulation. Apical dendrites express NOS-dependent components of LTP; therefore it is possible that LTD at the apical dendrites is also mediated by NOS, whereas the basal dendrites tend to express NOS-independent synaptic plasticity. Therefore, if theta phase-dependent plasticity has NOS-dependent components, it would be less likely for basal dendrites to express LTD.

	Basal Dendritic Synapses	Apical dendritic synapses
Stimulation parameter	Single burst (5 pulses @ 200 Hz)	Single burst (5 pulses @ 200 Hz)
Stimulation intensity	~3.5x threshold intensity for inducing bursts 1.5x threshold for test pulses	~3.5x threshold intensity for inducing bursts 1.5x threshold for test pulses
Reference theta	SLM	SLM
Response analysis	EPSP slope	EPSP slope
Level of analysis	Stratum oriens sink	Stratum radiatum sink
Optimal phase for LTP	Rising phase (306°-30°)	Rising phase (334°-24°)
Optimal phase for LTD	No LTD observed	Trough

Table 1. Comparison between experimental paradigms where a single stimulating burst was delivered to either the basal or apical dendrites.

4.5 Optimal phase of theta rhythm for inducing synaptic plasticity

From previous in vivo studies, the optimal phase for inducing LTP was at the peak of extracellular stratum radiatum theta. The optimal phase for inducing LTD was at the trough, although this was only observed in behaving rats (Holscher et al., 1997; Hyman et al., 2003). Although these studies only used a qualitative phase analysis, they still attempted to deliver stimulation during other phases of the theta rhythm (i.e., falling phase and rising phase). Delivering stimulation at the rising and falling phase did not induce LTP or LTD. However, our experiments showed that a gradient of LTP exists as stimulation approaches the optimal phase for maximal LTP. A gradient of synaptic modulation is likely to exist physiologically because this allows for greater diversity in processing information. Furthermore, my experiments showed that maximal LTP occurred at the rising phase of SLM theta. Some phase shift in the theta rhythm may occur from the stratum radiatum to SLM (Leung, 1984; Ylinen et al., 1995). Thus the peak of stratum radiatum theta could correspond to somewhere close to the rising phase of SLM theta. This phase of theta rhythm is proposed to correspond to the optimal conditions for inducing LTP. During the peak of stratum radiatum theta, membrane depolarization may be at its greatest, while Ca^{2+} levels are large enough at the apical dendrites to elicit high-threshold spikes, and are therefore likely to create the appropriate dynamics for LTP (Cummings et al., 1996). As the theta wave reaches its trough, intracellular membrane potential levels decrease along with Ca^{2+}, but Ca^{2+} levels at the dendrites are still elevated enough to create the appropriate dynamics for LTD (Cummings et al., 1996). Levels of depolarization are significant for inducing synaptic plasticity because activation of the NMDA receptor requires sufficient depolarization to

relieve the Mg^{2+} block. Sufficient levels of depolarization are also needed to activate VDCCs, which may be involved in non-NMDA receptor dependent types of synaptic plasticity. LTP and LTD in CA1 are both proposed to be NMDA receptor-dependent phenomena, but some studies have observed NMDA-receptor independent synaptic plasticity in CA1 (Grover and Teyler, 1990; Cavus and Teyler, 1998). Therefore, the degree to which NMDA receptors are activated plays a significant role in determining the direction of synaptic plasticity. The modulation of synaptic plasticity by different phases of the theta rhythm supports the model of hippocampal function proposed by Hasselmo et al. (2002). In this model, synaptic input from the entorhinal cortex is at its greatest at the peak of pyramidal layer theta and weakest at the trough of pyramidal layer theta. Thus entorhinal input is weakest at the peak of stratum radiatum theta, and CA3 to CA1 connections are most active at this time, promoting LTP. If LTP was possible during the time of strongest entorhinal input (trough of radiatum theta), this could interfere with previously stored associations. Hyman et al. (2003) predicted that the peak induction of LTP might be 80° before the weakest entorhinal cortex input, which corresponds to the rising phase of stratum radiatum or SLM theta. Therefore, the results from this study agree with Hyman's prediction.

Due to the phase shifting that could occur at the level of stratum radiatum, using a phase reference where theta is known to experience less shift may provide more consistent interpretation of results. The difficulty in interpreting theta phase is compounded by the fact that different experiments use different phase references, and the animals' behavioural state influences the theta profile. In my study, I used a phase reference at the SLM because this was where theta amplitude was at its greatest. Amplitude of theta was

important for the peak detection program, and extending the recording probe into the hippocampal fissure would be too deep to record the stratum oriens response. However, an attempt was made to reference a consistent theta at the level of stratum oriens/alveus. By using this phase reference, a better correlation was observed between the phase of theta rhythm where stimulation occurred and the magnitude of induced LTP. The optimal phase of stratum oriens/alveus theta for inducing LTP was at the falling phase, which is consistent with the approximate 180° phase shift that occurs from stratum oriens to SLM (Ylinen et al., 1995). The extracellular theta rhythm profile in my study also showed a phase reversal of approximately 180° from stratum oriens to SLM **(Fig. 34)**. Therefore, future studies would benefit from using a more stable phase reference either at the level of stratum oriens/alveus or the hippocampal fissure.

4.6 Multiple bursts delivered to different phases of theta rhythm

A greater magnitude of induced basal dendritic LTP was found when multiple stimulation bursts were delivered to the basal dendritic synapses at the positive phase of the SLM theta rhythm. Similar to what was observed for single burst experiments, LTD did not occur from burst stimulation during the negative phase. A brief comparison between the two experimental paradigms can be found in **Table 2**. Using the sum alignment of multiple bursts to the negative versus the positive peak of theta, it may be inferred that stimulation of the basal dendrites during the negative phase of theta rhythm may contribute very little to synaptic plasticity, inducing neither LTD nor depotentiation. These findings are consistent with previous experiments that found apical dendritic LTP when multiple bursts were delivered specifically to the peak of theta rhythm (Holscher et al., 1997; Hyman et al., 2003). However, my experiments were the first to show that

different magnitudes of potentiation can be achieved when bursts are delivered to different phases of theta rhythm, suggesting that synaptic efficacy can be modulated to a fine degree when bursts do not land on the same phase. Study of physiological neuronal firing patterns show that CA3 pyramidal cells can fire at all phases of theta rhythm with no particular phase preference (Fox et al., 1986). Therefore, my experiments more closely mimic physiological conditions. However, interpreting the results from multiple burst experiments may be difficult because the contribution of each burst to synaptic plasticity is unknown. Temporal sequence of bursts, and saturation of LTP are likely to play a role in how synapses are modified.

	Single burst	Multiple burst
Stimulation parameter	Single burst (5 pulses @ 200 Hz)	5 bursts of 4-6 pulses/burst with interpulse frequency of 200 Hz Minimum interburst frequency of 4 seconds
Stimulation intensity	~3.5 x threshold intensity for inducing bursts 1.5x threshold for test pulses	~2.5-3 x threshold intensity for inducing bursts 1.5x threshold for test pulses
Reference theta	SLM	SLM
Response Analysis	EPSP slope	EPSP slope
Phase analysis	Raw phase	Combined phase index (CPI) Positive combined phase index (PPI)
Optimal phase for LTP	Rising phase (306°-30°)	Positive phase (0°-180°)
Optimal phase for LTD	No LTD observed	No LTD observed

Table 2. Comparison between single burst and multiburst experiments. Single burst experiments are those where a single burst was delivered to the basal dendrites during different phases of theta rhythm in an attempt to induce either LTP or LTD. Multiburst experiments are those where multiple bursts were delivered to the basal dendrites during different phases of the theta rhythm in an attempt to induce either LTP or LTD.

4.7 Modulation of CA1 pyramidal cell excitability by different phases of theta rhythm

A population spike is an increasing function of the number of synchronously discharging cells (Andersen, 1971). Thus, a larger population spike corresponds to a greater number of cells firing in synchrony. At low stimulation intensities, increases in the population spike amplitude correspond to an increase in the recruitment of units. However, at higher stimulation intensities, an increase in the population spike amplitude is likely due to an increase in synchrony of neuronal firing (Leung and Au, 1994). The optimal phase for CA1 pyramidal cell excitability may correspond to when membrane depolarization levels are at their highest, making it more likely for cells to reach firing threshold from afferent stimulation; thus increasing population recruitment. Similar to what was observed by Kloosterman et al. (2001), basal dendritic excitation evoked a spike that started near the cell body or initial segment and then invaded the proximal apical dendrites. Apical dendritic excitation resulted in an orthodromic spike that started at the proximal apical dendrites and propagated to the cell body and basal dendrites. In contrast, low-threshold stimulus in vitro initiates an action potential at the initial segment (Spruston et al., 1995; Stuart et al., 1997) or the axon (Colbert and Johnston, 1996). Low intensity stimulation may induce action potentials at the axon or initial segment of single neurons, but they may be too temporally dispersed to result in a population spike (Andersen et al., 1971). Spike sinks are mediated by voltage-dependent Na^+ currents (Miyakawa and Kato, 1986; Turner et al., 1989). Therefore greater depolarization during stimulation onset is likely to increase unit recruitment: greater depolarization at the level of the cell body or initial segment is likely to produce a larger population spike from basal dendritic excitation, whereas the population spike from apical excitation is likely to depend on depolarization

at the proximal apical dendrites. My results show that the largest evoked population spike occurs at the falling phase (120°-160°) of SLM theta for both apical and basal dendritic stimulation. Similar to my observations from LTP experiments, an increasing gradient of excitability exists as stimulation approaches the optimal phase. Many studies have investigated neuronal firing and excitability in relation to the theta rhythm, and my results are in agreement with their findings. The maximum EPSP occurred when stimulation landed on the falling phase of theta rhythm in a study by Schall et al. (2008); however their reference theta was unclear. Presumably, it was at the level of stratum radiatum which would be in phase with the dentate theta that other studies used as a reference (Ylinen et al., 1995). Action potentials in CA1 tend to be phase locked to the negative peak of extracellular theta recorded from CA1 pyramidal cell layer (Ylinen et al., 1995), and the phase of maximum firing of pyramidal cells in CA1 is narrowly distributed around the positive peak of dentate theta (Fox et al., 1986). The phase of maximum firing corresponds to when cells are most excitable or closest to threshold potential; hence why the amplitude of the evoked population spike is also largest during this phase. In a separate study by Kamondi et al. (1998), the probability of pyramidal cell discharge was highest at or slightly after the negative peak of extracellular theta at the pyramidal cell layer. Pyramidal cells can be discharged with the least amount of excitation during the negative phase of pyramidal cell layer theta, which also explains why peak discharge of the CA1 cell population is phase-locked to the negative phase. However, if the stimulation intensity is too high, the probability of discharging cells increases; thus variation in population spike amplitude will less likely be observed. I used a moderate stimulation intensity (~1.5 x spiking threshold) in my study so that sensitive changes in

the population spike amplitude can be observed. With reference to the dentate theta, a maximum excitability evoked by apical dendritic (or commissural stimulation) was located slightly after the positive peak for urethane-anaesthetized rats (Wyble et al., 2000; Rudell and Fox, 1984). In walking rats however, the phase of maximum excitability shifted later in the theta cycle at 111° after the positive peak (Rudell et al., 1980). The smallest EPSPs, however, were evoked 198° after the peak of dentate theta, which corresponds to the trough (288°) of the dentate theta (Wyble et al., 2000). Dentate and SLM theta were similar in phase, and in my experiments, apical stimulation resulted in lowest cell excitability from 280°-320° of the SLM theta, confirming results from previous studies. However, basal stimulation resulted in lowest cell excitability from 320°-360°, although this was not significantly different from the excitability found at 280°-320°. Therefore, the results from apical and basal dendritic stimulation experiments agree with each other. In summary, maximum excitability of CA1 pyramidal cells from apical stimulation is likely to be near the falling phase of SLM theta, and minimum excitability is near the trough. My study was the first to examine how theta rhythm modulates CA1 pyramidal cell excitability from basal dendritic stimulation, and results support the idea that the falling phase of SLM theta corresponds to when the CA1 pyramidal cell is most excitable, whereas the trough corresponds to when the CA1 pyramidal cell is least excitable. The falling phase of SLM theta likely corresponds to when somatic hyperpolarization is minimal.

4.8 Modulation of CA1 pyramidal cell excitability by theta rhythm

CA1 pyramidal cell excitability is not only modulated by different phases of the theta rhythm, but also by the presence of theta rhythm itself. Excitability from apical dendritic

stimulation was suppressed during theta activity, compared to non-theta activity, whereas excitability from basal dendritic stimulation was greater during theta activity, compared to non-theta activity. My results are in agreement with previous findings that both CA1 population spike amplitude and apical evoked EPSPs were suppressed during theta activity (Herreras et al., 1988; Wyble et al., 2000; Leung, 1980). PnO stimulation releases acetylcholine in the hippocampus and results in a 4-7.5 Hz hippocampal theta rhythm (Leung and Peloquin, 2010). Endogenous acetylcholine release in the hippocampus is normally accompanied by hippocampal theta rhythm (Dudar et al., 1979; Keita et al., 2000). PnO activation of the hippocampus decreases the evoked apical excitatory sink and population spike (Leung and Peloquin, 2010). In my study, non-theta activity was predominantly slow-wave activity with a larger power from the 1-2 Hz (delta) range. The non-theta activity classified in my study may resemble the slow oscillations (SO) defined by Schall et al. (2008). Apical dendritic evoked potentials were enhanced during SO compared to periods of theta rhythm. The inhibitory system operating at the apical dendritic level may be involved with the reduction in population spike amplitude from apical dendritic stimulation (Herreras et al., 1988b). Presynaptic inhibition of excitatory fibers in the hippocampus (Schaeffer collaterals) may also play a role (Valentino and Dingledine, 1981; Hounsgaard, 1978). In summary, my results are consistent with previous findings that CA1 pyramidal cell excitability from apical stimulation is suppressed by theta rhythm. However, I present a novel finding that CA1 pyramidal cell excitability from basal stimulation is enhanced by spontaneously occurring theta rhythm. Hippocampal theta rhythm elicited by PnO stimulation also enhances the basal dendritic population spike. The differential modulation of basal and apical dendritic excitation by

PnO stimulation is believed to be facilitated by acetylcholine. In vitro perfusion of the hippocampal slice with carbachol, a cholinergic agonist, attenuates the apical dendritic EPSP more than the basal dendritic EPSP. Endogenous acetylcholine mediates stronger presynaptic inhibition of the midapical dendrites than basal dendrites mainly through M1 muscarinic receptors (Leung and Peloquin, 2010). Therefore, apical dendritic synapses are less excitable during periods of theta activity when acetylcholine release is high. Acetylcholine may block K^+ conductance in pyramidal cells, enhances cation channels (Dutar and Nicoll, 1988; Fisahn et al., 2002), and decreases inhibition (Yim and Leung, 1988; Behrends and ten Bruggencate, 1993), resulting in increased depolarization and spiking from basal dendritic stimulation. It is also possible that septohippocampal GABAergic neuron activation during theta rhythm inhibits hippocampal inhibitory interneurons; thus providing disinhibition of pyramidal cells (Freund and Buzsáki, 1996; Toth et al., 1997).

4.9 Relation of spike excitability to synaptic plasticity

Synaptic plasticity and spike excitability are both events that depend on the level of membrane depolarization. An intracellular theta oscillation in membrane potential exists during theta rhythm, and providing a model of theta generation may assist in interpreting results where the depths of extracellular reference theta are different. The theta profile in the behaving rat shows a gradual phase shift across stratum radiatum. However, once the entorhinal cortex (EC) is lesioned, the theta profile resembles that of urethane-anaesthetized rats (Ylinen et al., 1995; Kamondi et al.,1998). This suggests that theta generation in the behaving rat may be due to two inputs: one IPSP input at the level of the soma, and an excitatory input at the level of the distal apical dendrites. These two inputs

are out of phase with each other: rhythmic hyperpolarization at the soma of principal cells by their interneurons precedes rhythmic dendritic excitation by perforant path input (Buzsáki et al., 1983; Buzsáki et al., 1986). The theta profile in urethane-anaesthetized rats is believed to be driven by only a somatic IPSP input, although a weak distal apical dendritic input may also be present, depending on the depth of anaesthesia. The peak of intracellular depolarization slightly lagged behind the trough of local extracellular theta at the pyramidal cell layer by 0°-60° (Ylinen et al., 1995). Kamondi et al. (1998) found similar results where the peak of somatic depolarization corresponded to the negative phase of pyramidal cell layer theta; thus that should be where CA1 pyramidal cell discharge should be at its greatest. However, the depolarizing phase of intradendritic theta coincided with the positive phase of pyramidal cell layer theta. Therefore, somatic hyperpolarization and dendritic depolarization appear to be mainly in phase. The negative phase of pyramidal cell layer theta corresponds to approximately the positive phase of SLM theta in the urethane-anaesthetized rat because theta rhythm phases shifts approximately 180° in urethane-anaesthetized rats (Ylinen et al., 1995).

From my experiments, stimulation during the rising phase was optimal for inducing maximal LTP, whereas stimulation during the falling phase resulted in greatest CA1 pyramidal cell excitability (comparison between the two paradigms can be found in **Table 1**). Although I used a phase reference at the SLM, this does not fully explain the discrepancy in my findings. Previous studies that used a stratum radiatum reference found that LTP was induced at the peak, whereas the falling phase corresponded to where cell excitability was at its greatest. This suggests <90° difference in the optimal phase that LTP and cell excitability occurred, although Hasslemo et al. (2005) argued for

difference phases of LTP and cell excitability. However, in my study, I found an almost 180° phase difference between optimal phase for LTP and cell excitability. The most parsimonious explanation is that somatic hyperpolarization and dendritic depolarization occur at the same phase of theta rhythm in the urethane-anaesthetized rat (Kamondi et al., 1998). Cell excitability, as measured from the population spike at the pyramidal cell layer, depends on depolarization of the soma. However, the excitatory response at the basal and apical dendrites depends on the level of depolarization at these dendritic compartments. Thus, optimal phase for inducing synaptic plasticity at the dendrites and exciting the cell body should be approximately 180° apart. In previous studies, the optimal phase for LTP was 180° after the least optimal phase for LTP. Assuming intracellular theta oscillates at the same frequency, these phases should correspond to when the membrane potential is most depolarized and hyperpolarized. However, the intracellular theta oscillation is always less regular than rhythmicity of the extracellular theta (Ylinen et al., 1995); therefore the phase of extracellular theta may not always correspond to the same intracellular phase. In my study, I found that the optimal phase for inducing LTP closely followed the least optimal phase for inducing LTP (approximately 90° phase difference). It is possible that the hyperpolarizing phase is necessary to remove inactivation of T-type Ca^{2+} channels (Makram and Sakmann, 1994); thus increasing Ca^{2+} entry during the rising phase. High intracellular Ca^{2+} levels favour the induction of LTP. Thus, burst stimulation during the rising phase activates NMDA receptors, allowing Ca^{2+} to flow into the cell. This event coupled with the inactivation of T-type Ca^{2+} channels presents the optimal conditions for LTP, where intracellular Ca^{2+}concentrations are highest.

CA1 pyramidal cell excitability was lowest at the trough of SLM theta. Although this also corresponds to the phase where apical LTD can be induced from single burst stimulation, LTD is not likely a result of dendritic depolarization levels being at their lowest. Somatic hyperpolarization and dendritic depolarization occur at the same phase of theta rhythm; therefore the phase of theta rhythm where population spike excitability is lowest should correspond to when the dendrites are most depolarized. Although the phase for optimal LTP at the apical dendrites (rising phase) does not correspond to the trough, it is likely that dendritic depolarization is still elevated during this phase. Elevated depolarization levels will allow for activation of some NMDA-receptors, but less than if depolarization was at its highest. Therefore, stimulation delivered during the trough of theta rhythm results in a moderate Ca^{2+} influx. LTD occurs when intracellular Ca^{2+} levels are lower, yet still elevated, whereas LTP occurs when Ca^{2+} levels are at their highest (Cummings et al., 1996). Burst stimulation delivered to the apical dendrites during a time of lowest depolarization is unlikely to result in neither LTP nor LTD due to insufficient activation of NMDA receptors. Therefore, the trough of SLM theta may correspond to when apical dendritic depolarization levels are elevated, but not at their maximum, providing the optimal conditions for LTD to occur.

	Synaptic plasticity	Excitability
Stimulation parameter	Single burst (5 pulses @ 200 Hz)	Single pulse
Stimulation intensity	~3.5x threshold intensity for inducing bursts 1.5x threshold for test pulses	1.5x threshold intensity for inducing population spike
Reference theta	SLM	SLM
Response analysis	EPSP slope	Population spike amplitude
Level of analysis	Stratum oriens or stratum radiatum sink	Pyramidal cell layer
Optimal theta phase	Rising phase for LTP Trough for LTD at apical dendrites only	Greatest excitability at falling phase Least excitability at trough
Basal versus apical dendrites	LTD observed only at apical dendrites	No difference

Table 3. Comparison between synaptic plasticity and excitability experiments. Synaptic plasticity experiments are those where a single burst was delivered during different phases of theta rhythm in an attempt to induce either LTP or LTD. Excitability experiments are those where a single high intensity pulse, sufficient to evoke a population spike, was delivered during different phases of the theta rhythm.

4.10 Conclusion

In this study, I demonstrate, for the first time, that synaptic plasticity at the basal dendrites is modulated by the hippocampal theta rhythm. CA1 pyramidal cell excitability from basal stimulation is also modulated by different phases of the theta rhythm, and theta rhythm enhances cell excitability arising from basal dendritic stimulation. A gradient of increasing excitability was observed as stimulation approached the falling phase of theta rhythm, while a gradient of increasing LTP was observed as stimulation approached the rising phase. The optimal phase for inducing LTP at the basal and apical dendrites is at the rising of SLM theta, whereas the least optimal phase is at the trough. Stimulation of the apical dendrites during the trough of theta resulted in LTD, whereas for the basal dendrites, trough stimulation did not induce LTD. The experimental finding that the optimal phase for LTP and cell excitability are approximately 180° apart is consistent with the finding that somatic hyperpolarization and dendritic depolarization occur at the same phase of theta in the urethane-anesthetized rat. The optimal phase for LTP follows the least optimal phase for LTP because the hyperpolarizing phase is necessary to remove inactivation of T-type Ca^{2+} channels, which in turn contribute to the induction of LTP. Synaptic plasticity at the basal dendrites was modulated in a unidirectional manner, only favouring LTP, whereas the apical dendrites were susceptible to bidirectional modulation, favouring either LTP or LTD. My results propose a physiological mechanism by which synaptic plasticity in CA1 can be modulated by the hippocampal theta rhythm.

5. REFERENCES

Abraham WC (2003). How long will long-term potentiation last?.*Philosophical Transactions of the Royal Society B: Biological Sciences*, *358*(1432), 735-744.

Abraham WC, Otani S (1991). Macromolecules and the maintenance of long-term potentiation. *Kindling and synaptic plasticity*, 92-109.

Abraham WC, Williams JM (2003). Properties and mechanisms of LTP maintenance. *The Neuroscientist*, *9*(6), 463-474.

Alger BE, Nicoll RA (1982). Feed-forward dendritic inhibition in rat hippocampal pyramidal cells studied in vitro. *The Journal of Physiology*, *328*(1), 105-123.

Amaral DG, Witter MP (1989). The three-dimensional organization of the hippocampal formation: a review of anatomical data. *Neuroscience*, *31*(3), 571-591.

Andersen P, Bliss TVP, Skrede KK (1971). Lamellar organization of hippocampal excitatory pathways. *Experimental Brain Research*, *13*(2), 222-238.

Arai A, Black J, Lynch G (1994). Origins of the variations in long-term potentiation between synapses in the basal versus apical dendrites of hippocampal neurons. Hippocampus 4, 1-9.

Bashir ZI, Jane DE, Sunter DC, Watkins JC, Collingridge GL (1993). Metabotropic glutamate receptors contribute to the induction of long-term depression in the CA1 region of the hippocampus. *European journal of pharmacology*, *239*(1), 265-266.

Bashir ZI, Collingridge GL (1994). An investigation of depotentiation of long-term potentiation in the CA1 region of the hippocampus. *Experimental brain research*, *79*(2), 437-443.

Bear MF, Abraham WC (1996). Long-term depression in hippocampus. Annu Rev Neurosci*19*: 437–62.

Bi GQ, Poo MM (2001). Synaptic modification by correlated activity: Hebb's postulate revisited. *Annual review of neuroscience*, *24*(1), 139-166.

Bienenstock EL, Cooper LN, Munro PW (1982). Theory for the development of neuron selectivity: orientation specificity and binocular interaction in visual cortex. *The Journal of Neuroscience*, *2*(1), 32-48.

Behrends JC, ten Bruggencate G (1993). Cholinergic modulation of synaptic inhibition in the guinea pig hippocampus in vitro: excitation of GABAergic interneurons and inhibition of GABA-release. *Journal of Neurophysiology*, *69*(2), 626-629.

Benke TA, Luthi A, Isaac JT, Collingridge GL (1998). Modulation of AMPA receptor unitary conductance by synaptic activity. Nature 393, 793-797.

Blackstad TW (1958). On the termination of some afferents to the hippocampus and fascia dentata. *Cells Tissues Organs*, *35*(3), 202-214.

Bredt DS, Nicoll RA (2003). AMPA receptor trafficking at excitatory synapses. Neuron 40, 361-379.

Bliss TV, Lømo T (1973). Long-lasting potentiation of synaptic transmission in the dentate area of the anaesthetized rabbit following stimulation of the perforant path. *The Journal of physiology*, *232*(2), 331-356.

Bullock TH, Buzsaki G, McClune MC (1990). Coherence of compound field potentials reveals discontinuities in the CA1-subiculum of the hippocampus in freely-moving rats. *Neuroscience*, *38*(3), 609-619.

Bunsey M, Eichenbaum H (1996). Conservation of hippocampal memory function in rats and humans. *Nature*, *379*(6562), 255-257.

Buzsáki G, Eidelberg E (1983). Phase relations of hippocampal projection cells and interneurons to theta activity in the anesthetized rat. *Brain research*, *266*(2), 334-339.

Buzsáki G, Leung L,VanderwolfCH (1983). Cellular bases of hippocampal EEG in the behaving rat. *Brain Research Reviews*, *6*(2), 139-171.

Buzsáki G, Czopf J, Kondakor I, Kellenyi L (1986). Laminar distribution of hippocampal rhythmic slow activity (RSA) in the behaving rat: current-source density analysis, effects of urethane and atropine. *Brain research*, *365*(1), 125-137.

Capocchi G, Zampolini M, Larson J (1992). Theta burst stimulation is optimal for induction of LTP at both apical and basal dendritic synapses on hippocampal CA1 neurons. *Brain research*, *591*(2), 332-336.

Çavus I, Teyler TJ (1998). NMDA receptor-independent LTP in basal versus apical dendrites of CA1 pyramidal cells in rat hippocampal slice. *Hippocampus*, *8*(4), 373-379.

Colbert CM, Johnston D (1996). Axonal action-potential initiation and Na+ channel densities in the soma and axon initial segment of subicular pyramidal neurons. *The Journal of neuroscience*, *16*(21), 6676-6686.

Collingridge GL, KehlSJ,McLennan HT (1983). Excitatory amino acids in synaptic transmission in the Schaffer collateral-commissural pathway of the rat hippocampus. *The Journal of physiology*, *334*(1), 33-46.

Connors BW,Gutnick MJ (1990). Intrinsic firing patterns of diverse neocortical neurons. *Trends in neurosciences*, *13*(3), 99-104.

Cummings JA, Nicola SM, Malenka RC (1994). Induction in the rat hippocampus of long-term potentiation (LTP) and long-term depression (LTD) in the presence of a nitric oxide synthase inhibitor. *Neuroscience letters*, *176*(1), 110-114.

Cummings JA, Mulkey RM, Nicoll RA, Malenka RC (1996). Ca2+ signaling requirements for long-term depression in the hippocampus. Neuron*16*(4): 825–33.

Cull-Candy S, Brickley S, Farrant M (2001). NMDA receptor subunits: diversity, development and disease. Curr. Opin. Neurobiol. 11, 327-335.

Dan Y, Poo M (2004). Spike timing-dependent plasticity of neural circuits. Neuron *44*(1):23-30.

Derkach VA, Oh MC, Guire ES, Soderling TR (2007). Regulatory mechanisms of AMPA receptors in synaptic plasticity. Nat. Rev. Neurosci. 8, 101-113.

Dudar J, Whishaw IQ, Szerb JC (1979). Release of acetylcholine from the hippocampus of freely moving rats during sensory stimulation and running. *Neuropharmacology*, *18*(8), 673-678.

Dudek SM, Bear MF (1992). Homosynaptic long-term depression in area CA1 of hippocampus and effects of N-methyl-D-aspartate receptor blockade. *Proceedings of the National Academy of Sciences*, *89*(10), 4363-4367.

Dunah AW, Yasuda RP, Wang YH, Luo J, Davila-Garcia M, Gbadegesin M, Vicini S, Wolfe BB (1996). Regional and ontogenic expression of the NMDA receptor subunit NR2D protein in rat brain using a subunit-specific antibody. J. Neurochem. 67, 2335-2345.

Dutar P, Nicoll RA (1988). Classification of muscarinic responses in hippocampus in terms of receptor subtypes and second-messenger systems: electrophysiological studies in vitro. *The Journal of neuroscience*, *8*(11), 4214-4224.

Duvernoy HM (1988). *The human hippocampus: an atlas of applied anatomy*. Springer Verlag.

Fisahn A, Yamada M, Duttaroy A, Gan JW, Deng CX, McBain CJ, Wess J (2002). Muscarinic induction of hippocampal gamma oscillations requires coupling of the M1 receptor to two mixed cation currents. *Neuron*, *33*(4), 615-624.

Fox SE, Ranck JB (1975). Localization and anatomical identification of theta and complex spike cells in dorsal hippocampal formation of rats. *Experimental neurology*, *49*(1), 299-313.

Fox SE, Wolfson S, Ranck Jr JB (1986). Hippocampal theta rhythm and the firing of neurons in walking and urethane anesthetized rats. *Experimental Brain Research*, *62*(3), 495-508.

Freeman JA, Nicholson C (1975). Experimental optimization of current source-density technique for anuran cerebellum. J. Neurophysiol. 38, 369-382.

Freund TF, Buzsáki, GY (1996). Interneurons of the hippocampus. *Hippocampus*, *6*(4), 347-470.

Fritschy JM, Weinmann O, Wenzel A, Benke D (1998). Synapse-specific localization of NMDA and GABA(A) receptor subunits revealed by antigen-retrieval immunohistochemistry. J. Comp. Neurol. 390, 194-210.

Fujita Y (1979). Evidence for the existence of inhibitory postsynaptic potentials in dendrites and their functional significance in hippocampal pyramidal cells of adult rabbits. *Brain research*, *175*(1), 59-69.

Ge Y, Dong Z, Bagot RC, Howland JG, Phillips AG, Wong TP, Wang YT (2010). Hippocampal long-term depression is required for consolidation of spatial memory. Proc Natl Acad Sci U S A *107*(38): 16697-702.

Grover LM, Teyler TJ (1990). Two components of long-term potentiation induced by different patterns of afferent excitation. Nature 347: 477–9.

Haley JE, Schaible E, Pavlidis P, Murdock A, Madison DV (1996). Basal and apical synapses of CA1 pyramidal cells employ different LTP induction mechanisms. *Learning & Memory*, *3*(4), 289-295.

Hanse E, Gustafsson B (1992). Long-term Potentiation and Field EPSPs in the Lateral and Medial Perforant Paths in the Dentate Gyrus In Vitro: a Comparison. *European Journal of Neuroscience*, *4*(11), 1191-1201.

Hasselmo M, Bodelón C, Wyble B (2002). A proposed function for hippocampal theta rhythm: separate phases of encoding and retrieval enhance reversal of prior learning. *Neural computation*, *14*(4), 793-817.

Hebb DO (1949). *The organization of behavior: A neuropsychological theory*. Psychology Press.

Henze DA, Cameron WE, Barrionuevo G (1996). Dendritic morphology and its effects on the amplitude and rise-time of synaptic signals in hippocampal CA3 pyramidal cells. J. Comp. Neurol. 369, 331-344.

Herreras O, Solís JM, Mun MD, Del Rio RM, Lerma J (1988a). Sensory modulation of hippocampal transmission. I. Opposite effects on CA1 and dentate gyrus synapsis. *Brain research*, *461*(2), 290-302.

Herreras O, Solís JM, Herranz AS, Del Rio RM, Lerma J (1988b). Sensory modulation of hippocampal transmission. II. Evidence for a cholinergic locus of inhibition in the Schaffer-CA1 synapse. *Brain research*, *461*(2), 303-313.

Holscher C, Anwyl R, Rowan MJ (1997). Stimulation on the positive phase of hippocampal theta rhythm induces long-term potentiation that can be depotentiated by stimulation on the negative phase in area CA1 in vivo. J Neurosci*17*(16): 6470–6477.

Hölscher C (1999). Synaptic plasticity and learning and memory: LTP and beyond. J Neurosci Res*58*(1): 62–75.

Hounsgaard J (1978). Presynaptic inhibitory action of acetylcholine in area CA1 of the hippocampus. *Experimental neurology*, *62*(3), 787-797.

Hyman JM, Wyble BP, Goyal V, Rossi CA, Hasselmo ME (2003). Stimulation in hippocampal region CA1 in behaving rats yields long-term potentiation when delivered to the peak of theta and long-term depression when delivered to the trough. J Neurosci*23*(37): 11725–31.

Ishizuka N, Weber J, Amaral DG (1990). Organization of intrahippocampal projections originating from CA3 pyramidal cells in the rat. *Journal of Comparative Neurology*, *295*(4), 580-623.

Izumi Y, Zorumski CF (1993). Nitric oxide and long-term synaptic depression in the rat hippocampus. *Neuroreport*, *4*(9), 1131-1134.

Johnston D, Williams S, Jaffe D, Gray R (1992). NMDA-receptor-independent long-term potentiation. *Annual Review of Physiology*, *54*(1), 489-505.

Johnston D, Wu SMS (1995). *Foundations of cellular neurophysiology* (pp. 392-395). Cambridge, MA: MIT press.

Kaibara T, Leung LS (1993). Basal versus apical dendritic long-term potentiation of commissural afferents to hippocampal CA1: a current-source density study. J. Neurosci. 13, 2391-2404.

Keita MS, Frankel-Kohn L, Bertrand N, Lecanu L, Monmaur P (2000). Acetylcholine release in the hippocampus of the urethane anaesthetised rat positively correlates with both peak theta frequency and relative power in the theta band. *Brain research*, *887*(2), 323-334.

Klausberger T, Somogyi P (2008). Neuronal diversity and temporal dynamics: the unity of hippocampal circuit operations. *Science*, *321*(5885), 53-57.

Kloosterman F, Peloquin P, Leung LS (2001). Apical and basal orthodromic population spikes in hippocampal CA1 in vivo show different origins and patterns of propagation. *Journal of neurophysiology*, *86*(5), 2435-2444.

Knowles WD (1992). Normal anatomy and neurophysiology of the hippocampal formation. *Journal of Clinical Neurophysiology*, *9*(2), 253-263.

Lacaille JC, Schwartzkroin PA (1988). Stratum lacunosum-moleculare interneurons of hippocampal CA1 region. II. Intrasomatic and intradendritic recordings of local circuit synaptic interactions. J. Neurosci. 8, 1411-1424.

Larson J, Lynch G (1986). Induction of synaptic potentiation in hippocampus by patterned stimulation involves two events. Science 232: 985-988.

Lashley KS (1950). In search of the engram.

Laurberg S (1979). Commissural and intrinsic connections of the rat hippocampus. *Journal of Comparative Neurology*, *184*(4), 685-708.

Léránth C, Frotscher M (1987). Cholinergic innervation of hippocampal GAD-and somatostatin-immunoreactive commissural neurons. *Journal of Comparative Neurology*, *261*(1), 33-47.

Leung LWS, Da Silva FL, Wadman WJ (1982). Spectral characteristics of the hippocampal EEG in the freely moving rat. *Electroencephalography and clinical neurophysiology*, *54*(2), 203-219.

Leung LWS, Yim CY (1986). Intracellular records of theta rhythm in hippocampal CA1 cells of the rat. *Brain research*, *367*(1), 323-327.

Leung LS, Au AS (1994). Long-term potentiation as a function of test pulse intensity: a study using input/output profiles. *Brain research bulletin*, *33*(4), 453-460.

Leung LS, Shen B (1995). Long-term potentiation at the apical and basal dendritic synapses of CA1 after local stimulation in behaving rats. J Neurophysiol*73*(5): 1938–46.

Leung LS, Roth LISA, Canning KJ (1995). Entorhinal inputs to hippocampal CA1 and dentate gyrus in the rat: a current-source-density study. *Journal of Neurophysiology*, *73*(6), 2392-2403.

Leung LW (1984). Model of gradual phase shift of theta rhythm in the rat. J Neurophysiol *52*(6): 1051–65.

Leung LS, Shen B, Kaibara T (1992). Long-term potentiation induced by patterned stimulation of the commissural pathway to hippocampal CA1 region in freely moving rats. Neuroscience 48, 63-74.

Leung LS (1998). Generation of theta and gamma rhythms in the hippocampus. Neurosci Biobehav Rev*22*(2): 275–90.

Leung LS and Shen B (1999a) LTP at apical and basal synapses of CA1 in awake rats has different sensitivity to NMDA receptor antagonists. Hippocampus 9: 617-630.

Leung LS, Shen B (1999b). N-methyl-D-aspartate receptor antagonists are less effective in blocking long-term potentiation at apical than basal dendrites in hippocampal CA1 of awake rats. *Hippocampus*, *9*(6), 617-630.

Leung LS, Shen B, Rajakumar N, Ma J (2003). Cholinergic activity enhances hippocampal long-term potentiation in CA1 during walking in rats. J Neurosci *23*(28): 9297–304.

Leung LS (2010) Field potential generation and current source density analysis. In: Electrophysiological Recording Techniques,Vertes RP, Stackman RW (Eds.), Humana Press, Clifton, N.J., NeuroMethods Volume 54: 1-26

Leung LS, Péloquin P (2010). Cholinergic modulation differs between basal and apical dendritic excitation of hippocampal CA1 pyramidal cells. *Cerebral Cortex*, *20*(8), 1865-1877.

Li XG, Somogyi P, Ylinen A, Buzsaki G (1994). The hippocampal CA3 network: an in vivo intracellular labeling study. *Journal of Comparative Neurology*, *339*(2), 181-208.

Lorente de Nó R (1934). Studies on the structure of the cerebral cortex. II. Continuation of the study of the ammonic system. *Journal fürPsychologie und Neurologie*.

Lynch G, Larson J, Kelso S, BarrionuevoG,Schottler F (1983). Intracellular injections of EGTA block induction of hippocampal long-term potentiation. *Nature*, *305*(5936), 719-721.

M'Harzi M, Palacios A, Monmaur P, Willig F, HoucineO,Delacour, J. (1987). Effects of selective lesions of fimbria-fornix on learning set in the rat. *Physiology & behavior*, *40*(2), 181-188.

MacDonald CJ, Lepage KQ, Eden UT, Eichenbaum H (2011). Hippocampal “time cells” bridge the gap in memory for discontiguous events. *Neuron*, *71*(4), 737-749.

Markram H, Sakmann B (1994). Calcium transients in dendrites of neocortical neurons evoked by single subthreshold excitatory postsynaptic potentials via low-voltage-activated calcium channels. *Proceedings of the National Academy of Sciences*, *91*(11), 5207-5211.

Malenka RC, Kauer JA, Zucker RS, Nicoll RA (1988). Postsynaptic calcium is sufficient for potentiation of hippocampal synaptic transmission. *Science*, *242*(4875), 81-84.

Malenka RC, Bear MF (2004). LTP and LTD: an embarrassment of riches. Neuron 44, 5-21.

Malinow R, Malenka RC (2002). AMPA receptor trafficking and synaptic plasticity. Annu. Rev. Neurosci. 25, 103-126.

McBain CJ, Mayer ML (1994). N-methyl-D-aspartic acid receptor structure and function. *Physiological reviews*, *74*(3), 723-760.

Megias M, Emri Z, Freund TF, Gulyas AI (2001). Total number and distribution of inhibitory and excitatory synapses on hippocampal CA1 pyramidal cells. Neuroscience 102, 527-540.

Milner B (1962). Les troubles de la memoire accompagnant des lesions hippocampiquesbilaterales. *Physiologie de l’hippocampe*, 257-72.

Miyakawa H, Kato H (1986). Active properties of dendritic membrane examined by current source density analysis in hippocampal CA 1 pyramidal neurons. *Brain research*, *399*(2), 303-309.

Monaghan DT, Olverman HJ, Nguyen L, Watkins JC, Cotman CW (1988). Two classes of N-methyl-D-aspartate recognition sites: differential distribution and differential regulation by glycine. *Proceedings of the National Academy of Sciences*, *85*(24), 9836-9840.

Monyer H, Burnashev N, Laurie DJ, Sakmann B, Seeburg PH (1994). Developmental and regional expression in the rat brain and functional properties of four NMDA receptors. *Neuron*, *12*(3), 529-540.

Moser EI, Kropff E, Moser MB (2008). Place cells, grid cells, and the brain's spatial representation system. *Annu. Rev. Neurosci.*, *31*, 69-89.

Mott DD, Lewis DV (1991). Facilitation of the induction of long-term potentiation by GABAB receptors. *Science*, *252*(5013), 1718-1720.

Mulkey RM, Malenka RC (1992). Mechanisms underlying induction of homosynaptic long-term depression in area CA1 of the hippocampus. *Neuron*, *9*(5), 967-975.

Nadel L, Moscovitch M (1997). Memory consolidation, retrograde amnesia and the hippocampal complex. *Current opinion in neurobiology*, *7*(2), 217-227.

Nishiyama M, Hong K, Mikoshiba K, Poo MM, Kato K (2000). Calcium stores regulate the polarity and input specificity of synaptic modification. *Nature*, *408*(6812), 584-588.

Numan R (1978). Cortical-limbic mechanisms and response control: A theoretical review. *Physiological Psychology*, *6*(4), 445-470.

O'Keefe J, Dostrovsky J (1971). The hippocampus as a spatial map. Preliminary evidence from unit activity in the freely-moving rat. *Brain research*, *34*(1), 171-175.

O'Keefe J, Recce ML (1993). Phase relationship between hippocampal place units and the EEG theta rhythm. Hippocampus*3*(3): 317–30.

Petsche H, Stumpf C, Gogolak G (1962). The significance of the rabbit's septum as a relay station between the midbrain and the hippocampus I. The control of hippocampus arousal activity by the septum cells. *Electroencephalography and clinical neurophysiology*, *14*(2), 202-211.

Petsche H, Gogolak G, Van Zwieten PA (1965). Rhythmicity of septal cell discharges at various levels of reticular excitation. *Electroencephalography and clinical neurophysiology*, *19*(1), 25-33.

Raymond CR (2007). LTP forms 1, 2 and 3: different mechanisms for the 'long'in long-term potentiation. *Trends in neurosciences*, *30*(4), 167-175.

Roth LR, Leung LS (1995). Difference in LTP at basal and apical dendrites of CA1 pyramidal neurons in urethane-anesthetized rats. Brain Res. 694, 40-48.

Rudell AP, Fox SE, Ranck JB (1980). Hippocampal excitability phase-locked to the theta rhythm in walking rats. *Experimental neurology*, *68*(1), 87-96.

Rudell AP, Fox SE (1984). Hippocampal excitability related to the phase of the theta rhythm in urethanized rats. *Brain research*, *294*(2), 350-353.

Schall KP, Kerber J, Dickson CT (2008). Rhythmic constraints on hippocampal processing: state and phase-related fluctuations of synaptic excitability during theta and the slow oscillation. *Journal of neurophysiology*, *99*(2), 888-899.

Scoville WB & Milner B (1957). Loss of recent memory after bilateral hippocampal lesions. *Journal of neurology, neurosurgery, and psychiatry*, *20*(1), 11.

Soderling TR, Derkach VA (2000). Postsynaptic protein phosphorylation and LTP. Trends Neurosci. 23, 75-80.

Son H, Hawkins RD, Martin K, Kiebler M, Huang PL, Fishman MC, Kandel ER (1996). Long-term potentiation is reduced in mice that are doubly mutant in endothelial and neuronal nitric oxide synthase. *Cell*, *87*(6), 1015-1023.

Song I, Huganir RL (2002). Regulation of AMPA receptors during synaptic plasticity. Trends Neurosci. 25, 578-588.

Spruston N, Schiller Y, Stuart G, Sakmann B (1995). Activity-dependent action potential invasion and calcium influx into hippocampal CA1 dendrites. *Science*, *268*(5208), 297-300.

Squire L (1992). Declarative and nondeclarative memory: Multiple brain systems supporting learning and memory. *Cognitive Neuroscience, Journal of*, *4*(3), 232-243.

Staubli U, Lynch G (1987). Stable hippocampal long-term potentiation elicited by 'theta'pattern stimulation. *Brain research*, *435*(1), 227-234.

Steward O, Scoville SA (1976). Cells of origin of entorhinal cortical afferents to the hippocampus and fascia dentata of the rat. *Journal of Comparative Neurology*, *169*(3), 347-370.

Stewart M, Fox SE (1990). Do septal neurons pace the hippocampal theta rhythm?.*Trends in neurosciences*, *13*(5), 163-169.

Stuart G, Schiller J, Sakmann B (1997). Action potential initiation and propagation in rat neocortical pyramidal neurons. *The Journal of physiology*, *505*(3), 617-632.

Thinschmidt JS, Kinney GG, Kocsis B (1995). The supramammillary nucleus: is it necessary for the mediation of hippocampal theta rhythm?.*Neuroscience*, *67*(2), 301-312.

Toth K, Freund TF (1992). Calbindin D 28k-containing nonpyramidal cells in the rat hippocampus: their immunoreactivity for GABA and projection to the medial septum. *Neuroscience*, *49*(4), 793-805.

Toth K, Freund TF, Miles R (1997). Disinhibition of rat hippocampal pyramidal cells by GABAergic afferents from the septum. *The Journal of Physiology*, *500*(2), 463-474.

Tsien JZ, Huerta PT, Tonegawa S (1996). The essential role of hippocampal CA1 NMDA receptor–dependent synaptic plasticity in spatial memory. *Cell*, *87*(7), 1327-1338.

Turner RW, Meyers DE, Barker JL (1989). Localization of tetrodotoxin-sensitive field potentials of CA1 pyramidal cells in the rat hippocampus. *Journal of neurophysiology*, *62*(6), 1375-1387.

Valentino RJ, Dingledine R (1981). Presynaptic inhibitory effect of acetylcholine in the hippocampus. *The Journal of Neuroscience*, *1*(7), 784-792.

Vanderwolf CH (1969). Hippocampal electrical activity and voluntary movement in the rat. *Electroencephalography and clinical neurophysiology*, *26*(4), 407-418.

Vanderwolf CH, Baker GB (1986). Evidence that serotonin mediates non-cholinergic neocortical low voltage fast activity, non-cholinergic hippocampal rhythmical slow activity and contributes to intelligent behavior. *Brain research*, *374*(2), 342-356.

Vertes RP, Colom LV, Fortin WJ, Bland BH (1993). Brainstem sites for the carbachol elicitation of the hippocampal theta rhythm in the rat. *Experimental brain research*, *96*(3), 419-429.

Wagner JJ, Alger BE (1995). GABAergic and developmental influences on homosynaptic LTD and depotentiation in rat hippocampus. *The Journal of neuroscience*, *15*(2), 1577-1586.

Wagner JJ,Alger BE (1996). Homosynaptic LTD and depotentiation: do they differ in name only?.*Hippocampus*, *6*(1), 24-29.

Watanabe M, Mishina M, Inoue Y (1994). Distinct spatiotemporal expressions of five NMDA receptor channel subunit mRNAs in the cerebellum. J. Comp. Neurol. 343, 513-519.

Wenzel A, Scheurer L, Kunzi R, Fritschy JM, Mohler H, Benke D (1995). Distribution of NMDA receptor subunit proteins NR2A, 2B, 2C and 2D in rat brain. Neuroreport 7, 45-48.

Wexler EM, Stanton PK (1993). Priming of homosynaptic long-term depression in hippocampus by previous synaptic activity. *Neuroreport*, *4*(5), 591-594.

Whishaw IQ, Tomie JA (1997). Perseveration on place reversals in spatial swimming pool tasks: further evidence for place learning in hippocampal rats. *Hippocampus*, *7*(4), 361-370.

Winson J (1974). Patterns of hippocampal theta rhythm in the freely moving rat. *Electroencephalography and clinical neurophysiology*, *36*, 291-301.

Winson J (1976). Hippocampal theta rhythm. I. Depth profiles in the curarized rat. *Brain Research*, *103*(1), 57-70.

Wolansky T, Clement EA, Peters SR, Palczak MA, Dickson CT (2006). Hippocampal slow oscillation: a novel EEG state and its coordination with ongoing neocortical activity. *The Journal of neuroscience*, *26*(23), 6213-6229.

Wyble BP, Linster C, Hasselmo ME (2000). Size of CA1-evoked synaptic potentials is related to theta rhythm phase in rat hippocampus. *Journal of Neurophysiology*, *83*(4), 2138-2144.

y Cajal SR (1911). Histogénèse du cervelet. In *Histologie du SystèmeNerveux de l'Hommeet des Vertébrés* (Vol. 2, pp. 80-106). Instituto Ramón y Cajaldel CSIC Madrid.

Yashiro K, Philpot BD (2008). Regulation of NMDA receptor subunit expression and its implications for LTD, LTP, and metaplasticity. Neuropharmacology 55, 1081-1094.

Yim CY, Leung LWS (1988). Effects of carbachol perfusion on evoked responses and excitability of pyramidal cells in the hippocampal slice. *Neurosci Res Commun*, *2*, 47-52.

Zalutsky RA, Nicoll RA (1990). Comparison of two forms of long-term potentiation in single hippocampal neurons. *Science*, *248*(4963), 1619-1624.

Zola-Morgan S, Squire LR, Amaral DG (1986). Human amnesia and the medial temporal region: enduring memory impairment following a bilateral lesion limited to field CA1 of the hippocampus. *The Journal of Neuroscience*, *6*(10), 2950-2967.

6. APPENDIX

6.1 ETHICAL APPROVAL FOR ANIMAL USE

2010-261::3:

AUP Number: 2010-261

AUP Title: Neural plasticity of the forebrain

Yearly Renewal Date: 12/01/2013

The YEARLY RENEWAL to Animal Use Protocol (AUP) 2010-261 has been approved, and will be approved for one year following the above review date.

1. This AUP number must be indicated when ordering animals for this project.

2. Animals for other projects may not be ordered under this AUP number.

3. Purchases of animals other than through this system must be cleared through the ACVS office. Health certificates will be required.

REQUIREMENTS/COMMENTS

Please ensure that individual(s) performing procedures on live animals, as described in this protocol, are familiar with the contents of this document.

The holder of this Animal Use Protocol is responsible to ensure that all associated safety components (biosafety, radiation safety, general laboratory safety) comply with institutional safety standards and have received all necessary approvals. Please consult directly with your institutional safety officers.

Submitted by: Kinchlea, Will D

on behalf of the Animal Use Subcommittee

AUP Number: 2010-261

PI Name: Leung, Stan (lai-wo)

AUP Title: Neural Plasticity Of The Forebrain

Approval Date: 03/13/2015

Official Notice of Animal Use Subcommittee (AUS) Approval: Your new Animal Use Protocol (AUP) entitled "Neural Plasticity Of The Forebrain" has been APPROVED by the Animal Use Subcommittee of the University Council on Animal Care. This approval, although valid for four years, and is subject to annual Protocol Renewal.2010-261::5

1. This AUP number must be indicated when ordering animals for this project.
2. Animals for other projects may not be ordered under this AUP number.
3. Purchases of animals other than through this system must be cleared through the ACVS office. Health certificates will be required.

The holder of this Animal Use Protocol is responsible to ensure that all associated safety components (biosafety, radiation safety, general laboratory safety) comply with institutional safety standards and have received all necessary approvals. Please consult directly with your institutional safety officers.

Submitted by: Copeman, Laura
on behalf of the Animal Use Subcommittee
University Council on Animal Care

6.2 SUPPLEMENTARY FIGURES

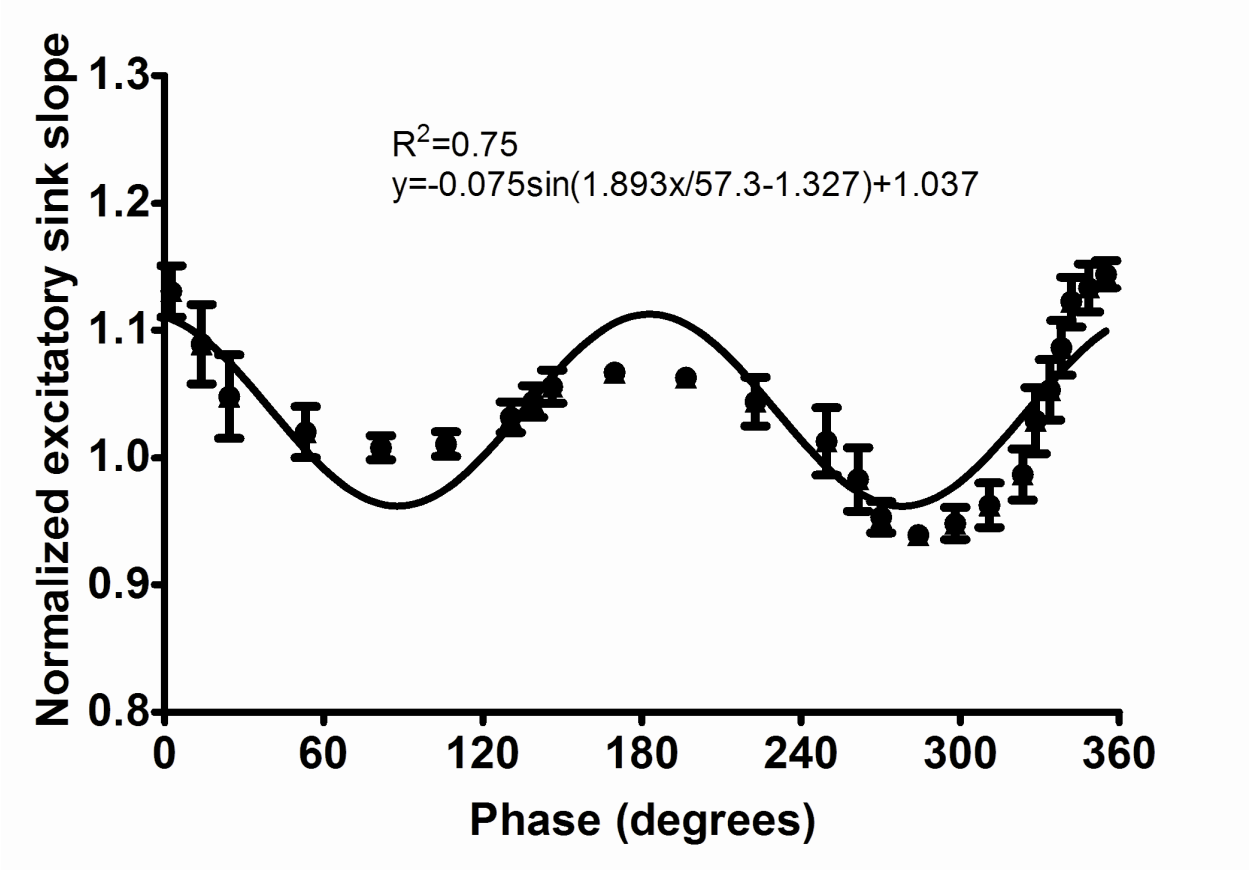

Figure 1. Sine wave correlation of plot of apical running averages plot shown in **Fig. 14**. A sine wave was fitted based on the equation y=Asin(Dx/57.2958+B)+C, where A=amplitude, B= offset, C=baseline, and D=frequency. The optimized parameters for a best-fitting sine wave were A=-0.075, B=-1.327, C=1.037 and D=1.893.

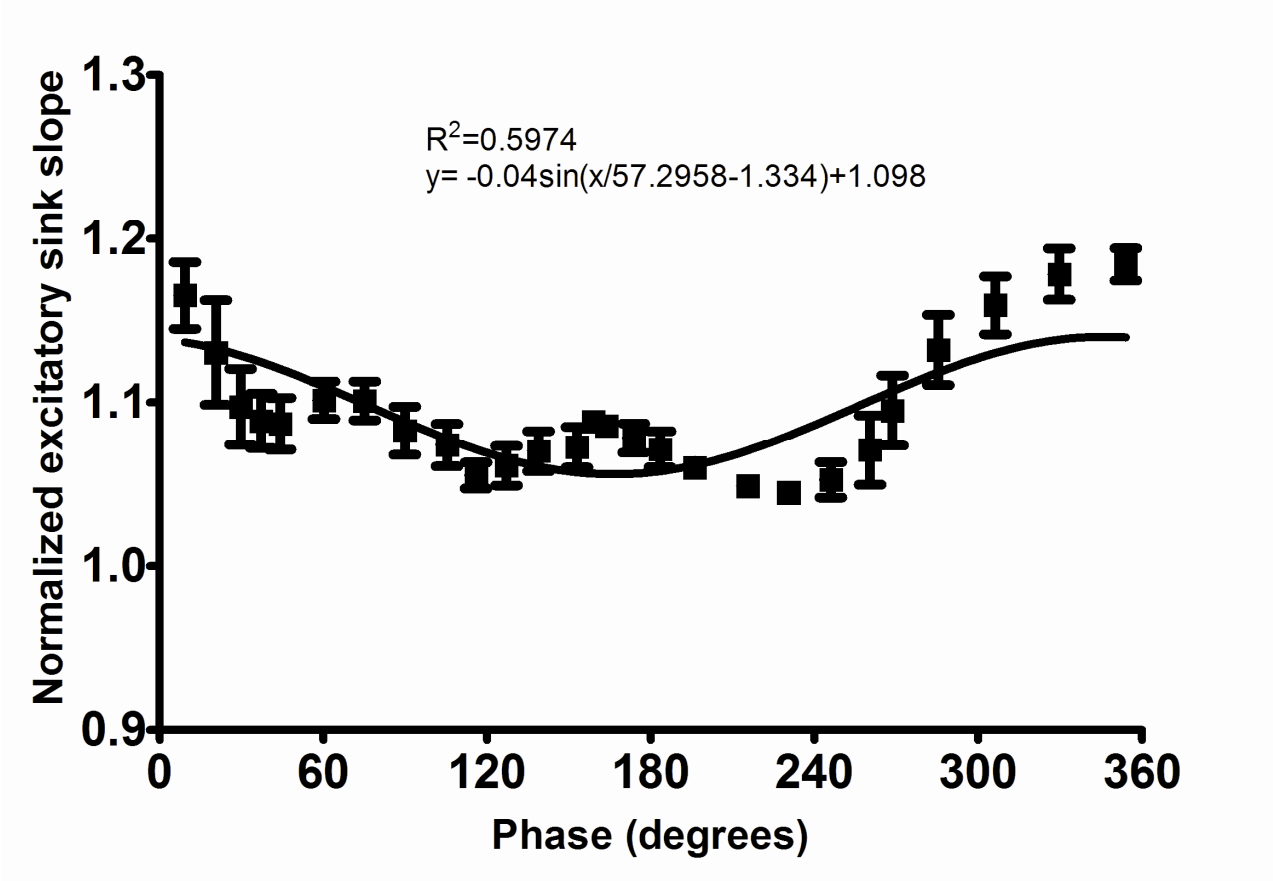

Figure 2. Sine wave correlation of plot of basal running averages plot shown in **Fig. 18**. A sine wave was fitted based on the equation y=Asin(x/57.2958+B)+C, where A=amplitude, B= offset, and C=baseline. The optimized parameters for a best-fitting sine wave were A=-0.04, B=-1.334, and C=1.098.

7. CURRICULUM VITAE

Name:	Clayton S.H. Law
Post-secondary Education and Degrees:	University of Western Ontario London, Ontario, Canada 2009-2013, Honours B.MSc. Pharmacology University of Western Ontario London, Ontario, Canada 2013-2015, M.Sc. Physiology
Honours and Awards:	Ontario Graduate Scholarship 2014-2015
Related Work Experience:	Teaching Assistant University of Western Ontario 2013-2015 Physiology 3130Y/Z
Publications:	Law, C.S., and Leung, L.S. (2015). Hippocampal theta rhythm provides different modulation of long-term potentiation and spike excitability at the basal and apical dendrites of hippocampal CA1 pyramidal cells. Accepted abstract for SFN 2015 meeting. Law, C.S., Fung T.K., and Leung, L.S. (2014). LTP induced by pairing subthreshold basal dendritic excitation with backpropagating apical dendritic evoked spike in vivo. Accepted abstract for SFN 2014 meeting.